CHAPTER 5
RESULTS AND DISCUSSION

In this chapter, the results related to the thermal and catalytic pyrolysis of waste expanded polystyrene (WEPS) are discussed in detail in two parts. In the first part **(Part-I)**, thermal pyrolysis and effect of various parameters are discussed. The catalytic pyrolysis of WEPS in three different reactor arrangements i.e., A-type/liquid phase, B-type/vapour phase and AB-type/multiphase) are discussed in the second part **(Part-II)**. The catalytic pyrolysis was performed using two commercial catalysts i.e., ZSM-5 ammonium powder and Nickel on silica-alumina and one synthesized catalysts from natural red clay. The catalysts synthesized from natural red clay were characterized by scanning electron microscope/energy dispersive X-ray spectroscopy (SEM-EDX), X-ray diffraction (XRD), Brunauer-Emmet-Teller (BET) surface area, Fourier transformed infrared spectroscopy (FTIR). The effect of various parameters on the pyrolysis of WEPS like holding time, feed to catalyst ratio, reaction temperature, heating rate and calcination temperature of synthesized catalyst for the production of target molecules benzene, toluene and ethylbenzene (BTE) are discussed. The pyrolysis oil was characterized by various characterization methods such as gas chromatography (GC) coupled with flame ionization detector mode (FID) mode, Fourier transformed infrared spectroscopy (FTIR), gross calorific value (GCV), carbon residue and flash and fire point. The reusability of catalyst after regeneration was also discussed at the end of this chapter. It should be noted that the, thermal pyrolysis of WEPS was conducted for the comparison of performance between thermal and catalytic process for the production of BTE content.

5.1 Feed characterization

5.1.1 Proximate analysis of WEPS

The proximate analysis of WEPS was performed as per ASTM test methods (IS 1350-1959) guidelines. The results of proximate analysis of WEPS in Table 5.1 shows that WEPS contains very high amount volatile matter of 99.8 wt.% and negligible amount of ash content 0.02 wt.% which indicate that high conversion of WEPS to liquid and gaseous hydrocarbon products with small amount of solid residue (Ahmad et al., 2020) during pyrolysis of WEPS.

Table 5.1 Proximate analysis of WEPS.

Physicochemical property	Amount (wt.%)
Moisture content	0.0
Volatile matter	99.8
Fixed carbon	0.18
Ash content	0.02

5.1.2 Thermo-chemical behaviour of WEPS

Thermogravimetry analysis (TGA) is a very useful analysis for investigating the behaviour of material and stability with temperature in an inert or in an oxidizing atmosphere. In short, this method provides exact information regarding the decomposition of the material at various temperatures. The weight loss due to decomposition of WEPS at various significant temperature zone is shown in Table 5.2. Figure 5.1 shows the TGA and DTG curves of WEPS. It is seen from the Figure 5.1 that the degradation of WEPS starts at a temperature of about 360 ^{o}C and 99 wt.% degradation occurs at a temperature of 600 ^{o}C. It is also seen from Figure

5.1 that 10 wt.% WEPS was degraded at a temperature of 394 ºC while 90 wt.% degradation takes place at about 440 ºC.

Table 5.2 TGA data of waste expanded polystyrene.

Weight loss (%)	**Temperature (ºC)**
Initial Decomposition Temperature (IDC)	T_{IDC} =360
10	T_{10} = 394
50	T_{50} = 422
90	T_{90} = 440
99	T99 = 600

The rate of weight loss becomes slow after 90 wt.% of conversion and only 9 wt.% weight loss is achieved for the increase in temperature of about 160 ºC. The TGA curve confirms that the thermal degradation of WEPS occurs in a single step. The DTG curve of WEPS confirms a single decomposition peak temperature of 428 ºC which indicates the dominating step during maximum degradation of WEPS (Yu et al., 2018).

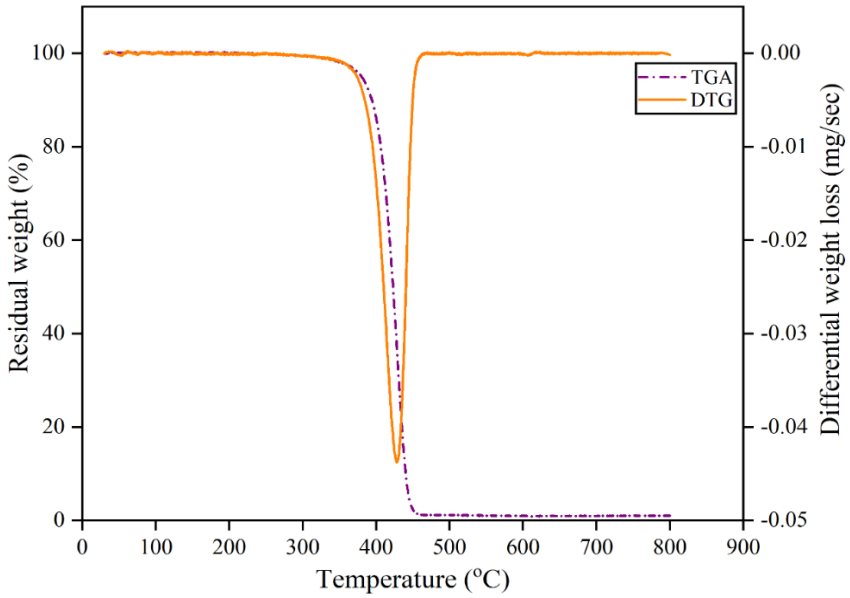

Figure 5.1 TGA/DTG curve of waste expanded polystyrene (WEPS).

5.2 Thermal pyrolysis of WEPS: Part I

The thermal pyrolysis of WEPS was studied in the reactor as discussed in experimental method using reactor arrangement for thermal pyrolysis (Figure 3.4a, page no. 50). The effect of different parameters and characterization of pyrolysis oil are described in the following section.

5.2.1 Effect of process parameters on product yield

5.2.1.1 Effect of temperature and holding time

Effect of temperature on product yield at zero hold time and effect of hold time on product yield was carried out for thermal pyrolysis (Figure 5.2a-b) at a heating rate of 15 ^{o}C/min. The temperature interval of 50 ^{o}C was maintained for both the pyrolysis to measure the pyrolysis yield at different temperatures. To see the effect of temperature on product yield at zero hold time, the experiment starts from ambient condition and process ends when it reaches to the maximum set temperature. It means, at zero hold time, no additional time was allowed to continue the reaction process once it reaches at a maximum set temperature (Figure 5.2a). In the second case, to see the effect of hold time, after reaching at set point temperature, the experiment was continued for additional 1 hr with an interval of 10 min for maximizing the liquid yield (Figure 5.2b). This experiment was performed to determine the optimum reaction time to achieve the highest conversion of WEPS to valuable fuel range hydrocarbons rich in BTE. It is seen in the Figure 5.2a, that the highest liquid yield of 85.93 wt.% was obtained at a temperature of 650 ^{o}C for thermal pyrolysis of WEPS when the hold time was zero (Figure 5.2a). However, there is no decomposition of WEPS up to 350 ^{o}C for thermal pyrolysis (Figure 5.2a). The TGA analysis (Figure 5.1) of WEPS also shows a similar trend as seen in the present study (Figure 5.2a).

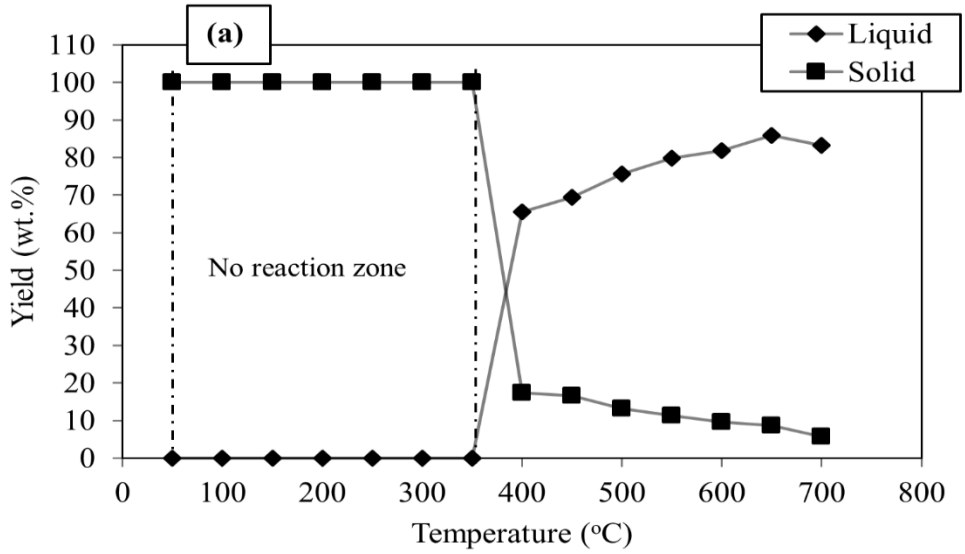

Figure 5.2a Effect of temperature on liquid and solid yield for thermal pyrolysis at 15 °C/min heating rate and zero holding time.

Figure 5.2b shows that the, liquid yield increases with the increase in hold time after reaching the pyrolysis set temperature of 650 °C and the highest liquid yield of 94.37 wt.% was obtained for the hold time of 30 min. Beyond 30 min of hold time no more liquid yield was collected, it means no further reaction takes place beyond this time (Figure 5.2b).

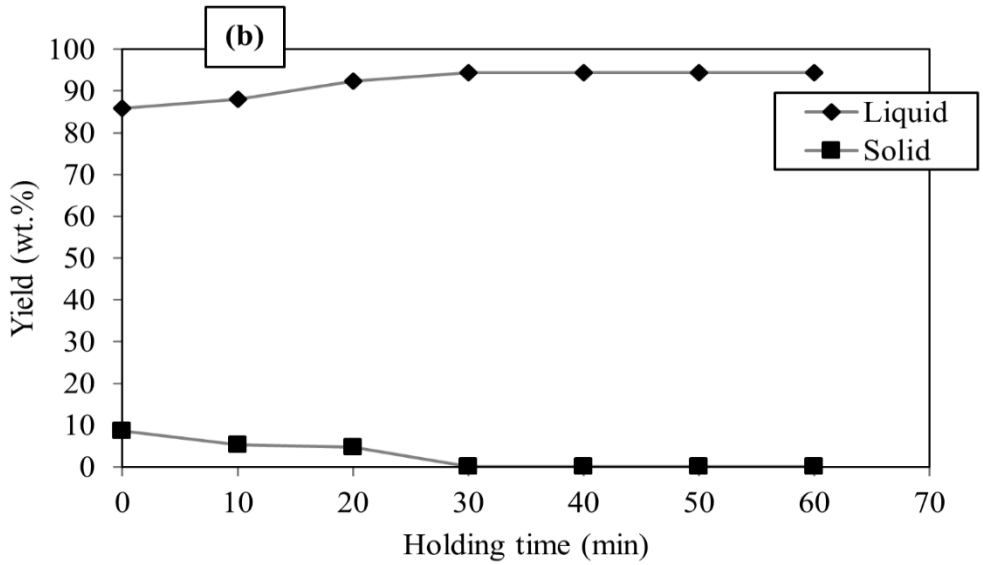

Figure 5.2b Effect of holding time on liquid and solid yield for thermal pyrolysis at a heating rate of 15 °C/min and at a temperature of 650 °C.

The solid yield also decreases with the increase in hold time up to 30 min. Thus, holding time of 30 min was considered as an optimum hold time in order to obtain a highest liquid yield for the thermal pyrolysis process.

5.2.1.2 Effect of heating rate

Figure 5.3 shows the effect of heating rate on the product yield obtained from thermal pyrolysis of WEPS at different heating rates ranging from 5 ^{o}C/min to 25 ^{o}C/min and at the pyrolysis temperature of 550 ^{o}C. It should be noted that the, liquid yield increases with the increase in heating rate up to 15 ^{o}C/min and a further increase in heating rate beyond 15 ^{o}C/min, the liquid yield decreases. This type of increasing trend of liquid yield up to 15 ^{o}C/min may be due to the low residence time of cracked hydrocarbon molecules at higher heating rate of 10 ^{o}C/min and 15 ^{o}C/min in comparison to low heating rate of 5 ^{o}C/min, and thus, cracked hydrocarbon molecules will go to the condenser where it is collected as liquid yield.

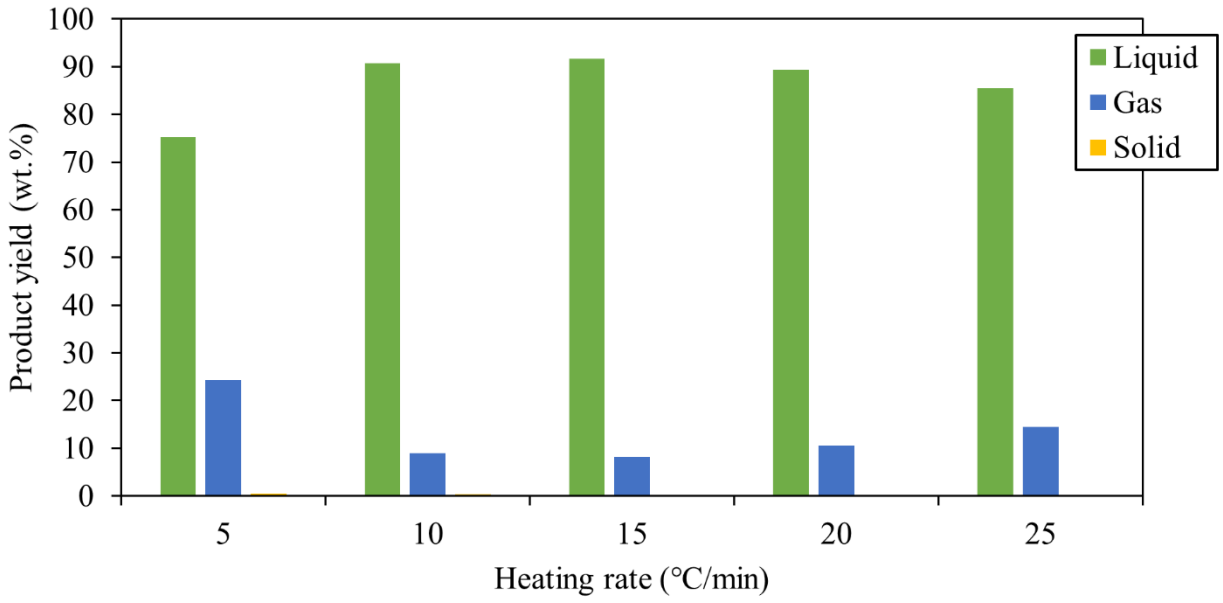

Figure 5.3 Effect of heating rate on product yield obtained from thermal pyrolysis of WEPS at a temperature of 550 ^{o}C.

It is seen from the Figure 5.3 that the maximum liquid yield of 91.69 wt.% was obtained at a heating rate of 15 ^{o}C/min. However, very high heating rate (20 ^{o}C/min) beyond 15 ^{o}C/min favours the β-scission reaction on polymeric hydrocarbon chain resulting in more gaseous hydrocarbon molecules and less liquid yield and reported by Sundararajan and Bhagavathi (2016). The liquid yield of 89.33 wt.% and 85.51 wt.% were obtained at heating rate of 20 ^{o}C/min and 25 ^{o}C/min, respectively. It should be noted that the solid residue decreases from 0.46 wt.% to 0.07 wt.%, with the increase in heating rate from 5 ^{o}C/min to 25 ^{o}C/min, as a slow heating rate favours the solid residue formation (Papari et al., 2021). In the preset study, 15 ^{o}C/min was recorded as the optimum heating rate in terms of liquid yield of (91.69 wt.%). The similar trend between heating rate and solid residue was also reported by Sundararajan and Bhagavathi, 2016 and Tao et al., 2013.

5.2.1.3 Effect of temperature

Figure 5.4 shows the product yield for the thermal pyrolysis of WEPS at a various temperatures ranging from 400 ^{o}C-700 ^{o}C with an interval of 50 ^{o}C at the optimum heating rate of 15 ^{o}C/min. It is seen from the Figure 5.4 that the liquid yield increase with the increase in reaction temperature up to 650 ^{o}C and then goes down beyond the temperature of 650 ^{o}C. The maximum liquid yield of 94.37 wt.% was obtained at a temperature of 650 ^{o}C for the thermal process. Whereas, the gaseous yield of 5.55 wt.% was obtained at a same pyrolysis temperature of 650 ^{o}C. Beyond the temperature of 650 ^{o}C the gaseous yield increases because of the stronger cracking of C-C bonds at higher temperature which gives rise to more gaseous range hydrocarbons (Lopez et al., 2011b). The liquid and gaseous yield of 93.64 wt.% and 6.27 wt.%, respectively were obtained at a reaction temperature of 700 ^{o}C. Thus, based on the maximum

liquid yield of 94.37 wt.%, the reaction temperature of 650 ºC was considered as the optimum temperature for the thermal pyrolysis process.

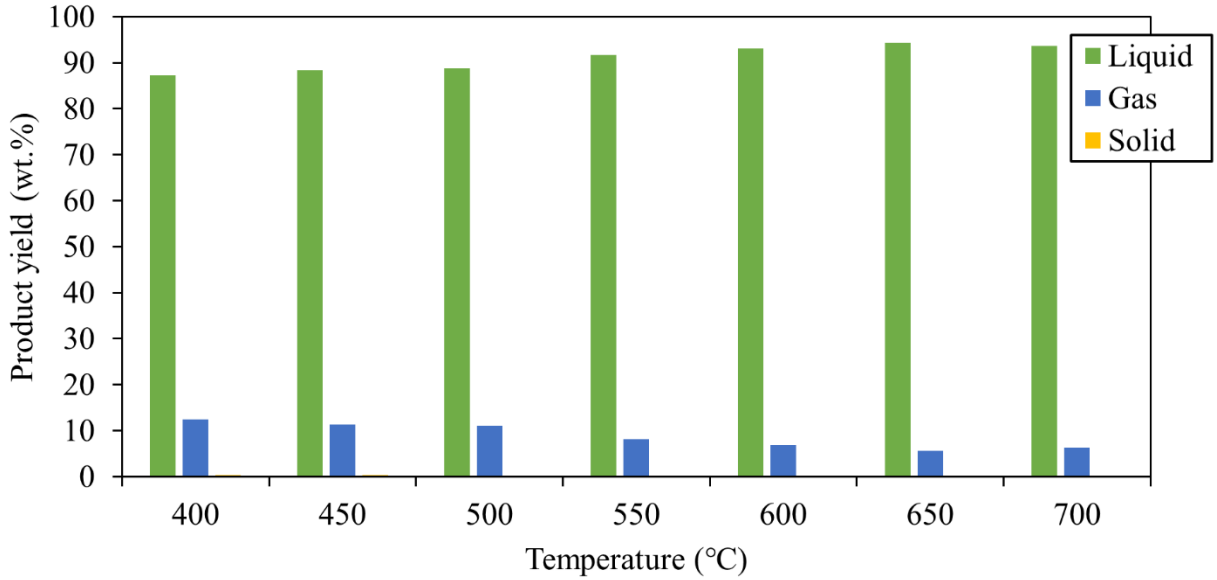

Figure 5.4 Effect of temperature on product yield obtained from thermal pyrolysis of WEPS at a heating rate of 15 ºC/min.

Interestingly, the solid residue obtained from thermal pyrolysis of WEPS was always low and it, decreased from 0.37 wt.% to 0.08 wt.% when the pyrolysis temperature was increased from 400 ºC to 650 ºC. Beyond the temperature of 650 ºC, the solid yield slightly increased to 0.09 wt.% may be due to the re-polymerization reaction (Lopez et al., 2011b).

5.2.2 Analysis of thermal pyrolysis oil

5.2.2.1 Estimation of aromatic content/BTE and styrene in pyrolysis oil

The BTE and styrene content of thermal pyrolysis oil was measured for determining the quality of product oil. In addition, the BTE and styrene content of thermal pyrolysis oil was measured to compare its quality with catalytic pyrolysis oil in terms of BTE and styrene content. The concentration of benzene, toluene, ethylbenzene and styrene were calculated from the

calibration characteristics Figure 3.8 (page no. 59). The BTE and styrene content of thermal pyrolysis oil was measured at each pyrolysis temperature and it is given in Table 5.3. The main aim of the present study is the enhancement in BTE content and reduction of a styrene in the pyrolysis oil. Thus, the process temperature were optimized in terms of composition and liquid yield both.

Table 5.3 Product yield and BTE content obtained from thermal pyrolysis of WEPS in the temperature range of 400-700 ^{o}C at 15 ^{o}C/min heating rate.

Pyrolysis Temperature (^{o}C)	Liquid (wt.%)	Gas (wt.%)	Benzene (wt.%)	Toluene (wt.%)	Ethylbenzene (wt.%)	Styrene (wt.%)	Total BTE (wt.%)
400	87.18	12.45	0.12	3.55	0.29	91.61	3.96
450	88.33	11.33	0.25	4.58	0.32	91.07	5.15
500	88.73	11.1	0.35	6.77	0.34	88.34	7.46
550	91.69	8.17	0.41	6.90	0.36	87.63	7.68
600	93.06	6.85	0.55	8.82	0.49	87.15	9.86
650	**94.37**	**5.55**	**0.62**	**10.21**	**0.55**	**84.74**	**11.38**
700	93.64	6.27	0.50	7.90	0.56	83.27	8.97

It should be noted that the maximum BTE content and minimum styrene content were found only at optimum temperature of 650 ^{o}C and heating rate of 15 ^{o}C/min (Table 5.3). It is seen from the Table 5.3, thermal pyrolysis produced very low BTE content of 11.38 wt.% and very high undesired styrene content of 84.74 wt.% at optimum conditions due to the non-selective cracking. Many authors (Nisar et al., 2019; Park et al., 2003) have also reported that the thermal pyrolysis of polystyrene produces mainly styrene monomer. However, styrene yield was strongly affected by the temperature of reaction. As the temperature is increased from 400 ^{o}C to 650 ^{o}C, the styrene yield decreased from 91.61 wt.% to 84.74 wt.%. The decreasing trend of styrene yield and enhancement of benzene, toluene and ethylbenzene, may be due to the further decomposition of styrene at high temperature (Artetxe et al., 2015; Bartoli et al., 2015)

via secondary reactions i.e., cracking and hydrogenation. Figure 5.5 shows the comparison of GC-FID characteristics of thermal pyrolysis oil obtained at optimum conditions i.e., temperature of 650 ºC and heating rate of 15 ºC/min and standard fuels gasoline and kerosene.

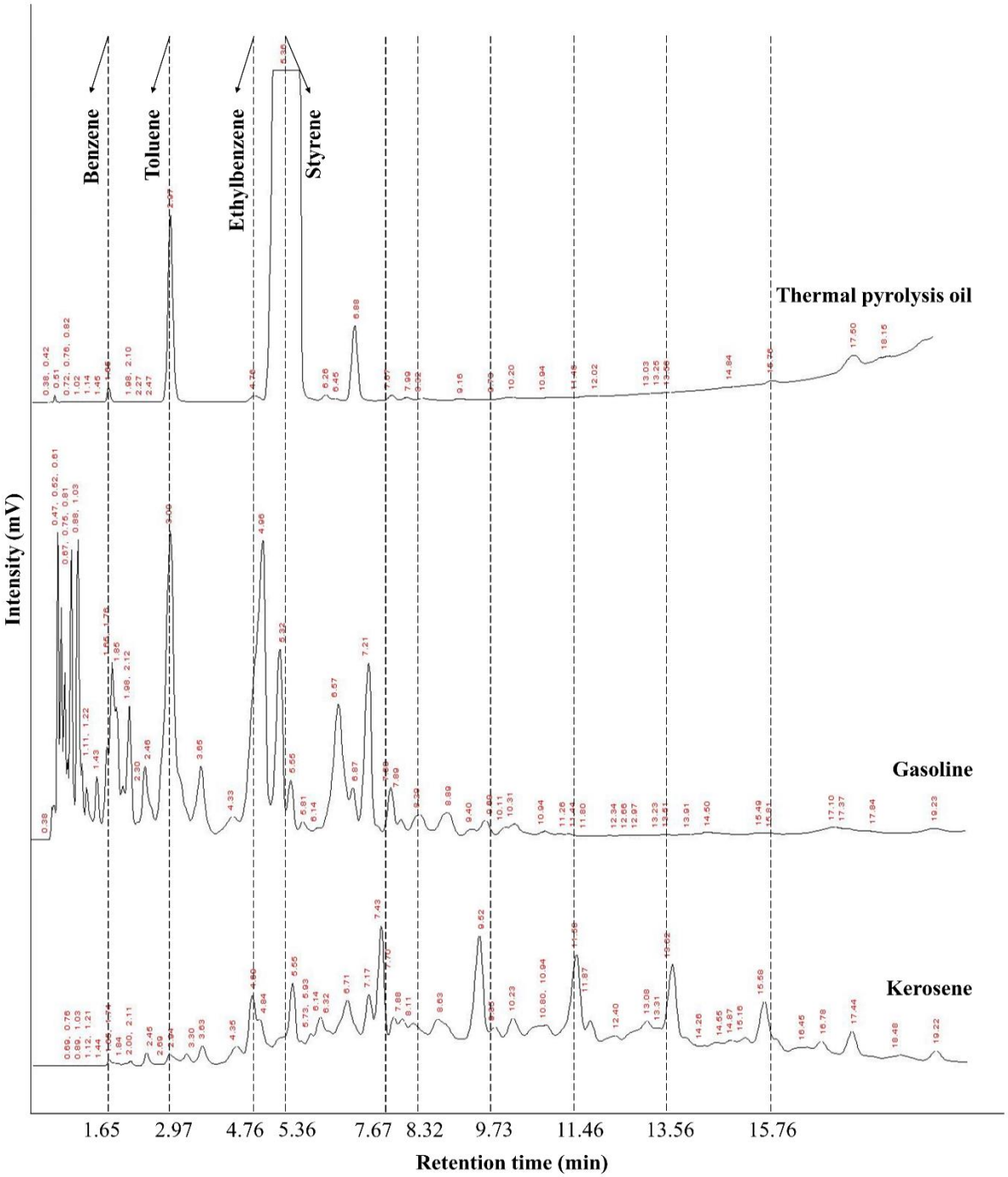

Figure 5.5 Comparison of gas chromatographs of thermal pyrolysis oil obtained at optimum conditions with commercial fuel gasoline and kerosene.

The peaks of target molecules i.e., benzene at a retention time of 1.65 min, toluene at retention time of 2.97 min and ethylbenzene at a retention time of 4.76 min and styrene at retention time of 5.36 min were highlighted with marker. Thus, the peaks of benzene, toluene, and ethylbenzene (BTE) appears within the initial zone of retention time of 6 min. It is also clear from Figure 5.5 that, most of the peaks of thermal pyrolysis oil was matches with the standard fuel kerosene at high retention time.

5.2.2.2 FTIR analysis of thermal pyrolysis oil

The FTIR is an important technique for the identification of various functional groups present in pyrolysis oil. The FTIR spectrum of thermal pyrolysis oil obtained at optimum conditions i.e., temperature of 650 ^{o}C and heating rate of 15 ^{o}C/min is shown in Figure 5.6. The important FTIR peaks at their various finger print region of wavenumber (cm^{-1}) are shown in Table 5.4.

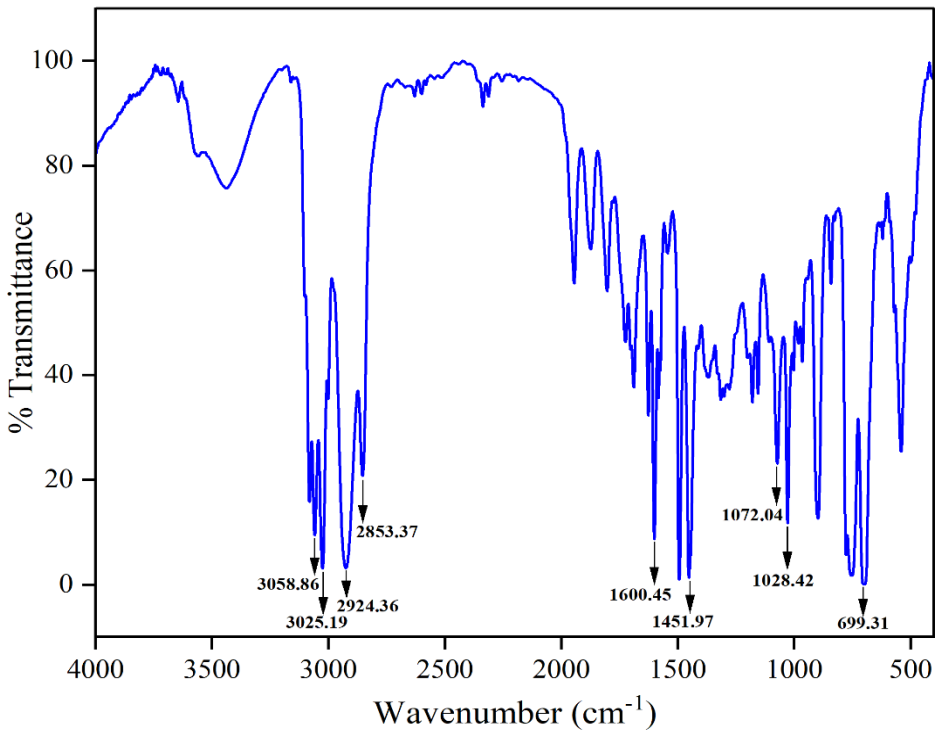

Figure 5.6 FTIR spectra of pyrolysis oil obtained from thermal pyrolysis of WEPS at optimum conditions.

The aromatic C-H stretching was observed at wavenumbers of 3081.44 cm^{-1}, 3058.86 cm^{-1}, 3025.19 cm^{-1}, and 3000.87 cm^{-1} (Budsaereechai et al., 2019). The methylene C-H asymmetric stretching and methylene C-H symmetric stretching were observed at a wavenumber of 2924.86 cm^{-1} and 2853.37 cm^{-1}, respectively. The peaks related to the methyl C-H asymmetric bending and methyl C-H symmetric bending were also observed at a wavenumber of 1451.97 cm^{-1} and 1367.31 cm^{-1}, respectively.

Table 5.4 Peak assignments for functional groups present in the thermal pyrolysis oil obtained at optimum conditions (temperature of 650 ºC and heating rate of 15 ºC/min).

Functional group	**Wavelength (cm^{-1})**	
	Standard finger print region	**Thermal pyrolysis oil**
Aromatic C-H stretching	Above 3000 cm^{-1}	3081.44 3058.86 3025.19 3000.87
Methylene C-H asymmetric stretching	2935-2915	2924.86
Methylene C-H symmetric stretching	2865-2845	2853.37
C=C-C aromatic ring stretching	1615-1580	1600.45 1582.57
C=C-C aromatic ring stretching	1510-1450	1493.31
Methyl C-H asymmetric bending	1470-1430	1451.97
Methyl C-H symmetric bending	1380-1370	1367.31
Aromatic C-H in plane bending	1225-950	1179.73 1155.09 1072.04
Cyclohexane ring vibrations	1055-1000/1005-925	1028.42 965.07
Aromatic C-H out of plane bending	900-670	842.13 777.54 752.77 699.31

Furthermore, the peaks at wavenumber of 1600.45 cm^{-1} and 1582.57 cm^{-1} and 1493.73 cm^{-1} are seen due to the C = C-C aromatic ring stretching. The aromatic C-H in plane bending was noticed at a wavenumber of 1179.73 cm^{-1}, 1155.09 cm^{-1} and 1072.04 cm^{-1}. Whereas, aromatic C-H out of plane bending was also detected at a wavenumber of 842.13 cm^{-1} and 777.54 cm^{-1} and 752.77 cm^{-1} and 699.31 cm^{-1}. Moreover, cyclohexane ring vibrations were also observed at a wavenumber of 1028.42 cm^{-1} and 965.07 cm^{-1} (Coates 2006). Thus, FTIR spectra of pyrolysis oil obtained from thermal process confirms the presence of alkanes, alkenes, napthenes and aromatics hydrocarbons.

5.2.2.3 Physicochemical properties of thermal pyrolysis oil

The physicochemical properties of thermal pyrolysis oil such as gross calorific value (GCV), carbon residue, flash and fire point were estimated as per the ASTM standard methods mentioned in chapter 3 (page no. 59-61) and they are reported in Table 5.5. The physicochemical properties of thermal pyrolysis oil were also compared with the commercial fuel gasoline and kerosene as mentioned in Table 5.5. It should be noted that the physicochemical properties found to be best only at optimum condition i.e., temperature of 650 ^{o}C and heating rate of 15 ^{o}C/min. The calorific value of thermal pyrolysis oil at optimum condition was found to be 9816 Cal/g. The significant difference between calorific value of pyrolysis oil and standard fuels gasoline and kerosene (Gaurh and Pramanik, 2019) may be due to the presence of long-chain carbon compounds of lower calorific value (Lam et al., 2012). Similarly, the carbon residue of thermal pyrolysis oil obtained at optimum condition was found to be 1 wt.%, significantly higher than the gasoline and kerosene (Shakirullah et al., 2010) because of presence of heavy hydrocarbon molecules. The high carbon residue is responsible

for heavy smoke emissions (Murugan et al., 2008) and deposition on engine parts, leading to overheating and finally results in engine knocking (Alhassan et al., 2015).

Table 5.5 physicochemical properties of thermal pyrolysis oil obtained at a heating rate of 15 ^{o}C/min with standard fuel gasoline and kerosene.

Properties	**Test method**	**Pyrolysis temperature (^{o}C)**							**Commercial fuels**	
		400	**450**	**500**	**550**	**600**	**650**	**700**	**Gasoline**	**Kerosene**
GCV (Cal/g)	IP 12/63 T	9231	9354	9526	9672	9795	**9816**	9703	11315	11052
Carbon residue (wt.%)	IP 14/65	2.3	2.1	1.6	1.4	1.3	**1.01**	1.1	0.14	0.18
Flash point (^{o}C)	ASTM D 92	74	72	69	64	62	**58**	60	22	42
Fire point (^{o}C)	ASTM D 92	76	75	72	68	64	**62**	65	25	45

The flash point is a critical factor for evaluating the potential of fire and explosion during fuel production, storage and transportation (Fu, 2019). The flash and fire point of thermal pyrolysis oil was found to be 58 ^{o}C and 62 ^{o}C, which indicates the easy handling, storage and transportation of oil (Mahmudul et al., 2017). However, the lower the flash point of a fuel is, the easier the ignition of that fuel. The flash and fire point of thermal pyrolysis oil obtained at a temperature of 650 ^{o}C was higher than the commercial fuel gasoline (Mukhraiya and Yadav, 2015) because of high boiling range hydrocarbons. However, the flash and fire point of pyrolysis oil at 650 ^{o}C was close to the commercial kerosene (Ahmad et al., 2017). The physicochemical properties indicate that the thermal pyrolysis oil obtained at 650 ^{o}C may create trouble for generator set or as a fuel oil for stoves. In view of this, the catalytic pyrolysis of WEPS using various catalysts were investigated to obtained upgraded fuel oil in terms of

BTE content and other valuable hydrocarbons. The catalytic pyrolysis of WEPS is discussed in the next section **Part-II**.

5.3 Catalytic pyrolysis of waste expanded polystyrene (WEPS): Part II

The catalytic pyrolysis of WEPS was performed using three different types of catalysts i.e., ZSM-5 ammonium powder, nickel on silica-alumina catalyst and synthesized catalyst from natural red clay. The effect of various process parameters like holding time, feed to catalyst ratio and reaction temperature on the product yield and product composition for the various reactor arrangements (A-type, B-type and AB-type) are discussed for three different types of catalysts under the three following major sections 5.3.1 (page no. 84), 5.3.2 (page no. 102), and 5.3.3 (page no. 118), respectively.

5.3.1 Catalytic pyrolysis using ZSM-5 ammonium powder as catalyst

5.3.1.1 Effect of process parameters on product yield

5.3.1.1.1 Effect of feed to catalyst ratio

The catalyst plays an important role during the pyrolysis of waste plastics in selective cracking of the larger hydrocarbon molecules into value added products. It also reduces the time of reaction by driving the reaction through a pathway with lower activation energy comparatively at a lower temperature than the non-catalytic/thermal pyrolysis process (Anene et al., 2018). The effect of feed to catalyst ratio on product yield for A-type, B-type and AB-type catalytic pyrolysis were determined at different feed to catalyst ratio of 10:1, 20:1, 30:1 and 40:1 using ZSM-5 ammonium powder as catalyst. The reaction temperature of 600 ^{o}C and heating rate of 15 ^{o}C/min were maintained to determine the effect of feed to catalyst ratio on the product yield.

Figure 5.7 shows the effect of feed to catalyst ratio on product yield obtained from the catalytic pyrolysis of WEPS in the reactor arrangement liquid phase/A-type at a temperature of 600 ^{o}C and heating rate of 15 ^{o}C/min. However, effect of feed to catalyst ratio on the product yield obtained from B-type and AB-type catalytic pyrolysis at the same experimental conditions are mentioned in Appendix A2. Primarily, in A-type-/liquid phase catalytic pyrolysis, the reaction proceeds with the WEPS meltdown at the bottom of the reactor due to heating at the set temperature and then the melted mass of WEPS get mixed thoroughly with the catalyst particles due to the heating at a high temperature which results in boiling and simultaneous natural convection at the initial stage of the reaction. As long as liquid hydrocarbon remains in the reactor, the catalyst particle will be in good contact of liquid hydrocarbon which will be cracked into liquid and gaseous hydrocarbons further.

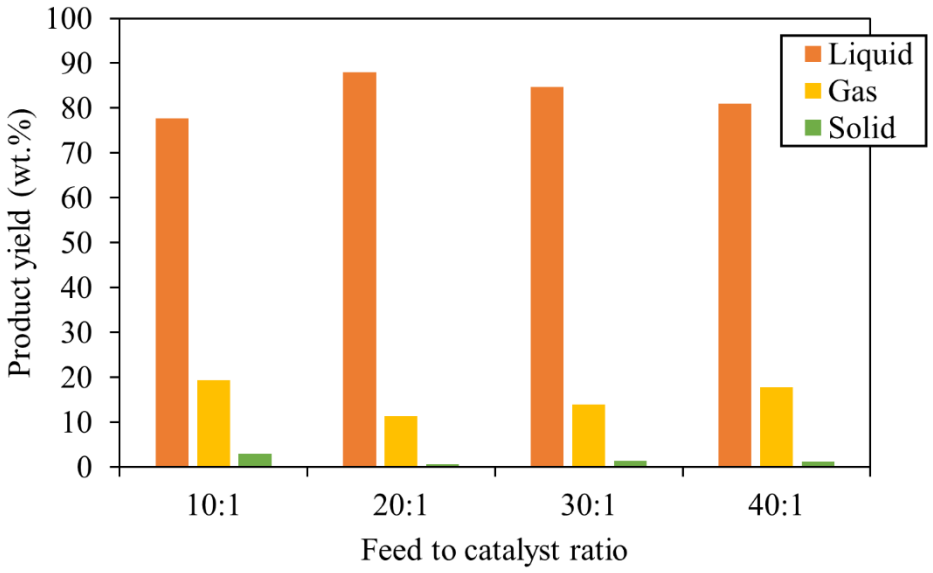

Figure 5.7 Effect of feed to catalyst ratio on product yield for liquid phase catalytic process/A-type at 600 ^{o}C and 15 ^{o}C/min using ZSM-5 ammonium powder catalyst.

It is seen from Figure 5.7 that the liquid yield increases with the increase in feed to catalyst ratio up to 20:1 and gives a maximum liquid yield of 88.05 wt.%. It may be due to the highest

active surface of catalyst available for interaction with the reactants. However, the liquid yield goes down to 84.7 wt. % with the increase in feed to catalyst ratio beyond 20:1. The feed to catalyst ratio of 30:1 and 40:1 produced a very low liquid yield of 84.70 wt.% and 80.97 wt.%, respectively (Table 5.6). It may be due to the low active sites of catalyst available in comparison to feed at very high feed to catalyst ratio. Although, active sites are high for the very low feed to catalyst ratio of 10:1, the reactant is not sufficient to produce high liquid yield (Gaurh and Pramanik, 2020, Verma et al., 2022). Thus, the liquid yield of 77.64 wt.% was obtained at a feed to catalyst ratio of 10:1. It is also seen from the Table 5.6 that the solid residue obtained was lowest (0.62 wt.%) for the feed to catalyst ratio of 20:1, and it may be due to the highest conversion of WEPS to liquid yield and gaseous yield in total. It should be noted that the lowest gaseous yield of 11.33 wt.% was obtained at the feed to catalyst ratio of 20:1. The optimum feed to catalyst ratio of 20:1was found to be 20:1 for the WEPS catalytic pyrolysis.

Table 5.6 Product yield of A-type/liquid phase catalytic pyrolysis at 600 ^{o}C and 15 ^{o}C/min using varying feed to catalyst ratio using ZSM-5 ammonium powder catalyst.

Feed to catalyst ratio	Liquid yield (wt.%)	Gaseous yield (wt.%)	Solid yield (wt.%)
10:1	77.64	19.4	2.96
20:1	88.05	11.33	0.62
30:1	84.7	13.93	1.37
40:1	80.97	17.76	1.27

5.3.1.1.2 Effect of temperature and holding time

The effect of temperature on liquid and solid yield at zero hold time and effect of hold time on product yield was determined for the liquid phase/A-type pyrolysis, vapour phase/B-type and

multiphase/AB-type catalytic pyrolysis using ZSM-5 ammonium powder catalyst. The effect of temperature and holding time on liquid and solid yield for A-type catalytic pyrolysis is shown in Figure 5.8(a-b). However, the effect of temperature and holding time on liquid and solid yield for B-type and AB-type catalytic pyrolysis are given in Appendix A3.

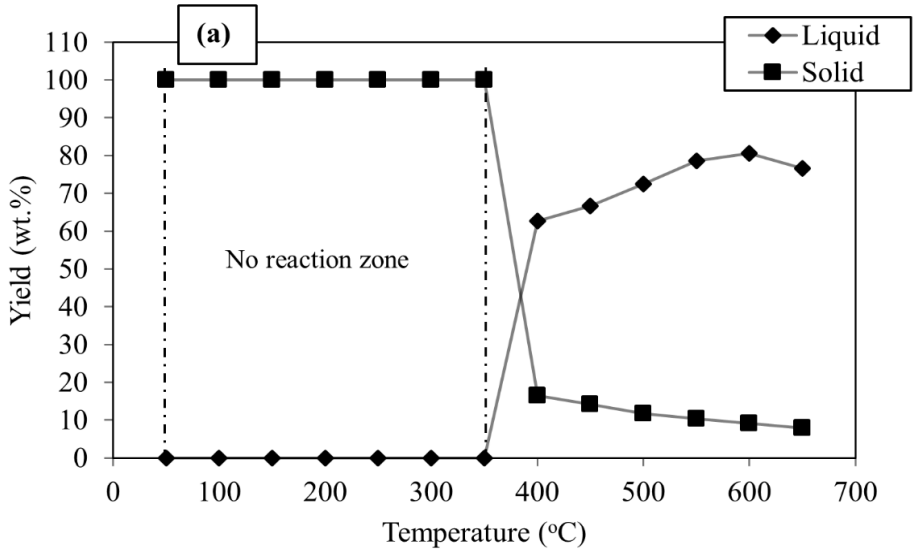

Figure 5.8a Effect of temperature on liquid and solid yield for liquid phase catalytic/A-type pyrolysis at 15 °C/min heating rate and zero hold time using ZSM-5 ammonium powder catalyst.

It is seen from the Figure 5.8a there is no decomposition of WEPS up to temperature 350 °C and thus, product yield/liquid yield is zero. However, beyond the temperature 350 °C, the reaction starts and highest liquid yield of 80.57 wt.% was obtained at a temperature of 600 °C for zero hold time (Figure 5.8a). Figure 5.8b shows that the effect of hold time on product yield. It is seen in the Figure 5.8b the liquid yield increases with the increase in hold time up to 30 min. However, liquid yield remains constant beyond the hold time of 30 min, as there is no molecules left over for further suitable conversion. The highest liquid yield of 88.05 wt.% was obtained for the hold time of 30 min (Figure 5.8b). Thus, the holding time of 30 min was

considered as the optimum time of pyrolysis at the respective reaction temperature to maintain the reaction temperature for the production of maximum liquid yield (Figure 5.8b).

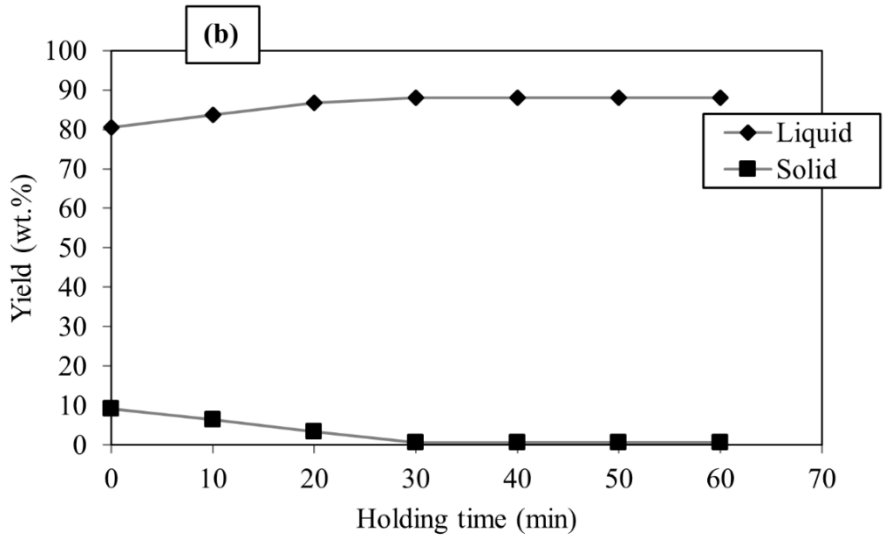

Figure 5.8b Effect of holding time on liquid and solid yield for liquid phase catalytic/A-type pyrolysis at 15 ^{o}C/min and 600 ^{o}C using ZSM-5 ammonium powder catalyst.

5.3.1.1.3 Effect of heating rate

Figure 5.9 shows the effect of heating rate on the product yield obtained from the catalytic pyrolysis i.e., liquid phase/A-type, vapour phase/B-type and multiphase/AB-type for the varying heating rates ranging from 5 ^{o}C/min to 25 ^{o}C/min at the fixed pyrolysis temperature of 550 ^{o}C using ZSM-5 ammonium powder catalyst. The optimum feed to catalyst ratio of 20:1 and holding time of 30 min were maintained for the study of heating rate on product yield. It is seen from the Figure 5.9 that the liquid yield is always lower for the catalytic pyrolysis of all reactor arrangements in comparison to that of thermal pyrolysis irrespective of magnitude of heating rates. It may be due to a more selective process i.e., catalytic pyrolysis which produces low molecular weight hydrocarbons. Thus, the gaseous yield is relatively high and liquid yield obtained is low in comparison to thermal pyrolysis (Kunwar et al., 2016; Miandad et al., 2017). However, the liquid yield increases with the increase in heating rate up to 15

°C/min and a further increase in heating rate beyond 15 °C/min, the liquid yield decreases for all three types of reactor arrangements i.e., A-type, B-type and AB-type. It is seen from the Figure 5.9 that the maximum liquid yield of 82.73 wt.%, 78.85 wt.% and 75.11 wt.% were obtained at the heating rate of 15 °C/min for the A-type, B-type, and AB-type reactor arrangements, respectively. Whereas, liquid yield of 80.51 wt.%, 73.33 wt.% and 71.07 wt.% were obtained at the heating rate of 20 °C/min for the A-type, B-type and AB-type reactor arrangements, respectively.

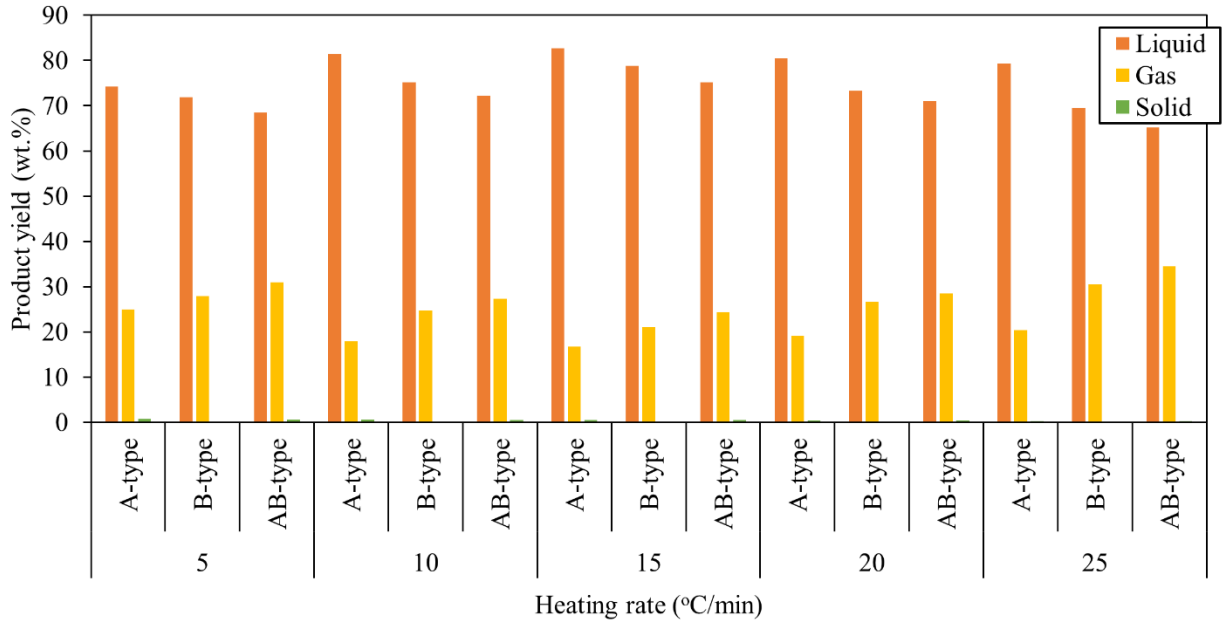

Figure 5.9 Effect of heating rate on product yield obtained from catalytic pyrolysis i.e., A-type, B-type and AB-type at a temperature of 550 °C using ZSM-5 ammonium powder catalyst.

At low heating rates of 5 °C/min and 10 °C/min, the gaseous yield was recorded high because, under slower heating rates, hydrocarbon molecules remained within the reactor at the set temperature for a longer duration which favours the formation of gaseous molecules (Aboulkas et al., 2012). The maximum liquid yield was obtained at the heating rate of 15 °C/min for all types of catalytic pyrolysis i.e., A-type, B-type and AB-type. It may be due to the selective

decomposition of relatively higher molecular weight hydrocarbon molecules which, favours the formation of mainly liquid range hydrocarbons. Beyond the heating rate of 15 ^{o}C/min the decreasing trend of liquid yield was observed and it may be due to the β-scission reaction at higher heating rate, which favours the formation of more gaseous molecules **(**Sundararajan and Bhagavathi, 2016). It should be noted that the optimum heating rate of 15 ^{o}C/min was also recorded for the thermal pyrolysis. However, the liquid yield of 91.69 wt.% was obtained for thermal pyrolysis at this heating rate.

5.3.1.1.4 Effect of temperature

Figure 5.10 shows the effect of temperature on the product yield for the catalytic pyrolysis of WEPS using ZSM-5 ammonium powder catalyst at a various temperatures ranging from 400 ^{o}C to 700 ^{o}C with an interval of 50 ^{o}C at the optimum heating rate of 15 ^{o}C/min and feed to catalyst ratio of 20:1. It is seen from Figure 5.10 that the liquid yield increases with the increase in reaction temperature up to 600 ^{o}C for A-type and temperature up to 550 ^{o}C for AB-type and B-type, respectively. Beyond these temperatures 600 ^{o}C (for A-type) and 550 ^{o}C (for B-type and AB-type), the liquid yield decreases surprisingly. The maximum liquid yield of 88.05 wt.% was obtained at the temperature of 600 ^{o}C for A-type/liquid phase catalytic pyrolysis. Interestingly, B-type/vapour phase and AB-type/multiphase catalytic pyrolysis produced liquid yield of 78.85 wt.% and 75.11 wt.% at the same temperature of 550 ^{o}C. It should be noted that the optimum reaction temperature to achieve the highest liquid yield is low for the catalytic pyrolysis of all types i.e., A-type (600 ^{o}C), B-type (550 ^{o}C) and AB-type (550 ^{o}C) in comparison to that of thermal pyrolysis (650 ^{o}C). Even comparison among all three types of reactor arrangements during catalytic pyrolysis shows that B-type/vapour phase and AB-

type/multiphase need lower temperature (550 ^{o}C) to achieve maximum liquid yield than the A-type/liquid phase catalytic pyrolysis (600 ^{o}C). It is well established that the catalytic pyrolysis needs low temperature in comparison to thermal pyrolysis and the catalytic pyrolysis provides the reaction route with low activation energy and selective products (Panda et al., 2010). Table 5.7 shows the quantitative values of products yield with the key product i.e., liquid yield obtained at the optimum temperature condition of various reactor arrangements.

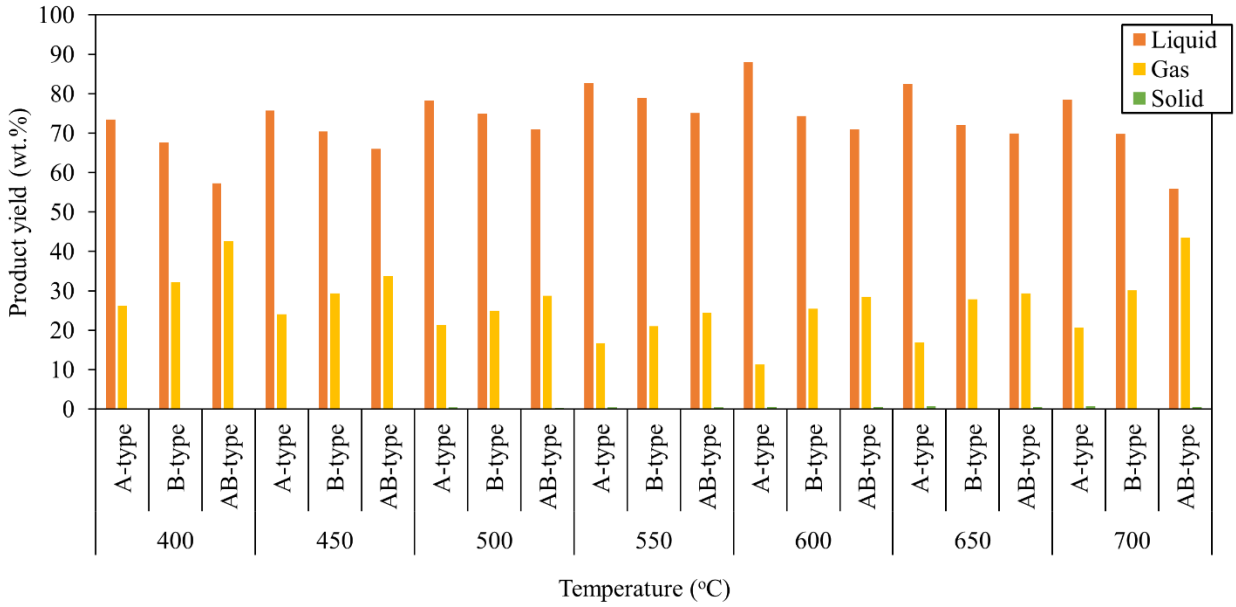

Figure 5.10 Effect of temperature on product yield obtained from catalytic pyrolysis i.e., A-type, B-type and AB-type at a heating rate of 15 ^{o}C/min using ZSM-5 ammonium powder catalyst.

It is seen from the quantitative analysis of products obtained by the catalytic pyrolysis in three types of reactor arrangements that the amount of liquid yield decreases in this order A-type > B-type > AB-type of reactor arrangements (Table 5.7). Although, liquid yield decreases as per the order showed above for the reactor arrangements, the gaseous yield increases in the order of A-type < B-type < AB-type. It means the highest gaseous yield is obtained for the AB-type/multiphase and lowest for the A-type/liquid phase reactor arrangements. It may be due to

the presence of catalyst ZSM-5 in liquid and vapour phase both for AB-type/multiphase pyrolysis. The interaction of the reactants with the catalyst particles take place in two stages i.e., the interaction of WEPS with ZSM-5 at liquid phase in primary reactor i.e., stage one which will results in the formation of fuel range hydrocarbon molecules with low amount of gaseous fractions as observed in A-type/liquid phase reactor arrangements.

Table 5.7 Product yield obtained from catalytic pyrolysis of WEPS using various reactor arrangements at optimum temperature and heating rate of 15^{o}C/min using ZSM-5 ammonium powder catalyst.

Reactor arrangement	Optimum temperature (^{o}C)	Liquid yield (wt.%)	Gaseous yield (wt.%)	Solid yield (wt.%)
A-type/liquid phase	600	88.05	11.33	0.62
B-type/vapour phase	550	78.85	21.07	0.08
AB-type/multiphase	550	75.11	24.40	0.49

In the second stage, hydrocarbon vapour coming of relatively larger molecular weight molecules escape through the catalytic bed placed in the secondary reactor (Figure 3.5a-b, page no. 51) fitted at the neck of the primary reactor as shown in Figure 3.4c-d (page no. 50) and thereby further catalytic cracking reaction of the liquid range hydrocarbon will takes place along with aromatization of paraffins (Seo et al., 2003). Obviously, two-stage catalytic cracking will enhance gaseous yield and reduce liquid yield with improved quality as seen in AB-type/multiphase reactor arrangement. It should be noted that AB-type/multiphase pyrolysis produced little low liquid yield 75.11 wt.% in comparison to thermal and catalytic pyrolysis of other types of arrangements i.e., A-type and B-type. The reactor arrangement of vapour phase/B-type produced liquid yield of 78.85 wt.% which is in between the liquid

phase/A-type and multiphase/AB-type reactor arrangements. In the B-type pyrolysis, purely thermal pyrolysis is takes place at the primary reactor followed by vapour phase catalytic pyrolysis of hydrocarbon molecules produced by random cracking by thermal pyrolysis only in the first stage. It gives more gaseous range hydrocarbon molecules than A-type. Thus, the liquid yield is little lower than the A-type. Irrespective of the reactor arrangements used in the catalytic pyrolysis, solid yield is always low except for the A-type/liquid phase pyrolysis (0.62 wt.%). It may be due to the re-polymerization of the hydrocarbon molecules in the liquid phase/A-type. It is clearly seen from the Figure 5.10 and Table 5.7, the solid of 0.62 wt.%, 0.08 wt.% and 0.49 wt.% were obtained for the reactor arrangement A-type, B-type and AB-type, respectively.

5.3.1.2 Analysis of pyrolysis oil obtained using ZSM-5 ammonium powder catalyst

5.3.1.2.1 Estimation of aromatic content/BTE and styrene in pyrolysis oil

The qualitative evaluation of pyrolysis oil is very much essential to determine the highest BTE content in the liquid yield obtained at the optimized condition. Thus, the calibration characteristics were plotted to measure the extent of enhancement benzene, toluene, and ethylbenzene (BTE) and reduction of styrene in liquid yield after incorporation of ZSM-ammonium powder catalyst using different reactor arrangements at various temperature conditions. The calibration characteristics have already been plotted in the chapter 3 (page no. 59) for the estimation of weight percent of individual target aromatic hydrocarbon molecules viz., benzene, toluene, ethylbenzene and styrene, as a function of their % peak area under the curve. The BTE content of all liquid yields obtained at different pyrolysis temperatures ranging

from 400 ºC to 700 ºC are presented in Table 5.8, which are being produced may be due to the reaction mechanism as proposed in Figure 2.10 (chapter-2).

Table 5.8 Product yield and BTE content obtained from catalytic pyrolysis of WEPS in the temperature range of 400-700 ºC at 15 ºC/min heating rate using ZSM-5 ammonium powder catalyst.

Pyrolysis temperature (ºC)	Reactor arrangement	Liquid (wt.%)	Gas (wt.%)	Benzene (wt.%)	Toluene (wt.%)	Ethylbenzene (wt.%)	Styrene (wt.%)	Total BTE (wt.%)
400	A-type	73.52	26.29	0.15	5.09	0.41	85.33	5.65
	B-type	67.69	32.12	0.22	5.52	0.70	83.29	6.44
	AB-type	57.27	42.63	2.09	6.75	1.74	77.72	10.57
450	A-type	75.74	24.02	0.92	7.67	0.63	79.25	9.22
	B-type	70.43	29.39	1.56	7.76	0.84	78.02	10.16
	AB-type	65.99	33.84	3.02	10.08	2.96	67.55	16.06
500	A-type	78.29	21.27	1.70	8.41	1.48	74.40	11.60
	B-type	74.98	24.91	4.12	10.05	2.19	63.61	16.36
	AB-type	70.88	28.81	8.10	10.92	3.03	50.80	22.04
550	A-type	82.73	16.77	3.32	8.91	2.23	56.13	14.47
	B-type	**78.85**	**21.07**	**10.13**	**10.14**	**4.00**	**46.42**	**24.28**
	AB-type	**75.11**	**24.4**	**11.68**	**12.18**	**4.26**	**46.30**	**28.12**
600	**A-type**	**88.05**	**11.33**	**5.56**	**12.10**	**1.32**	**55.78**	**18.98**
	B-type	74.41	25.51	7.68	10.12	2.39	51.93	20.18
	AB-type	70.92	28.51	10.83	11.01	3.80	43.33	25.64
650	A-type	82.46	16.84	4.27	9.59	1.07	46.25	14.94
	B-type	72.1	27.82	5.43	10.08	2.23	42.81	17.74
	AB-type	69.95	29.43	10.04	10.70	3.72	41.11	24.46
700	A-type	78.57	20.68	1.47	8.30	0.72	41.85	10.49
	B-type	69.83	30.1	4.39	8.54	1.09	39.92	14.02
	AB-type	55.88	43.48	8.78	9.31	3.68	39.36	21.76

As, the reduction of styrene and increasing BTE content in liquid yield are the main aim of the present study, thus the process temperature were optimized in terms of composition and liquid yield both. It is seen from the Table 5.8 that the liquid yield of AB-type pyrolysis oil is lowest (75.11 wt.%) in comparison to B-type (78.85 wt.%) and A-type (88.05 wt.%) at their optimum condition. However, the qualitative analysis shows that the BTE content is highest (28.12

wt.%) for AB-type pyrolysis with highest individual constituents benzene, toluene and ethylbenzene of 11.68 wt.%, 12.18 wt.% and 4.26 wt.%, respectively. While, liquid phase/A-type and vapour phase/B-type produced BTE content of 18.98 wt.% and 24.27 wt.%, respectively. The styrene content was lowest (46.30 wt.%) in the liquid yield of AB-type/multiphase pyrolysis. The reason for increase in BTE content and reduction in styrene content in the liquid yield of multiphase/AB-type pyrolysis may be due to the cracking and hydrogenation of hydrocarbon molecules via two stage catalytic process i.e., first stage where WEPS gets degraded to hydrocarbon molecules of wide range molecular weight mainly aromatics, styrene and BTE as noticed in the A-type/liquid phase pyrolysis followed by second stage catalytic reaction in the vapour phase where styrene get converted to ethylbenzene, toluene and ethylbenzene. Thus, multiphase/AB-type pyrolysis produced 2.23 times more ethylbenzene than A-type pyrolysis. On the other hand, vapour phase/B-type pyrolysis which also takes place in two steps i.e., thermal pyrolysis in the liquid phase without catalyst followed by catalytic pyrolysis of hydrocarbon molecules in the vapour phase in the second stage. Thus, ethylbenzene is higher (4 wt.%) in B-type pyrolysis than the A-type/liquid phase pyrolysis (1.32 wt.%) (Park et al., 2020). The thermal pyrolysis produced very low BTE content of 11.38 wt.% of and highest styrene content of 84.74 wt.% because of non-selective cracking (Table 5.3, page no. 78). It should be noted that although multiphase/AB-type pyrolysis gives low amount of liquid yield (78.85 wt.%) than thermal pyrolysis (94.37 wt.%), the quality of the AB-type liquid yield is excellent as it contains very low styrene (46.30 wt.%) and high amount BTE (28.12 wt.%). Thus, the liquid oil obtained from AB-type catalytic pyrolysis is expected to give better physicochemical properties which are suitable for the use in generator set and cooking stoves.

The comparison of GC characteristics obtained for the liquid yield of catalytic pyrolysis of A-type, B-type and AB-type at the optimum conditions is shown in Figure 5.11a.

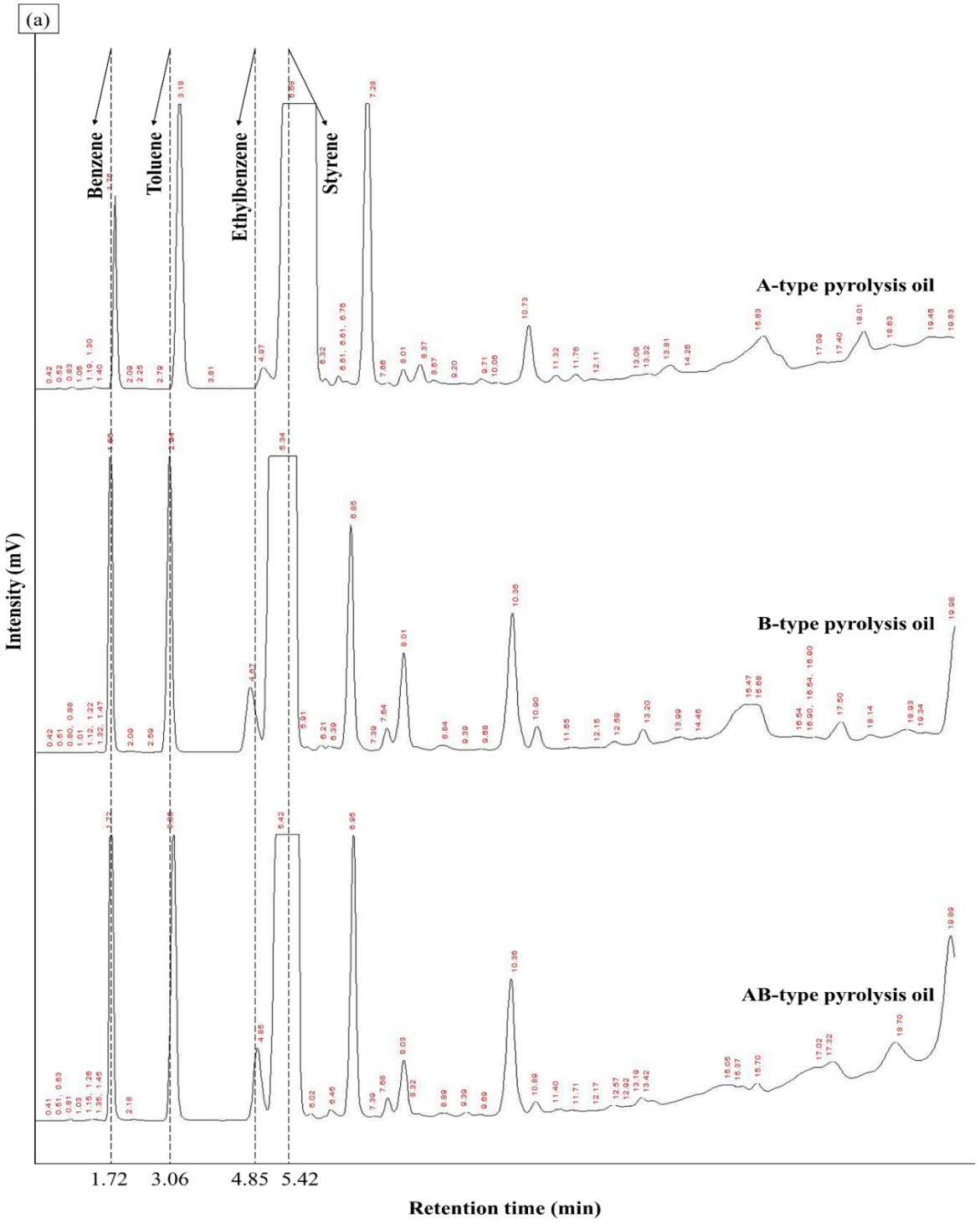

Figure 5.11a Gas chromatographs of catalytic pyrolysis oil A-type, B-type, and AB-type obtained at optimum conditions using ZSM-5 ammonium powder catalyst.

The target aromatic hydrocarbons mainly BTE and styrene are highlighted with markers. The key reaction pathways involved in the formation of benzene, toluene, ethylbenzene (BTE) and styrene during catalytic pyrolysis of waste expanded polystyrene (WEPS) (Verma et al., 2021; Ojha and Vinu, 2015) are presented in Figure 2.10 (Chapter 2, page no. 36). The catalytic cracking of polystyrene starts from either the aromatic ring or the aliphatic chain. However, aliphatic chain is more easily attacked by protons from Brønsted acid sites. The double bond in the aromatic ring is difficult to attack by Brønsted acid sites since it is more stable and sterically hindered, indicating higher dissociation energy and sufficient contact time between polystyrene and zeolites are required. Thus, slightly higher temperature (550 ^{o}C) provides the dissociation energy and *in-situ* mode improves the diffusion efficiency by enhancing the contact between catalyst and feed, which favoured the attack of aromatic double bonds by the surface-active sites in zeolites to produce more targeted aromatic hydrocarbons i.e., benzene, toluene and ethylbenzene (Wang et al., 2019). It is also seen in Figure 5.11a, that all four major aromatic hydrocarbons (BTE) and styrene are present in all types of catalytic pyrolysis oil. However, the intensity of peaks for styrene gradually decreases for the liquid yield depending on the type of pyrolysis in the order of A-type > B-type > AB-type. Lower peak intensity indicates low styrene in the liquid yield and thus, a better quality of the liquid oil. On the other hand, the peak of ethylbenzene, which is one of the important fuel component or octane number improver increases with the type of pyrolysis applied in the following order: A-type < B-type < AB-type. The ethylbenzene is formed either by the styrene dimer cracking or by the styrene hydrogenation through hydrogen transfer reaction (Marczewski et al., 2013). Similarly, the peak intensity of toluene and benzene are highest for the AB-type catalytic pyrolysis and it may be due to the cyclization of protonated styrene dimer which formed by the attack by

protons from Bronsted acid sites on aliphatic chain followed by cracking (Wang et al., 2019) during the two-stage multiphase catalytic pyrolysis in AB-type reactor arrangement. It is well known that the lower aromatics benzene, toluene and ethylbenzene (BTE) improve the octane number of gasoline fuel (Shim et al., 2006; Wang et al., 2014). However, the amount of benzene should be less than 1 wt.% (Gaurh and Pramanik, 2018a) to avoid the carbon deposition in the IC engines. Thus, benzene should be removed from the pyrolysis oil before it is used in IC engines for better performance of the engine. The comparison of GC characteristic of AB-type catalytic pyrolysis oil and commercial fuel mainly gasoline and kerosene is shown in the Figure 5.11b.

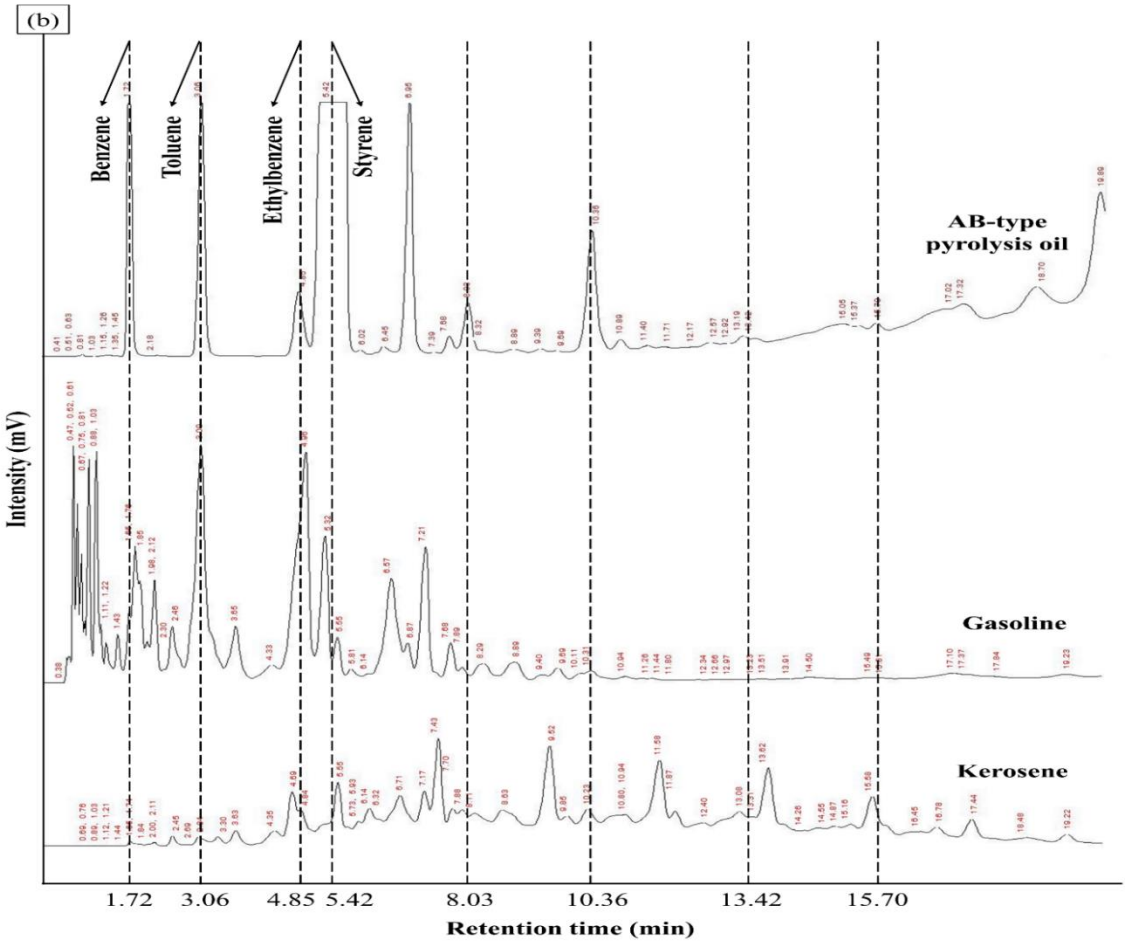

Figure 5.11b Comparison of gas chromatographs of AB-type catalytic pyrolysis oil obtained using ZSM-5 ammonium powder at optimized conditions with commercial gasoline and kerosene.

It is clearly seen from the Figure 5.11b that most of the aromatic components of AB-type pyrolysis match with gasoline fuel and to some extent kerosene as well up to retention time of 6 min. However, beyond the retention time of 6 min, most of the hydrocarbon molecules of AB-type pyrolysis matches with kerosene (Figure 5.11b).

5.3.1.2.2 FTIR analysis of pyrolysis oil

The FTIR is an important analytical technique for detecting the functional groups in the pyrolysis oil. Figure 5.12 shows the FTIR spectra of all types of catalytic pyrolysis oil obtained at their respective optimum conditions i.e., heating rate of 15 ^{o}C/min and temperature of 600 ^{o}C for liquid phase/A-type pyrolysis and 550 ^{o}C for vapour phase/B-type and multiphase/AB-type pyrolysis of WEPS using ZSM-5 ammonium powder as a catalyst.

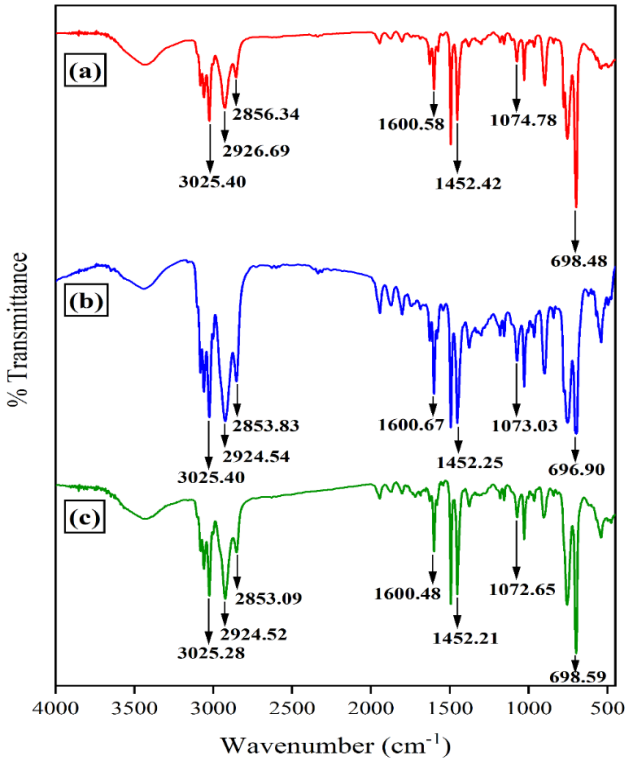

Figure 5.12 FTIR spectra of catalytic pyrolysis oil obtained at optimum conditions using ZSM-5 ammonium powder catalyst (a) A-type/liquid phase, (b) B-type/vapour phase and (c) AB-type/multiphase.

The functional groups obtained from the FTIR spectrum for the pyrolysis oil obtained different types of reactor arrangements at optimum condition are shown in Table 5.9. The vibrations at wavenumber of 3025.40 cm^{-1}, 3025.40 cm^{-1} and 3025.28 cm^{-1} were obtained due to the aromatic stretching for A-type, B-type and AB-type catalytic pyrolysis oil, respectively (Budsaereechai et al., 2019). The C=C-C aromatic ring stretching vibrations were observed at wavenumber of 1600.58 cm^{-1}, 1600.67 cm^{-1} and 1600.48 cm^{-1} for A-type, B-type and AB-type pyrolysis oil, respectively.

Table 5.9 Functional groups present in the pyrolysis oil obtained at optimum conditions using ZSM-5 ammonium powder catalyst.

Functional group	**Wavelength (cm^{-1})**			
	Standard finger print region	**A-type/liquid phase pyrolysis oil**	**B-type/vapour phase pyrolysis oil**	**AB-type/multiphase pyrolysis oil**
Aromatic C-H stretching	Above 3000	3081.75, 3059.25, 3025.40	3081.95, 3059.58 3025.40	3081.64, 3059.23, 3025.28
Methylene C-H asy/sym stretching	2935-2915/2865-2845	2926.69, 2856.34,	2924.54, 2853.83	2924.52, 2853.09
C=C-C aromatic ring stretch	1615-1580	1600.58	1600.67, 1582.89	1600.48
C=C-C aromatic ring stretch	1510-1450	1494.09	1493.61	1493.38
Methyl C-H asy/sym bend	1470-1430/1380-1370	1452.42, 1379.67	1452.25, 1377.23	1452.21, 1376.30
Aromatic C-H in plane bend	1225-950	1179.99, 1155.54, 1074.78	1180.50, 1154.97, 1073.03	1180.34, 1154.99, 1072.65
Cyclohexane ring vibrations	1055-1000/1005-925	1028.79, 964.97	1028.69, 964.61	1028.68, 964.88
Aromatic C-H out plane bending	860-680	777.71, 753.98, 698.48	841.94, 753.11, 696.90	841.95, 755.51, 698.55

The peaks obtained at wavenumber of 1179.99 cm^{-1}, 1180.50 and 1180.34 cm^{-1} were found for the aromatic C-H in plane bending vibration for liquid phase/A-type, vapour phase/B-type and multiphase/AB-type pyrolysis oil, respectively. However, cyclohexane ring vibrations were confirmed by the peaks obtained at 1028.79 cm^{-1}, 1028.69 cm^{-1}, 1028.68 cm^{-1}. The aromatic C-H out of plane bending vibrations were also confirmed by the peaks obtained at wavenumber of 777.71 cm^{-1}, 841.94 cm^{-1}, and 841.95 cm^{-1}, respectively (Coates, 2006).

5.3.1.2.3 Physicochemical properties of pyrolysis oil

The physicochemical properties such as calorific value, carbon residue, and flash and fire point were determined for the all types of catalytic pyrolysis oil obtained at optimum conditions i.e., heating rate of 15 ^oC/min for all types of pyrolysis and temperature of 600 ^oC for A-type/liquid phase pyrolysis and 550 ^oC for B-type/vapour phase and AB-type/multiphase pyrolysis, respectively. The calorific value, carbon residue and flash and fire point of all types of pyrolysis oil obtained at optimum conditions were compared with standard gasoline and kerosene for applications in IC engine and as a fuel oil for cooking stoves (Table 5.10). It is seen from Table 5.10, gross calorific value (GCV) of AB-type/multiphase pyrolysis oil was highest (12685.3 Cal/g), even higher than the commercial gasoline (11315 Cal/g) and kerosene (11052 Cal/g) (Gaurh and Pramanik, 2019) it may be due to the presence of low boiling hydrocarbon molecules. Thus, AB-type/multiphase pyrolysis oil could be a better replacement of fuel oil for IC engine and cooking stoves. It is also seen from the Table 5.10, the carbon residue of catalytic pyrolysis oil lie in the range between 0.6 and 0.99. Among all pyrolysis oil, AB-type/multiphase pyrolysis oil produced a lowest carbon residue of 0.6 wt.% which is

lower than the percentage limit (1 wt.%) (Gaurh and Pramanik, 2019). Thus, pyrolysis oil of AB-type has very less tendency towards the deposition of carbon in IC engines.

Table 5.10 Physicochemical properties of catalytic pyrolysis oil obtained at optimum conditions using ZSM-5 ammonium powder catalyst with standard commercial fuel gasoline and kerosene.

Physicochemical properties	Thermal	catalytic pyrolysis oil			Commercial fuels	
		A-type	B-type	AB-type	Gasoline	Kerosene
Gross calorific value (Cal/g)	9816	9945	10972	12685	11315	11052
Carbon residue (wt.%)	1.01	0.99	0.9	0.6	0.14	0.18
Flash point (^oC)	58	50	44	38	22	42
Fire point (^oC)	62	56	48	42	25	45

A fuel considered as highly flammable if it has flash point less than 60 ^oC (Wang et al., 1964). Thus, all types of catalytic pyrolysis oil comes under the category of flammable liquid fuel. Noticeably, pyrolysis oil of AB-type has the lowest flash point of 38 ^oC and fire point of 42 ^oC which are close to commercial gasoline (Mukhraiya and Yadav, 2015) and kerosene (Ahmad et al., 2017). Thus, pyrolysis oil of AB-type/multiphase can be recommended for IC engine mainly diesel generator set or as a fuel oil for cooking stoves.

5.3.2 Catalytic pyrolysis using Nickel on silica-alumina as catalyst

5.3.2.1 Effect of process parameters on product yield

5.3.2.1.1 Effect of feed to catalyst ratio

The effect of feed to catalyst ratio on the product yield obtained from A-type, B-type and AB-type catalytic pyrolysis were determined at a pyrolysis temperature of 600 ^oC and heating rate

of 15 ^{o}C/min for different feed to catalyst ratio of 10:1, 20:1, 30:1 and 40:1. Figure 5.13 shows the effect of feed to catalyst ratio on product yield obtained from liquid phase/A-type catalytic pyrolysis of WEPS using nickel on silica-alumina catalyst. Although, the effect of feed to catalyst ratio on product yield for B-type and AB-type catalytic pyrolysis are shown in Appendix A4. It is seen from the Figure 5.13 that the liquid yield increases with the increase in feed to catalyst ratio up to 20:1 and beyond 20:1 the liquid yield decreases. Thus, the highest liquid yield of 88.54 wt.% was obtained at the feed to catalyst ratio of 20:1 for A-type catalytic pyrolysis using Nickel on silica-alumina catalyst. It may be due to the higher active sites of catalyst available for the interaction with the reactant as already been discussed in page no. 85.

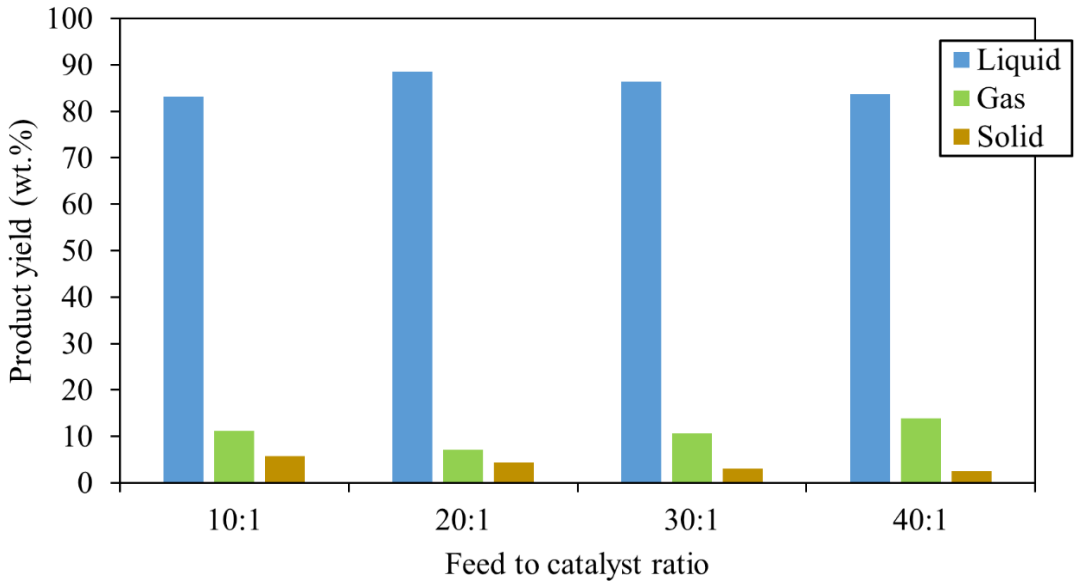

Figure 5.13 Effect of feed to catalyst ratio on product yield of liquid phase/A-type catalytic pyrolysis at 600 ^{o}C and heating rate of 15 ^{o}C/min using Nickel on silica-alumina catalyst.

The feed to catalyst ratio of 30:1 and 40:1 obtained a very low liquid yield of 86.32 wt.% and 83.65 wt.%, respectively. As it is already discussed earlier (page no. 86), at very low feed to catalyst ratio, the reactant is not sufficient to obtain the high liquid yield (Gaurh and Pramanik, 2020). Thus, the liquid yield of 83.11 wt.% was obtained at a feed to catalyst ratio of 10:1.

It is also seen from the Table 5.11 that the solid residue of 4.42 wt.% was obtained at feed to catalyst ratio of 20:1. Whereas, the lowest gaseous yield of 7.04 wt.% was obtained for A-type catalytic pyrolysis using Nickel on silica-alumina catalyst.

Table 5.11 Effect of feed to catalyst ratio on product yield of liquid phase/A-type catalytic pyrolysis at 600 ^{o}C and heating rate of 15 ^{o}C/min using Nickel on silica-alumina catalyst.

Feed to catalyst ratio	Liquid (wt.%)	Gas (wt.%)	Solid (wt.%)
10:1	83.11	11.14	5.75
20:1	88.54	7.04	4.42
30:1	86.32	10.61	3.07
40:1	83.65	13.81	2.54

5.3.2.1.2 Effect of temperature and holding time on liquid and solid yield

The effect of temperature on liquid and solid yield at zero hold time and effect of hold time on product yield were determined for liquid phase/A-type pyrolysis, vapour phase/B-type and multiphase/AB-type catalytic pyrolysis using Nickel on silica-alumina catalyst. The effect of temperature and holding time on liquid and solid yield for A-type catalytic pyrolysis is shown in Figure 5.14(a-b). However, the effect of temperature and holding time on liquid and solid yield for B-type and AB-type catalytic pyrolysis are given in Appendix A5.

Figure 5.14a shows the effect of temperature on the product yield at a heating rate of 15 ^{o}C/min and zero hold time. It is seen from the Figure 5.14a there is no conversion of WEPS up to reaction temperature of 350 ^{o}C. However, beyond the reaction temperature of 350 ^{o}C the liquid yield increases with the increase in temperature up to 600 ^{o}C. Thus, the highest liquid yield of 81.14 wt.% was obtained at a reaction temperature of 600 ^{o}C and zero hold time for A-type catalytic pyrolysis (Figure 5.14a).

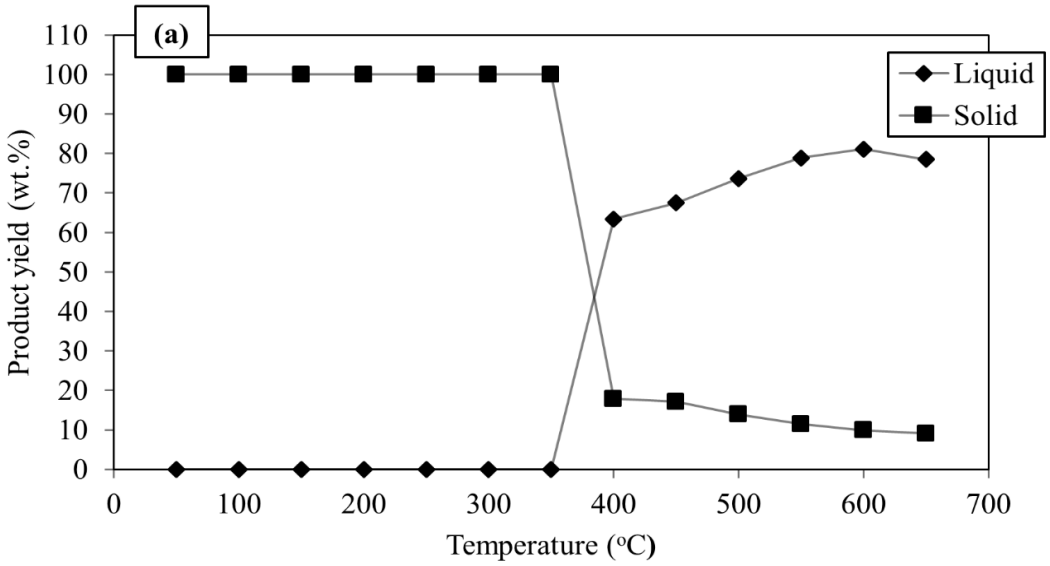

Figure 5.14a Effect of temperature on liquid and solid yield for liquid phase catalytic/A-type pyrolysis at 15 °C/min heating rate and zero hold time using Nickel on silica-alumina catalyst.

Figure 5.14b shows the effect of holding time on product yield at a reaction temperature of 600 °C. It is seen from Figure 5.14b that the liquid yield increases with the increase in holding time up to 30 min. However, liquid yield remains constant beyond the holding time of 30 min, as there is no molecules left over for further suitable conversion as already discussed earlier (page no. 87).

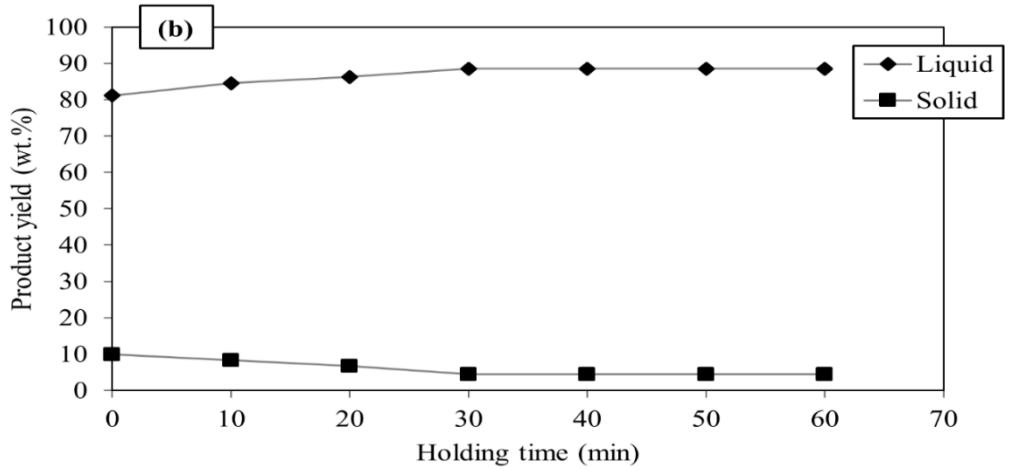

Figure 5.14b Effect of holding time on liquid and solid yield for liquid phase catalytic/A-type pyrolysis at 15 °C/min and 600 °C using Nickel on silica-alumina catalyst.

The highest liquid yield of 88.54 wt.% was obtained for the holding time of 30 min. Thus, the hold time of 30 min was considered as the optimum hold time of pyrolysis reaction. It should be noted that the optimum hold time of 30 min was also recorded for the catalytic pyrolysis using ZSM-ammonium powder catalyst. The liquid yield of 88.05 wt.% was obtained for the catalytic pyrolysis using ZSM-5 ammonium powder at a holding time of 30 min.

5.3.2.1.3 Effect of heating rate

The effect of heating rate on product yield obtained from catalytic pyrolysis i.e., A-type, B-type, and AB-type using Nickel on silica-alumina catalyst was determined at the varying heating rate ranging from 5 ^{o}C/min to 25 ^{o}C/min, pyrolysis temperature of 550 ^{o}C, optimum feed to catalyst ratio of 20:1 and holding time of 30 min. Figure 5.15 shows the effect of heating rate on product yield obtained from catalytic pyrolysis using nickel on silica-alumina catalyst. It is seen from the Figure 5.15 that the liquid yield increases with increase in heating rate up to 15 ^{o}C/min and beyond this heating rate, liquid yield get decreases for all types of catalytic pyrolysis. At low heating rates of 5 ^{o}C/min and 10 ^{o}C/min, the gaseous yield was recorded very high because, under slower heating rates, molecules remained within the reactor at the set temperature for a longer duration as already discussed in page no. 89. The A-type, B-type and AB-type pyrolysis produced very low liquid yield of 69.82 wt.%, 67.44 wt.%, and 66.17 wt.%, respectively at a heating rate of 5 ^{o}C/min. The gaseous yield of 25.93 wt.%, 30.19 wt.%, and 30.92 wt.% were obtained from A-type, B-type and AB-type pyrolysis, respectively at the same heating rate of 5 ^{o}C/min. The highest liquid yield was obtained at the heating rate of 15 ^{o}C/min for all types of catalytic pyrolysis. It may be due to the selective decomposition of relatively

higher molecular weight hydrocarbon molecules which, favours the formation of liquid range hydrocarbons.

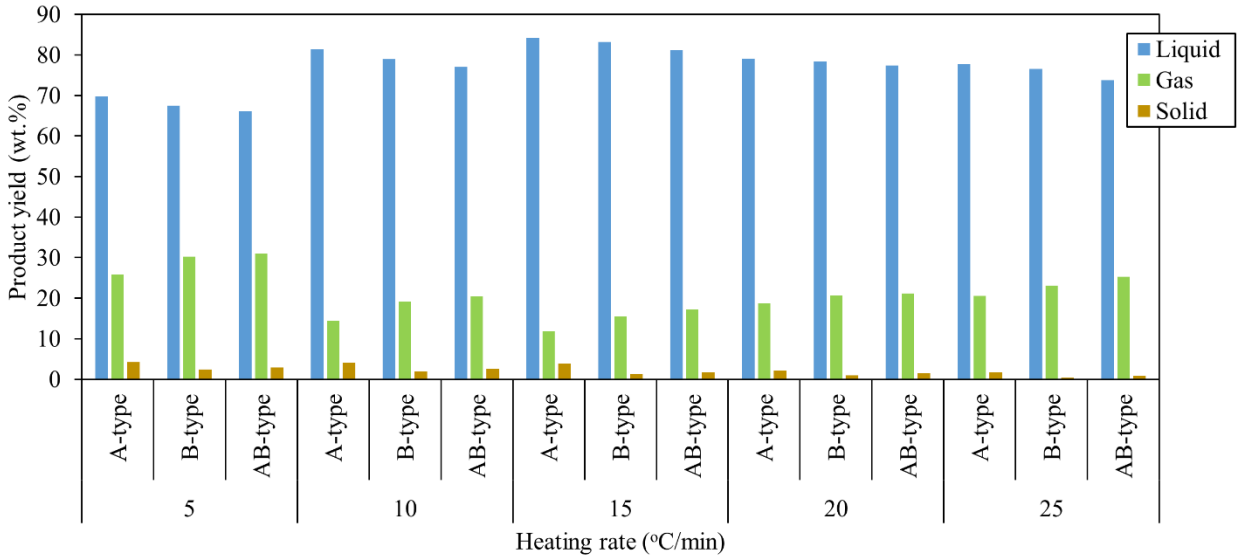

Figure 5.15 Effect of heating rate on product yield of catalytic pyrolysis i.e., A-type, B-type and AB-type at pyrolysis temperature of 550 °C using Nickel on silica-alumina catalyst.

The A-type, B-type and AB-type pyrolysis produced maximum liquid yield of 84.17 wt.%, 83.21 wt.%, and 81.15 wt.%, respectively at the heating rate of 15 °C/min. The gaseous yield of 11.89 wt.%, 15.50 wt.%, and 17.14 wt.% were obtained from A-type, B-type and AB-type catalytic pyrolysis, respectively at a heating rate of 15 °C/min. Beyond the heating rate of 15 °C/min the decreasing trend of liquid yield was observed and it may be due to the β-scission reaction at higher heating rate, which favours the formation of more gaseous molecules as already mentioned in page no. 90. The A-type, B-type and AB-type pyrolysis produced liquid yield of 79.06 wt.% 78.35 wt.%, and 77.40 wt.%, respectively and gaseous yield of 18.81 wt.%, 20.68 wt.%, 21.14 wt.%, respectively at the high heating rate of 20 °C/min.

It should be noted that the heating rate of 15 °C/min was also found to be optimum for the catalytic pyrolysis using ZSM- ammonium powder catalyst. The maximum liquid yield of

82.73 wt.%, 78.85 wt.% and 75.11 wt.% were obtained at the heating rate of 15 ºC/min for the A-type, B-type, and AB-type reactor arrangements, respectively using ZSM-5 ammonium powder catalyst.

5.3.2.1.4 Effect of temperature

The effect of temperature on product yield was obtained for catalytic pyrolysis i.e., A-type, B-type, and AB-type using varying temperature in the range of 400 ºC to 700 ºC, keeping the heating rate, holding time and feed to catalyst ratio at the optimum condition of 15 ºC/min, 30 min and 20:1, respectively using Nickel on silica-alumina catalyst (Figure 5.16).

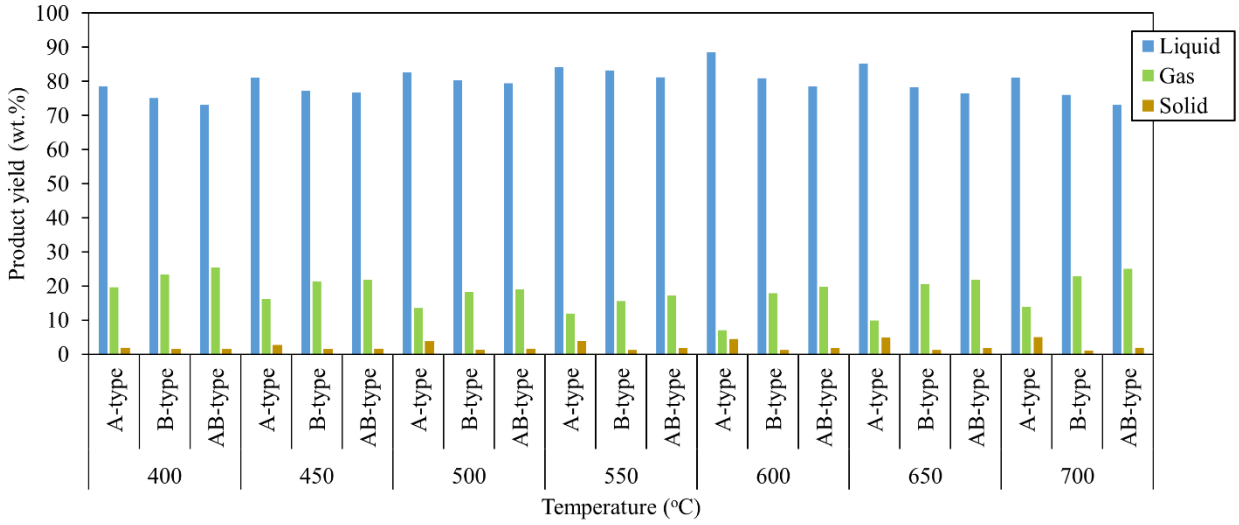

Figure 5.16 Effect of temperature on product yield for catalytic pyrolysis i.e., A-type, B-type and AB-type at a heating rate of 15 ºC/min using Nickel on silica-alumina catalyst.

It is seen from the Figure 5.16, the liquid yield increases with the increase in temperature up to 600 ºC for A-type catalytic pyrolysis. Beyond this temperature, the liquid yield decreases. It may be due to the cracking of C-C bonds at a higher temperature which increases the formation of gaseous range hydrocarbon molecules (Lopez et al., 2011b). The similar trend was also observed for the B-type and AB-type catalytic pyrolysis. The liquid yield increases

with the increase in temperature up to 550 ^{o}C for B-type and AB-type catalytic pyrolysis. It is also seen from the Figure 5.16 that the, maximum liquid yield of 88.54 wt.%, 83.21 wt.% and 81.15 wt.% were obtained for A-type at a temperature of 600 ^{o}C, B-type at a temperature of 550 ^{o}C, and for AB-type catalytic pyrolysis at a temperature of 550 ^{o}C, respectively. Moreover, among all types of pyrolysis, the AB-type catalytic pyrolysis always produced highest gaseous yield at each temperature due to the two stage catalytic contact of hydrocarbon molecules in liquid phase followed by selective vapour phase catalytic contact within the secondary reactor. Similarly, B-type catalytic pyrolysis also proceeds through multistage cracking i.e., in the first stage molecules cracked thermally in liquid phase without catalyst and then cracked hydrocarbon molecules passes through the catalytic bed installed in the secondary reactor as discussed earlier (page no. 92). Thus, the B-type catalytic pyrolysis produced little lower gaseous yield as compared to the AB-type catalytic pyrolysis. The AB-type and B-type pyrolysis produced gaseous yield of 17.14 wt.% and 15.50 wt.%, respectively at the optimum temperature of 550 ^{o}C. Whereas, A-type catalytic pyrolysis produced gaseous yield of 7.04 wt.% at the optimum temperature of 600 ^{o}C. The product yield obtained from all types of catalytic pyrolysis using Nickel on silica-alumina catalyst at their respective optimum temperature conditions are presented in Table 5.12.

Table 5.12 Product yield of catalytic pyrolysis at optimum temperature and heating rate of 15 ^{o}C/min using Nickel on silica-alumina catalyst.

Type of pyrolysis	Optimum temperature (^{o}C)	Liquid (wt.%)	Gas (wt.%)	Solid (wt.%)
Liquid phase/A-type	600	88.54	7.04	4.42
Vapour phase/B-type	550	83.21	15.50	1.29
Multiphase/AB-type	550	81.15	17.14	1.71

It should be noted that the, reaction temperature of 600 ^{o}C for A-type, 550 ^{o}C for B-type and AB-type was also found to be optimum for ZSM-5 ammonium powder catalyst. However, the liquid yield of 88.05 wt.%, 78.85 wt.% and 75.11 wt.% were obtained for A-type, B-type and AB-type catalytic pyrolysis using ZSM-5 ammonium powder catalyst.

5.3.2.2 Analysis of pyrolysis oil obtained using Nickel on silica-alumina catalyst

5.3.2.2.1 Estimation of aromatic content/BTE and styrene in pyrolysis oil

The qualitative analysis of pyrolysis oil obtained from catalytic pyrolysis is very much essential to determine its end use. In this context, the benzene, toluene and ethylbenzene (BTE) content were measured for the catalytic pyrolysis oil. The calibration characteristics (Figure 3.8, page no. 59) were used to measure the concentration of benzene, toluene, ethylbenzene (BTE) and styrene in the pyrolysis oil. The BTE and styrene content of pyrolysis oil obtained from catalytic pyrolysis i.e., A-type, B-type and AB- type at heating rate of 15 ^{o}C/min and at a temperature ranging from 400 ^{o}C to 700 ^{o}C is given in Table 5.13. It is clearly seen from the Table 5.13 that the pyrolysis oil contains maximum BTE content only at optimum temperature i.e., 600 ^{o}C, 550 ^{o}C and 550 ^{o}C for A-type, B-type and AB-type pyrolysis, respectively. The Nickel on silica-alumina catalyst significantly improve the conversion as well as the selectivity towards the desired products/target molecules BTE which are being produced may be due to the reaction mechanism as proposed in Figure 2.10 (chapter-2). Moreover, *in-situ* B-type and AB-type catalytic pyrolysis arrangements improve the diffusion efficiency, which favoured the attack of the aromatic double bond, as the low mass transfer resistance is offered in the vapour phase catalytic reaction in comparison to liquid phase catalytic reaction path of the vapour which produced from the primary reactor. In addition, vapour phase catalytic cracking

favoured the secondary reactions within the secondary reactor like cracking and hydrogenation (Marczewski et al., 2013) which, are responsible for the formation of gasoline range lower aromatic hydrocarbons mainly benzene, toluene and ethylbenzene.

Table 5.13 Aromatics BTE content of catalytic pyrolysis in the range of temperature 400 ^{o}C - 700 ^{o}C and at the heating rate of 15 ^{o}C/min using Nickel on silica-alumina catalyst.

Temperature (°C)	Reactor arrangement	Liquid (wt.%)	Gas (wt.%)	Benzene (wt.%)	Toluene (wt.%)	Ethylbenzene (wt.%)	Styrene (wt.%)	Total BTE (wt.%)
400	A-type	78.41	19.63	0.48	2.29	1.34	80.19	4.11
	B-type	75.03	23.45	1.81	3.25	4.48	75.78	9.54
	AB-type	73.12	25.44	2.68	4.27	7.21	69.39	14.17
450	A-type	81.06	16.19	0.62	3.26	2.13	77.14	6.01
	B-type	77.20	21.33	2.42	3.94	5.68	73.50	12.04
	AB-type	76.65	21.75	3.71	4.75	8.57	64.44	17.02
500	A-type	82.64	13.5	1.31	4.53	2.97	73.51	8.81
	B-type	80.34	18.28	4.16	5.12	7.40	69.56	16.68
	AB-type	79.42	18.94	5.53	6.16	11.58	59.28	23.27
550	A-type	84.17	11.89	1.96	5.52	3.62	71.06	11.10
	B-type	**83.21**	**15.5**	**5.57**	**6.53**	**9.28**	**65.67**	**21.38**
	AB-type	**81.15**	**17.14**	**8.05**	**7.55**	**12.96**	**55.55**	**28.56**
600	**A-type**	**88.54**	**7.04**	**3.18**	**6.48**	**4.33**	**69.94**	**13.99**
	B-type	80.85	17.9	4.28	5.68	6.59	60.99	16.55
	AB-type	78.43	19.82	6.29	4.75	10.33	52.04	21.37
650	A-type	85.20	9.93	2.53	5.71	3.45	66.43	11.69
	B-type	78.23	20.57	3.08	4.38	5.70	56.67	13.16
	AB-type	76.44	21.76	4.27	3.58	7.81	48.88	15.66
700	A-type	81.06	13.99	1.39	5.06	3.06	63.88	9.52
	B-type	76.03	22.84	2.31	3.03	4.48	54.52	9.82
	AB-type	73.11	25.02	3.30	2.19	6.17	45.82	11.66

As it is already discussed that the multiphase/AB-type catalytic pyrolysis involves two-stage catalytic cracking i.e., in a liquid phase and the vapour phase both. Thus, AB-type catalytic pyrolysis produced highest BTE content of 28.56 wt.% at a pyrolysis temperature of 550 ^{o}C and heating rate of 15 ^{o}C/min. The B-type catalytic pyrolysis produced little lower BTE content of 21.38 wt.% at a pyrolysis temperature of 550 ^{o}C and same heating rate of 15 ^{o}C/min. However, A-type catalytic pyrolysis produced lowest BTE content of 13.99 wt.% among all catalytic pyrolysis arrangements because of single stage liquid phase contact between hydrocarbon molecules and catalyst. Figure 5.17a shows the comparison of GC-FID characteristics of pyrolysis oil obtained at optimum heating rate i.e., 15 ^{o}C/min using optimum temperature of 600 ^{o}C for A-type, and 550 ^{o}C for B-type, and AB-type pyrolysis, respectively. The peaks of target molecules i.e., gasoline range lower aromatic hydrocarbons i.e., BTE and styrene are highlighted with marker. It is seen from the Figure 5.17a, multiphase/AB-type catalytic pyrolysis oil shows the highest intensity peak of ethylbenzene indicating the promotion of hydrogen transfer which causes the styrene hydrogenation to ethylbenzene (Marczewski et al., 2013). It is already reported by Onwudili et al., 2009 that there was no direct production of toluene and ethylbenzene. However, these are produced from the reaction of styrene itself. Lopez et al., 2011b also suggested that styrene decomposes into other aromatic hydrocarbon like benzene, toluene and ethylbenzene (BTE) as a consequence of the secondary reactions i.e., cracking and hydrogenation in the presence of acid catalyst. Figure 5.17b shows the comparison of liquid yield obtained from multiphase/AB-type catalytic pyrolysis using Nickel on silica-alumina catalyst with commercial fuel gasoline and kerosene. The peaks of benzene, toluene, and ethylbenzene (BTE) appears within the initial zone of residence time of 6 min. The multiphase/AB-type catalytic pyrolysis oil shows similarities with gasoline.

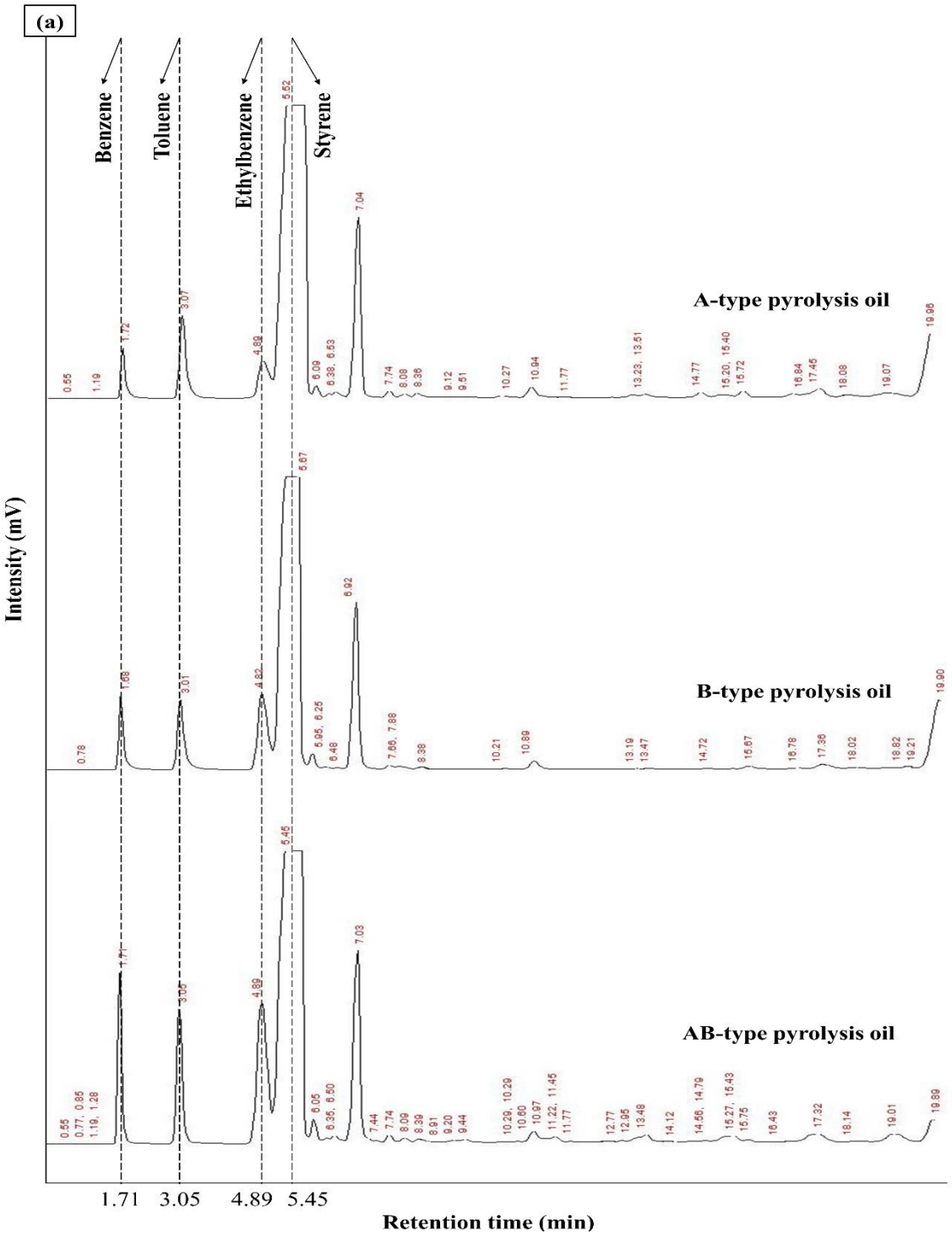

Figure 5.17a Gas chromatographs of catalytic pyrolysis oil A-type, B-type and AB-type obtained at optimum conditions using Nickel on silica-alumina catalyst.

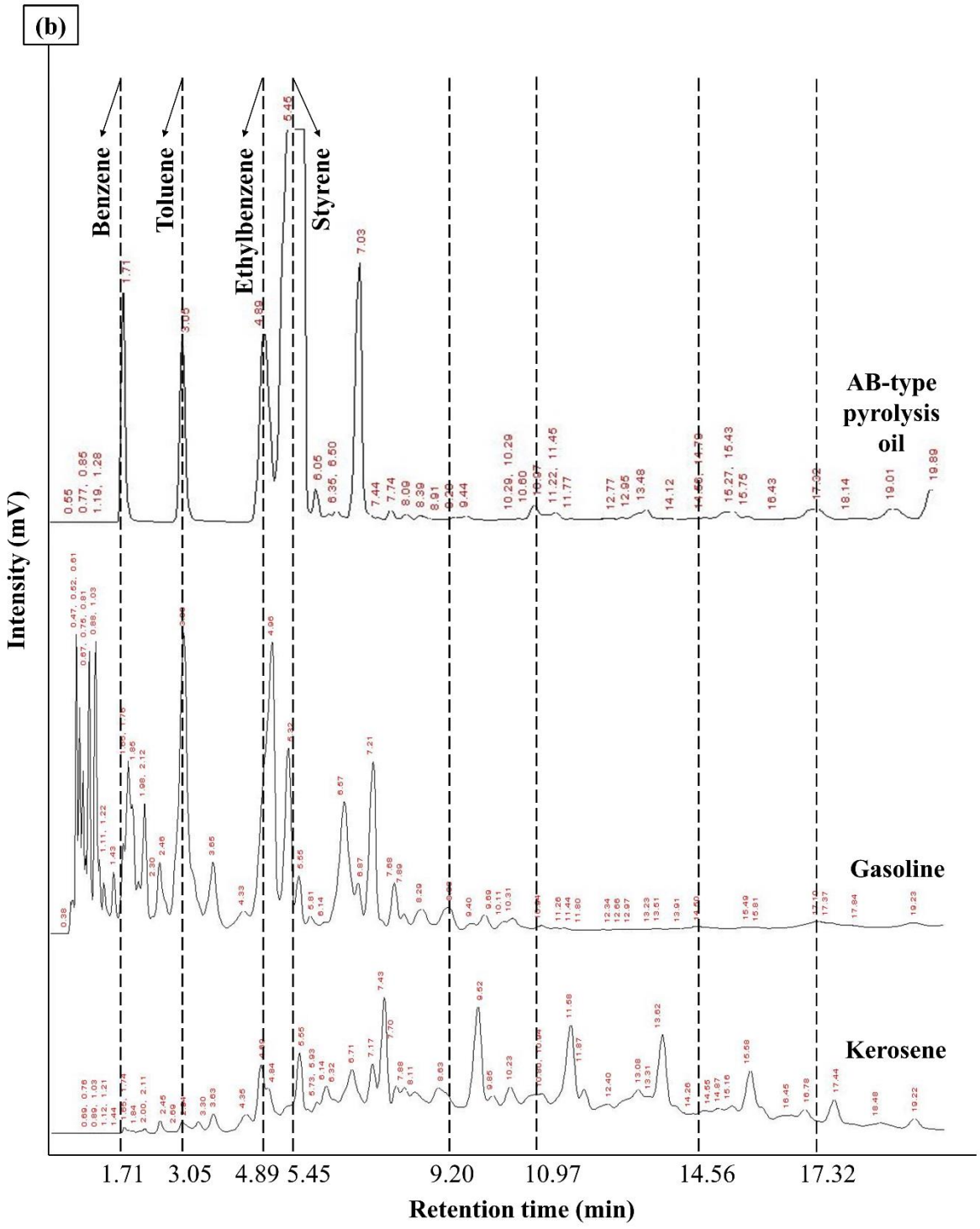

Figure 5.17b Comparison of gas chromatographs of AB-type pyrolysis oil obtained at optimum conditions using Nickel on silica-alumina catalyst with commercial gasoline and kerosene.

This indicates that the multiphase/AB-type catalytic pyrolysis oil contains gasoline range lighter hydrocarbons. Thus, quality-wise pyrolysis oil follows an order of multiphase/AB-type > vapour phase/B-type > liquid phase/A-type.

5.3.2.2.2 FTIR analysis of pyrolysis oil

The FTIR spectra of catalytic pyrolysis oil of A-type, B-type and AB-type obtained at their respective optimum process conditions i.e., optimum heating rate i.e., 15 ^{o}C/min for all types of pyrolysis and at the optimum temperature of 600 ^{o}C for A-type, and 550 ^{o}C for B-type, and AB-type pyrolysis, respectively using Nickel on silica-alumina catalyst is presented in Figure 5.18.

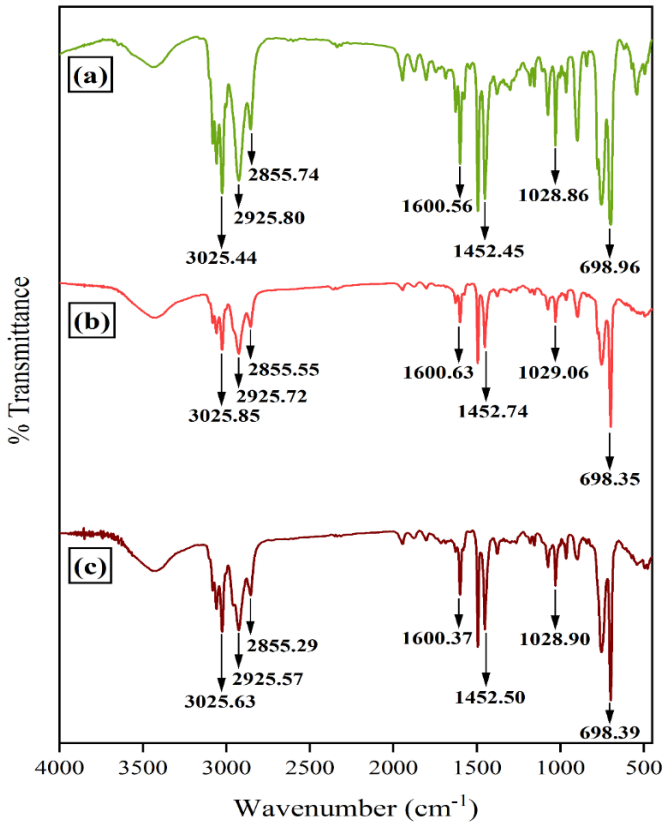

Figure 5.18 FTIR spectrum of catalytic pyrolysis oil obtained at optimum conditions using Nickel on silica-alumina catalyst (a) A-type/liquid phase (b) B-type/vapour phase (c) AB-type/multiphase.

The important FTIR peaks at their various finger print region of wavenumber are shown in Table 5.14. It is seen from the Table 5.14 that the aromatic C-H stretching was confirmed by the vibrations observed at the wavenumber of 3025.44 cm^{-1}, 3025.85 cm^{-1} and 3025.63 cm^{-1} for A-type, B-type and AB-type pyrolysis oil, respectively (Budsaereechai et al., 2019).

Table 5.14 Functional groups present in the catalytic pyrolysis oil obtained at optimum conditions using Nickel on silica-alumina catalyst.

Functional group	Wavenumber (cm^{-1})			
	Standard finger print region	**A-type/liquid phase oil**	**B-type/vapour phase oil**	**AB-type/ multiphase oil**
Aromatic C−H stretching	Above 3000	3081.86 3059.38 3025.44	3082.35 3059.95 3025.85	3081.93 3059.73 3025.63
Methylene C−H asym stretching	2935-2915	2925.80	2925.72	2925.57
Methylene C−H sym stretching	2865-2845	2855.74	2855.55	2855.29
C = C− C aromatic ring stretching	1615-1580	1600.56 1582.88 1493.89	1600.63 1494.62	1600.37 1494.22
Methyl C−H asym bend	1470-1430	1452.45	1452.74	1452.50
Methyl C−H sym bend	1380-1370	1379.44	1378.19	1377.81
Aromatic C−H in plane bend	1225-950	1180.33 1155.46 1074.46	1155.63 1074.80	1179.55 1155.53 1073.88
Cyclohexane ring vibrations	1055-1000/1005-925	1028.86 965.20	1029.06 965.14	1028.90 965.12
Aromatic C−H out of plane bend	860-680	842.30 777.51 754.22 698.96	753.06 698.35	753.32 698.39

The vibrations at wavenumber of 2925.80 cm^{-1}, 2925.72 cm^{-1}, 2925.57 cm^{-1} were related to the methylene C-H asymmetric stretching for A-type, B-type and AB-type, respectively. Whereas, methylene C-H symmetric stretching vibrations were found at the wavenumber of 2855.74

cm^{-1}, 2855.55 cm^{-1}, 2855.29 cm^{-1} for A-type, B-type and AB-type pyrolysis oil, respectively. The peaks noticed at wavenumber of 1600.56 cm^{-1}, 1600.63 cm^{-1}, and 1600.37 cm^{-1} were related to the C=C− C aromatic ring stretching for A-type, B-type and AB-type pyrolysis oil, respectively. Furthermore, the FTIR peaks detected at the wavenumber of 1028.86 cm^{-1}, 1029.06 cm^{-1} and 1028.90 cm^{-1} confirmed the cyclohexane ring vibrations for A-type, B-type and AB-type pyrolysis oil, respectively (Coates, 2006).

5.3.2.2.3 Physicochemical properties of pyrolysis oil

The important physicochemical properties viz gross calorific value (GCV), carbon residue, flash and fire point of pyrolysis oil obtained from catalytic pyrolysis at their respective optimum process conditions i.e., optimum heating rate i.e., 15 ^oC/min for all types of pyrolysis and at the optimum temperature of 600 ^oC for A-type, and 550 ^oC for B-type, and AB-type pyrolysis, respectively using Nickel on silica-alumina catalyst is reported in Table 5.15. It is seen from the Table 5.15 that the GCV of pyrolysis oil obtained by AB-type catalytic pyrolysis was highest in comparison to the other catalytic pyrolysis oil i.e., A-type and B-type, even higher than the calorific value of gasoline and kerosene (Gaurh and Pramanik, 2019). It may be due to the high concentration of low molecular weight hydrocarbons in the AB-type pyrolysis oil (Sonawane et al., 2017) as already discussed earlier. The carbon residue is another property of oil which decides the carbon deposit tendency (Yang et al., 2013) inside the IC engine due to cracking of higher molecular weight hydrocarbons. The fuel with high carbon residue > 1 wt.% results in deposition of carbon residue inside engine which causes overheating and knocking **(**Alhassan et al., 2016). The carbon residue of all types of catalytic pyrolysis oil with commercial gasoline and kerosene (Shakirullah et al., 2010) is also reported in Table 5.15.

Table 5.15 Physicochemical properties of catalytic pyrolysis oil obtained at optimum conditions using Nickel on silica-alumina catalyst.

Physicochemical properties	Catalytic pyrolysis			Commercial fuels	
	A-type	B-type	AB-type	Gasoline	Kerosene
Gross calorific value (Cal/g)	9985	11240	12750	11315	11052
Carbon residue (wt.%)	0.89	0.65	0.45	0.14	0.18
Flash point (^oC)	48	44	40	22	42
Fire point (^oC)	54	50	44	25	45

The carbon residue of multiphase/AB-type pyrolysis oil is quite low i.e., 0.45 wt.%. Thus, it can be recommended for the IC engines, generator sets and cooking stoves. The comparison of flash and fire point of catalytic pyrolysis oil with commercial fuels gasoline (Mukhraiya and Yadav, 2015) and kerosene (Ahmad et al., 2017) is presented in Table 5.15. It is seen from Table 5.15 that the multiphase/AB-type catalytic pyrolysis oil has the lowest flash and fire point i.e., 40 ^oC and 44 ^oC, respectively among all types of catalytic pyrolysis oil and close to the commercial fuel kerosene. Thus, it is highly flammable in nature and easily ignites inside the engines. However, it requires more attention during storage, handling and transportation.

5.3.3 Catalytic pyrolysis using synthesized catalyst from natural red clay

5.3.3.1 Catalyst characterization

5.3.3.1.1 SEM-EDX analysis

The surface morphology of natural raw red clay (RC) and calcined red clay catalyst i.e., RC-600, RC-700, RC-800, and RC-900 were examined by the SEM micrographs shown in Figure 5.19 (a-e). Whereas the surface concentration of various elements obtained by EDX analysis

of red clay catalysts is mentioned in Table 5.16, and corresponding EDX figures are given in Figure 5.20 (a-e).

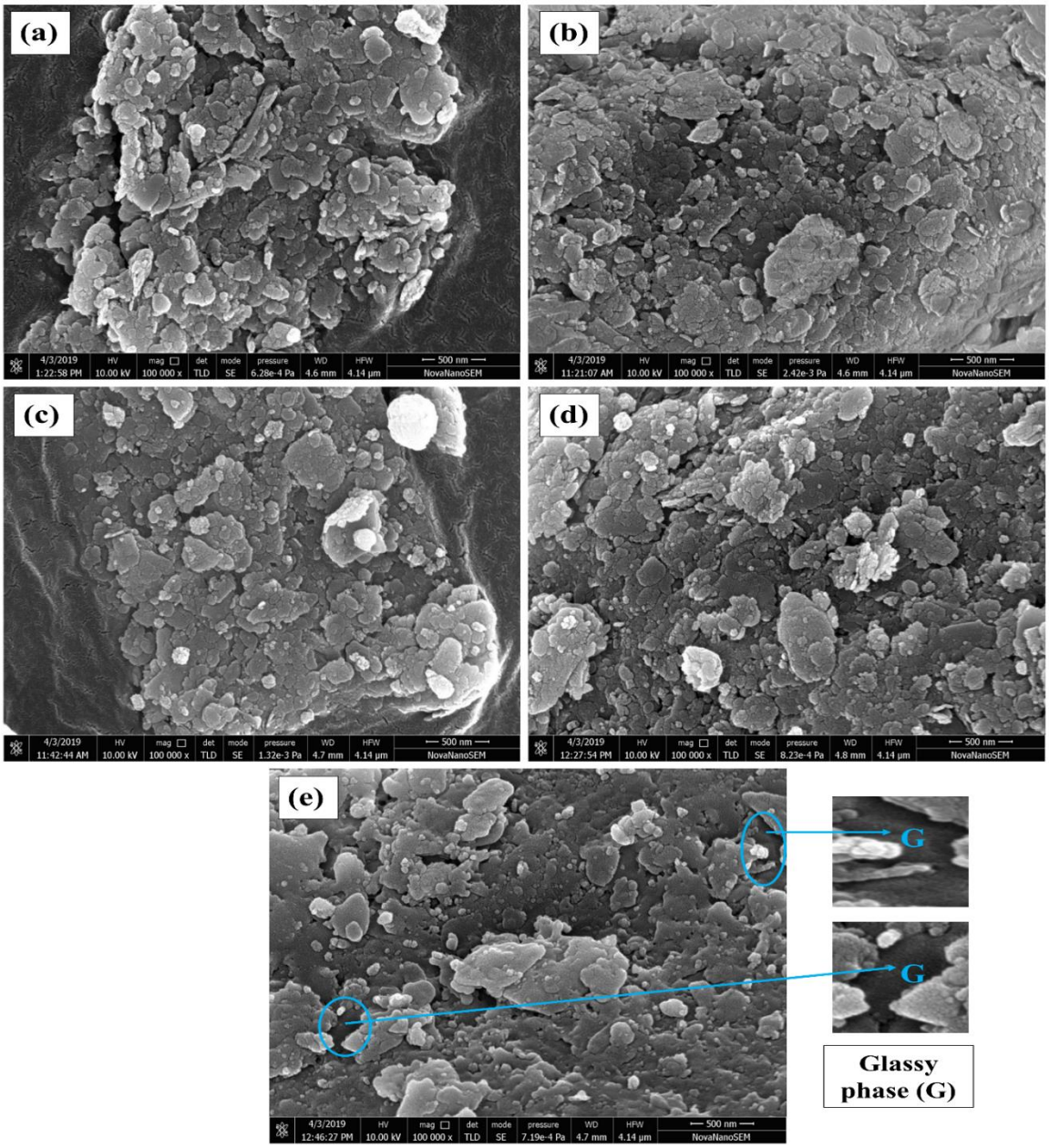

Figure. 5.19 SEM analysis of red clay catalysts (a) raw red clay, (b) red clay calcined at 600 ^{o}C, (c) red clay calcined at 700 ^{o}C, (d) red clay calcined at 800 ^{o}C, (e) red clay calcined at 900 ^{o}C.

It is observed that the natural red clay was composed of compact, thick irregular flaky particles (Figure 5.19a) (Messaoud et al., 2018). The particles in the uncalcined RC catalyst are present

in the form of large cluster with low porosity. However, the particles of nanosize cluster increases with the increase in calcination temperature up to 800 ^{o}C. In addition, surface morphology and surface elemental composition of calcined red clay also improve with the increase in calcination temperature up to 800 ^{o}C (Figure 5.19b-d). The surface morphology of calcined red clay RC-800 shows nano cluster form of particles with very high porosity **(**Figure 5.19d). When the red clay was calcined beyond the calcination temperature of 800 ^{o}C i.e., at a calcination temperature of 900 ^{o}C, the clay particles in RC-900 got sintered (Castillo et al., 2011). Which resulted in low surface area with low porosity and low surface concentration of active metals i.e., silica (Si) and alumina (Al). At the higher calcination temperature of 900 ^{o}C, most of the pores disappeared (Figure 5.19e) because the pores were filled by the glassy phase of silica (Mehta et al., 2018). It is also clear from Figure 5.19e, the structure becomes dense due to the glassy phase (G) (Jiang et al., 2017). The well distributed nano clusters of particle and surface morphology of RC-800 (Figure 5.19d**)** indicates that the elemental composition of this catalyst would be better than the other types of catalysts. Thus, the highest amount of silica (Si) of 56.82 wt.% was found for the RC- 800 catalyst (Figure 5.19e). However, the EDX analysis confirms the presence of silica and alumina in raw and calcined red clay catalysts i.e., RC-600, RC-700, RC-800 and RC-900 (Figure 5.20a-e and Table 5.16).

Table 5.16 Surface concentration of various elements obtained by EDX analysis of raw and calcined red clay catalyst.

Catalyst type	**EDX Composition**				
	O (wt.%)	**Mg (wt.%)**	**Al (wt.%)**	**Si (wt.%)**	**Ca (wt.%)**
RC	42.25	0.51	25.49	29.39	2.37
RC-600	41.56	2.50	22.38	31.87	1.69
RC-700	33.86	1.39	19.69	43.55	1.51
RC-800	31.15	0.09	10.97	56.82	0.96
RC-900	44.01	0.01	3.41	52.49	0.09

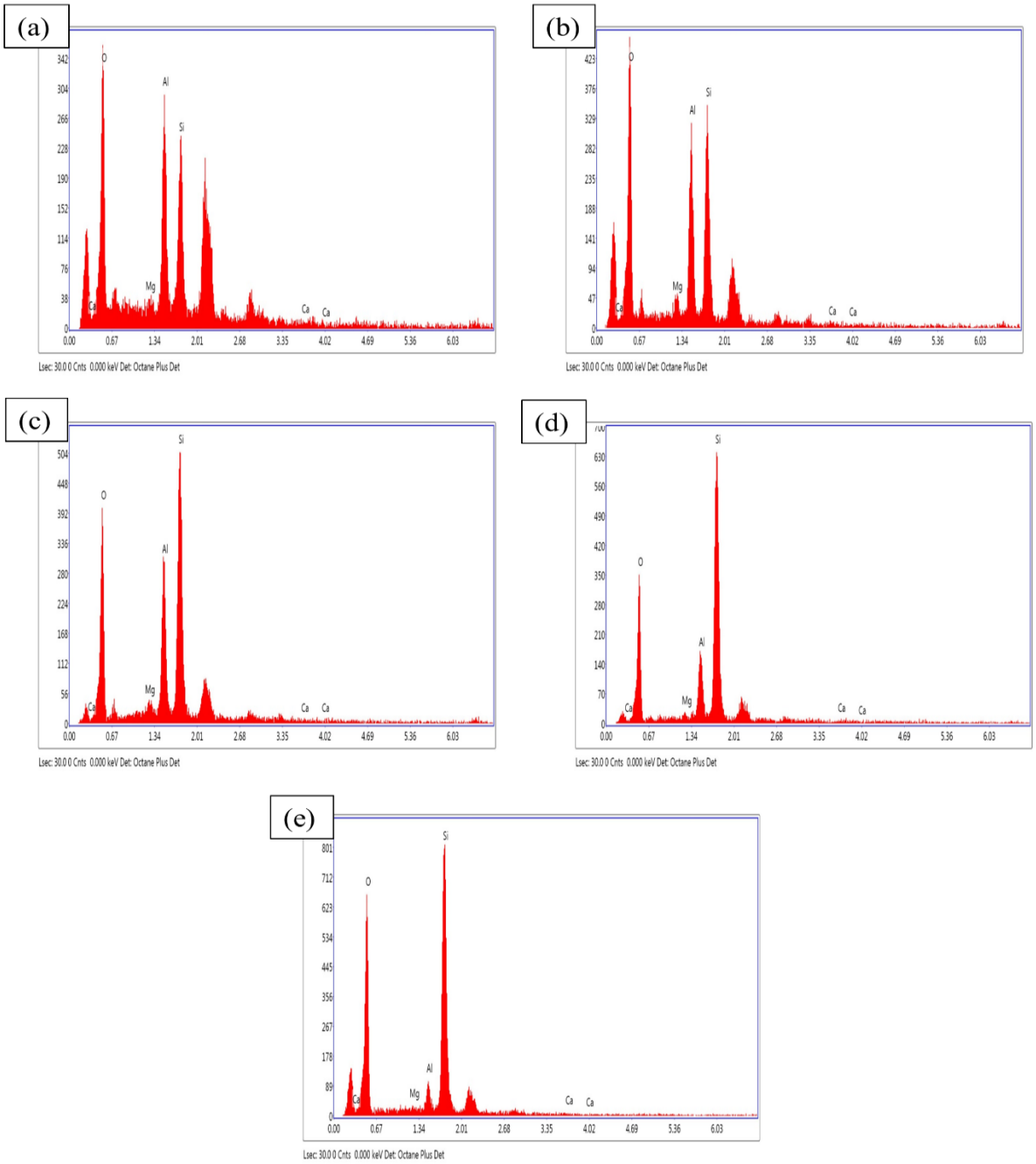

Figure 5.20 EDX analysis of red clay catalysts (a) raw red clay, (b) red clay calcined at 600 ^{o}C, (c) red clay calcined at 700 ^{o}C, (d) red clay calcined at 800 ^{o}C, (e) red clay calcined at 900 ^{o}C.

5.3.3.1.2 BET surface area analysis

The Brunauer Emmett Teller (BET) surface area analysis was conducted to determine the effect of calcination temperature on the surface area of raw and calcined clay particles. Figure

5.21a-e shows the N_2 adsorption/desorption isotherm for the synthesized red clay catalysts i.e., red clay in natural from (RC), red clay calcined at 600 ^oC (RC-600), red clay calcined at 700 ^oC (RC-700), red clay calcined at 800 ^oC (RC-800) and red clay calcined at 900 ^oC (RC-900), respectively.

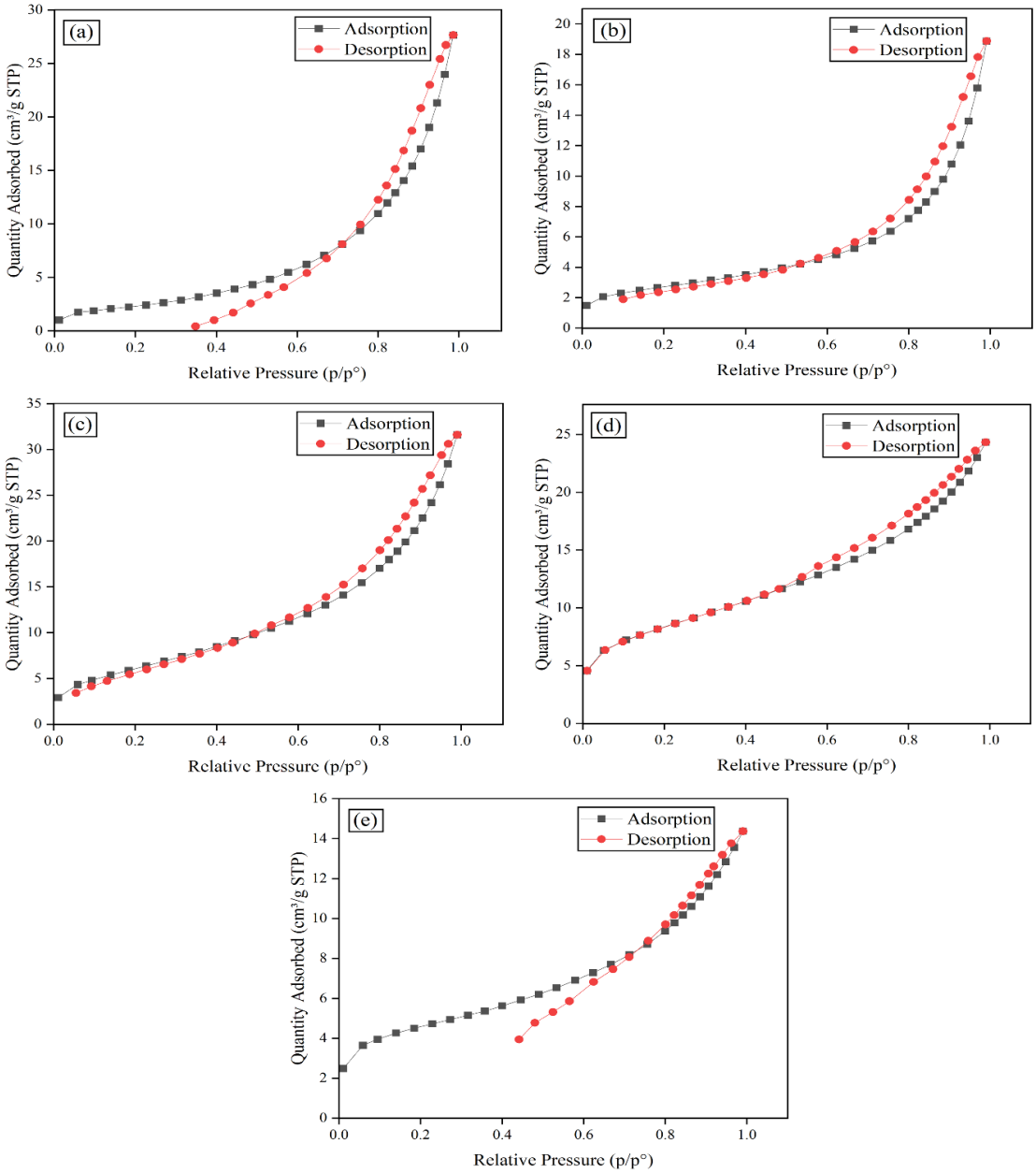

Figure 5.21 N_2 adsorption/desorption isotherm (a) raw red clay, (b) red clay calcined at 600 ^oC, (c) red clay calcined at 700 ^oC, (d) red clay calcined at 800 ^oC, (e) red clay calcined at 900 ^oC

The N_2 adsorption/desorption isotherm of raw red clay catalyst (Figure 5.21a) and calcined red clay catalysts i.e., RC-600 (Figure 5.21b), RC-700 (Figure 5.21c), RC-800 (Figure 5.21d) and RC-900 (Figure 5.21e) show the type IV isotherm and hysteresis loop of H4 (Zaitan et al., 2008). The most characteristic feature of the type IV isotherm is the hysteresis loop, which is associated to the pore condensation in mesoporous structure (Andoni et al., 2014). The calcination temperature significantly influences the surface area (Cases et al., 1991). The surface area of natural raw red clay particles was lowest i.e., 8.73 m^2/g. Whereas, surface area increases with an increase in calcination temperature from 600 ^oC to 800 ^oC i.e., 9.60 m^2/g for RC-600, 22.64 m^2/g for RC-700, and 29.25 m^2/g for RC-800 (Table 5.17). Beyond the calcination temperature of 800 ^oC, catalyst particles got sintered and leads to the dehydroxylation which resulted in low surface area of 15.70 m^2/g for RC-900 (Table 5.17) (Castillo et al., 2011). It is seen from Table 5.17 that the silica and alumina content of natural raw red clay were 29.39 wt.% and 25.49 wt.%, respectively. Whereas, the silica content increases from 31.87 wt.% to 56.82 wt.% with the increase in calcination temperature from 600 ^oC to 800 ^oC.

Table 5.17 BET surface area and silica-alumina content of synthesized red clay catalysts.

Type of catalyst sample	BET surface area (m^2/g)	Silica content (Si) (wt.%)	Alumina content (Al) (wt.%)
RC	8.73	29.39	25.49
RC-600	9.60	31.87	22.38
RC-700	22.64	43.55	19.69
RC-800	29.25	56.82	10.97
RC-900	15.70	52.49	3.41

It is reported in the literature that the number of pores increases with the increase in calcination temperature which results in high surface area of synthesized catalyst. Thus, the silica content

is also high at the calcination temperature of 800 ^{o}C (Gaurh and Pramanik, 2018b). However, at the higher calcination temperature of 900 ^{o}C, the silica content decreased to 52.49 wt.% due to pore blockage (Liang et al., 2009) or sintering (Castillo et al., 2011). There was a decreasing trend for alumina content (Al) from 22.38 wt.% to 3.41 wt.% when calcination temperature was increased from 600 ^{o}C to 900 ^{o}C. It is due to the dealumination as reported by Campbell et al., 1996.

5.3.3.1.3 XRD analysis

The clays mainly contain silicon dioxide and aluminium oxide as universal minerals (Tebandeke et al., 2017). In addition, silica-aluminas are a family of materials characterized by medium to strong tuneable acidity (Busca, 2020). The XRD characteristics of natural red clay catalyst (RC) is presented in the Figure 5.22a. The X-ray diffraction of natural red clay shows the presence for three major types of components/mineral consisting of silica or silica-alumina like α- quartz (Quartz-low/α-SiO_2), illite-micas $(K,H_3O)(Al,Mg,Fe)_2(Al,Si)_4O_{10}[(OH)_2,H_2O]$ and kaolinite $SiO_2Al_2O_5(OH)_4$ when the diffraction peaks were compared with JCPDS data (Figure 5.22a). The XRD characteristics of red clay catalyst (RC) shows the major peaks of α- quartz form at 2θ of 20.85 ^{o}, 26.62 ^{o}, 36.55 ^{o}, 39.46 ^{o}, 40.30 ^{o}, 42.46 ^{o}, 45.80 ^{o}, 50.15 ^{o}, 54.87 ^{o}, 55.31 ^{o}, 59.96 ^{o}, 64.04 ^{o}, 65.80 ^{o}, and 67.77 ^{o} corresponding to the d values of 4.26 ^{o}, 3.35 ^{o}, 2.46 ^{o}, 2.28 ^{o}, 2.24 ^{o}, 2.13 ^{o}, 1.98 ^{o}, 1.82 ^{o}, 1.67 ^{o}, 1.66 ^{o}, 1.54 ^{o}, 1.45 ^{o}, 1.42 ^{o}, and 1.38 ^{o} respectively (JCPDS 5-490). Similarly, diffraction peaks of illite and micas are found at the 2θ of 8.88 ^{o}, 17.79 ^{o}, and 26.76 ^{o} corresponding to d values of 9.95 ^{o}, 4.98 ^{o}, and 3.33 ^{o}, respectively (Pei and Chen, 1977).

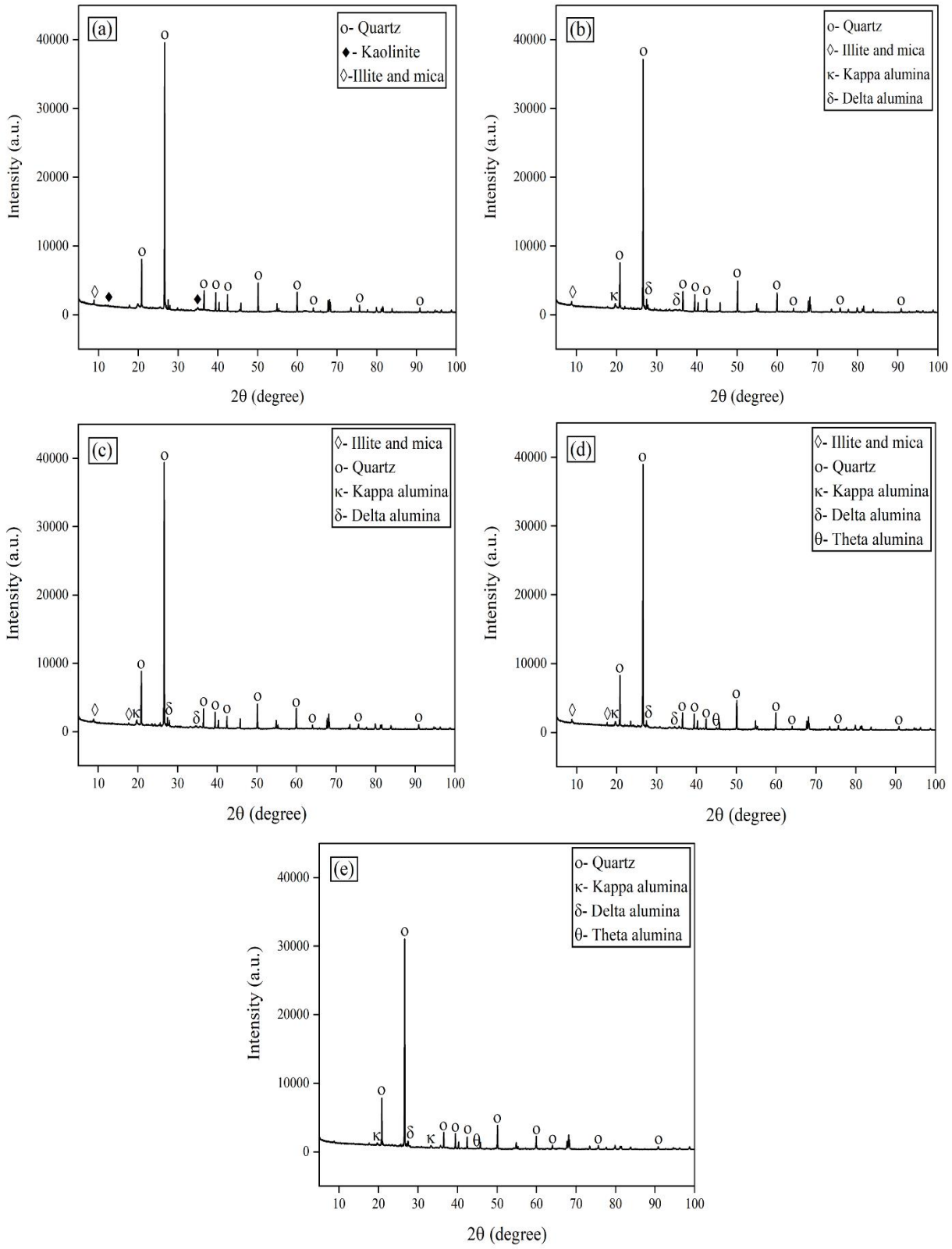

Figure 5.22 XRD characteristics of red clay catalysts (a) raw red clay, (b) red clay calcined at 600 ºC, (c) red clay calcined at 700 ºC, (d) red clay calcined at 800 ºC, (e) red clay calcined at 900 ºC

The kaolinite shows the diffraction peaks at the 2θ of 12.43 º and 34.95 º, corresponding to the basal spacing d of 7.11 º and 2.57 º, respectively (Pei and Chen, 1977; Flogeac et al., 2005). However, the peaks associated with kaolinite disappear after calcination of red clay due to the decomposition of kaolinite in to metakaolinite in the temperature range of 400 ºC to 630 ºC. Moreover, the gradual collapse of metakaolinite promotes the formation of free amorphous silica (Chargui et al., 2018). Thus, peaks corresponding to the kaolinite disappeared in the X-ray diffractograms of calcined red clay catalyst particles viz RC-600, RC-700, RC-800, and RC-900 (Figure 5.22b-e). It is also reported in the literature that the calcination of red clay promotes the formation of transition alumina like κ- kappa alumina, δ- delta alumina, and θ- theta alumina. The transition alumina has a non-crystalline and amorphous structure with important adsorptive and catalytic properties (Santos et al., 2003). It is clearly seen from Figure 5.22b and Figure 5.22c that the red clay calcined catalysts RC-600 and RC-700 come up with an additional peak for κ- kappa alumina and δ- delta alumina, respectively. Further, increase in calcination temperature of red clay to 800 ºC, the synthesized catalyst RC-800 gives one more phase of alumina i.e., θ- theta alumina apart from illite-micas, α- quartz, κ- kappa alumina, and δ- delta alumina (Figure 5.22d). Interestingly, illite-micas disappeared for the synthesized catalyst RC-900 at a calcination temperature of 900 ºC (Figure 5.22e). The peaks of transition alumina i.e., κ- kappa alumina were observed at the 2θ of 19.71 º and 33.15 º corresponding to the d value of 4.50 º and 2.70 º, respectively. The XRD peaks of δ-delta alumina were recorded at the 2θ of 27.62 º, 34.48 º, 41.82 º, and 50.42 º corresponding to the d value of 3.23 º, 2.60 º, 2.16 º, and 1.81 º, respectively. Whereas, θ- theta alumina shows the peaks at the 2θ of 44.89 º corresponding to the d value of 2.02 º. All the XRD peaks for κ-kappa alumina, δ- delta alumina and θ- theta alumina were verified with ICDD 16-0394, ICDD

16-0394, and ICDD 10-0425 standards, respectively. The high abundance of α-quartz in all red clay catalysts RC, RC-600, RC-700, RC-800, and RC-900 with high silica content obviously provides strong acidic sites for cracking (Tebandeke et al., 2015), hydrogenation, and aromatization of hydrocarbon molecules. It is also observed that peaks associated with α-quartz were more intense for raw and calcined red clay catalysts among all minerals. However, the intensity of peak for α-quartz got decreased for the catalyst RC-900 (Figure 5.22e) due to their partial dissolution into the glassy phase (Gralik et al., 2014), and a decrease in silica (Si) content was also observed in EDX study (Table 5.16) (Escalera et al., 2012). Thus, it is expected from the XRD analysis that the RC-800 catalyst may exhibit good catalytic properties due to the presence of enough silica and transition aluminas, which obviously enhance the performance of catalytic pyrolysis of WEPS and *in-situ* hydrogenation and aromatization of hydrocarbon molecules. It should be noted that RC-800 catalyst has the highest BET surface area i.e., 29.25 m^2/g, among all red clay catalysts. The silica (Si) and alumina (Al) content are also found in good amount for the RC-800 catalyst as is shown in Table 5.16. The high silica content (56.82 wt.%) in the RC-800 catalyst makes it a perfect acidic catalyst which can act as both Bronsted and Lewis acid in their natural and ion-exchanged form (Nagendrappa, 2002).

5.3.3.1.4 FTIR analysis of red clay catalysts

Figure 5.23 shows the Fourier transform spectroscopy (FTIR) analysis of synthesized red clay catalysts i.e., red clay in natural from (RC), red clay calcined at 600 ^oC (RC-600), red clay calcined at 700 ^oC (RC-700), red clay calcined at 800 ^oC (RC-800), red clay calcined at 900 ^oC (RC-900). The band at 3648 cm^{-1} corresponds to the frame work bridged hydroxyl groups in the form of Si−OH−Al confirms the strong Bronsted acid sites (BAS) (Ojha and Vinu, 2015) which are responsible for the production of valuable fuel range lower aromatic hydrocarbons

viz benzene, toluene, and ethylbenzene (BTE) (Marczewski et al., 2013). The vibration band corresponds to the asymmetric siloxane stretching observed in the range of 850-1350 cm^{-1} (Ojha and Vinu, 2015). Furthermore, the band corresponds to the 797 cm^{-1} belongs to the symmetric SiO_4 stretching (Ojha and Vinu, 2015).

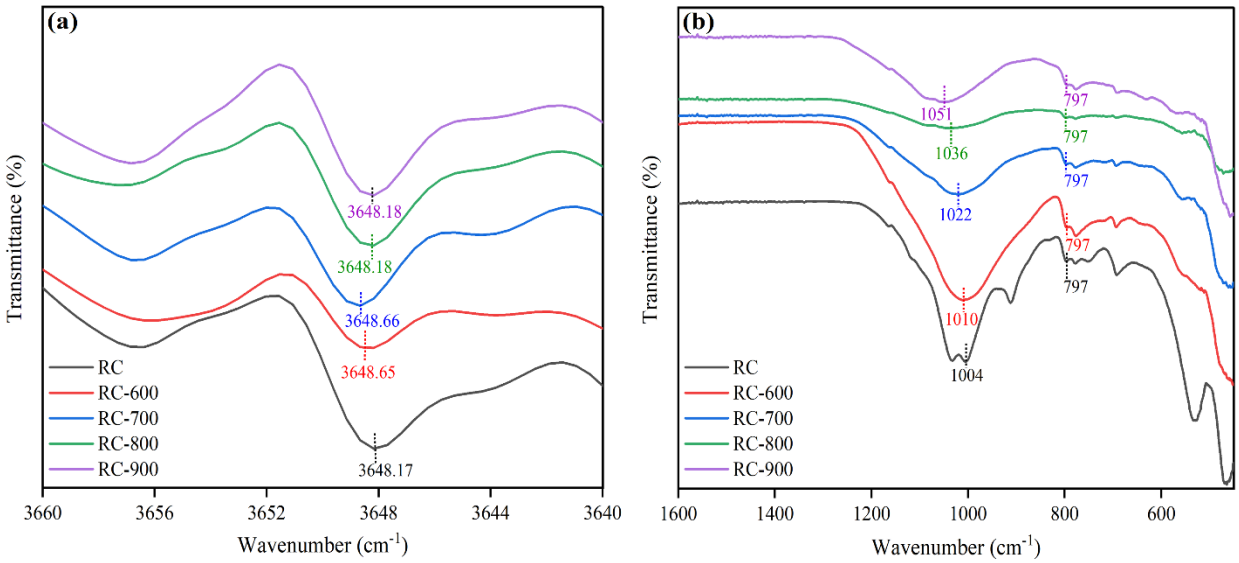

Figure 5.23 FTIR analysis of raw red clay (RC) catalyst and calcined red clay catalysts RC-600, RC-700, RC-800 and RC-900 into two different frequency regions (a) 3660-3640 cm^{-1} (b) 1600-450 cm^{-1}

5.3.3.2 Selection of best catalyst among all synthesized red clay catalysts

The catalytic pyrolysis of WEPS was examined using each type of red clay catalyst i.e., raw red clay (RC), red clay calcined at 600 ^oC (RC-600), red clay calcined at 700 ^oC (RC-700), red clay calcined at 800 ^oC (RC-800) and red clay calcined at 900 ^oC (RC-900) for the selection of best catalyst among all synthesized red clay catalysts. The liquid phase/A-type catalytic pyrolysis was performed at a temperature of 600 ^oC, heating rate of 15 ^oC/min using feed to catalyst ratio of 20:1. Whereas, vapour phase/ B-type and multiphase/AB-type catalytic pyrolysis were performed at a reaction temperature of 550 ^oC, heating rate of 15 ^oC/min using

feed to catalyst ratio of 20:1. Table 5.18 shows the liquid yield along with BTE and styrene content for each red clay catalyst. It should be noted that, the highest BTE and lowest styrene content was only found for red clay catalyst RC-800 for each type of reactor arrangement i.e., A-type, B-type and AB-type. The maximum BTE content of 27.61 wt.%, 23.51 wt.% and 18.58 wt.% were obtained for AB-type, B-type and A-type catalytic pyrolysis, respectively using RC-800 catalyst.

Table 5.18 Comparison between liquid yield and BTE content obtained all types of red clay catalyst i.e., RC, RC-600, RC-700, RC-800, RC-900.

Catalyst type	Temperature (ºC)	Reactor arrangement	Liquid (wt.%)	Benzene (wt.%)	Toluene (wt.%)	Ethyl benzene (wt.%)	Styrene (wt.%)	Total BTE (wt.%)
RC	600	A-type	92.93	0.21	8.37	2.97	79.23	11.55
	550	B-type	88.16	0.32	9.45	4.16	75.89	13.93
	550	AB-type	85.74	0.54	10.11	5.26	73.77	15.91
RC-600	600	A-type	92.19	0.33	9.13	3.17	76.89	12.63
	550	B-type	86.67	0.41	9.85	5.27	72.34	15.53
	550	AB-type	84.39	0.71	11.26	6.65	69.18	18.62
RC-700	600	A-type	90.59	0.43	11.97	4.47	71.23	16.87
	550	B-type	83.36	0.79	12.66	7.12	65.29	20.57
	550	AB-type	81.85	1.19	13.48	8.59	63.41	23.26
RC-800	**600**	**A-type**	**88.82**	**0.48**	**12.60**	**5.50**	**68.83**	**18.58**
	550	**B-type**	**80.81**	**0.97**	**13.86**	**8.68**	**63.68**	**23.51**
	550	**AB-type**	**79.47**	**1.47**	**15.42**	**10.72**	**60.75**	**27.61**
RC-900	600	A-type	91.84	0.36	10.87	3.91	74.89	15.14
	550	B-type	85.01	0.56	10.29	6.98	68.25	17.83
	550	AB-type	83.76	0.98	12.18	7.41	65.12	20.57

It may be due to the highest BET surface area of 29.25 m^2/g for RC-800 catalyst among all other red clay catalysts which, promotes the secondary reactions such as cracking and

hydrogenation for the formation of target molecules benzene, toluene and ethylbenzene (BTE). Moreover, the highest silica content of 56.82 wt.% was found for RC-800 catalyst. The presence of strong Bronsted acid sites in RC-800 catalyst was also confirmed by the FTIR analysis. Furthermore, the XRD analysis ensured the presence of illite-micas, α-quartz, and all possible transition aluminas i.e., κ-kappa alumina, δ-delta alumina, and θ-theta alumina in the RC-800 catalyst only. Thus, based on the analytical characterization and experimental results, red clay catalyst RC-800 was selected for the further detailed study.

5.3.3.3 Effect of process parameters on product yield

5.3.3.3.1 Effect of feed to catalyst ratio

Figure 5.24 shows the effect of feed to catalyst ratio on product yield produced for A-type/liquid phase catalytic pyrolysis at the reaction temperature of 600 ^{o}C and a heating rate of 15 ^{o}C/min. Various feed to catalyst ratios of 10:1, 20:1, 30:1, and 40:1 were taken to examine the effect of catalyst amount on the product yield obtained from A-type catalytic pyrolysis of WEPS using best RC-800 red clay catalyst. The effect of feed to catalyst ratio for B-type and AB-type catalytic pyrolysis were also examined at the similar experimental conditions. However, the effect of feed to catalyst ratio on product yield for B-type and AB-type catalytic pyrolysis are shown in Appendix A6. It is seen from Figure 5.24 that the liquid yield increases up to feed to catalyst ratio of 20:1. Beyond feed to catalyst ratio of 20:1, liquid yield decreases to 85.92 wt.% (30:1). Very low liquid yield of 83.71 wt.% was produced at a very high feed to catalyst ratio of 40:1 (Table 5.19). The optimum feed to catalyst ratio of 20:1 gives the highest liquid yield of 88.82 wt.% (Table 5.19), and it may be due to the highest active surface of catalyst available for interaction with the reactants. The reason has already been discussed in

page no. 85. Although, active sites are high for the very low feed to catalyst ratio of 10:1, the reactant is not sufficient to produce high liquid yield (Gaurh and Pramanik, 2020). Thus, the liquid yield of 81.30 wt.% was obtained at a feed to catalyst ratio of 10:1.

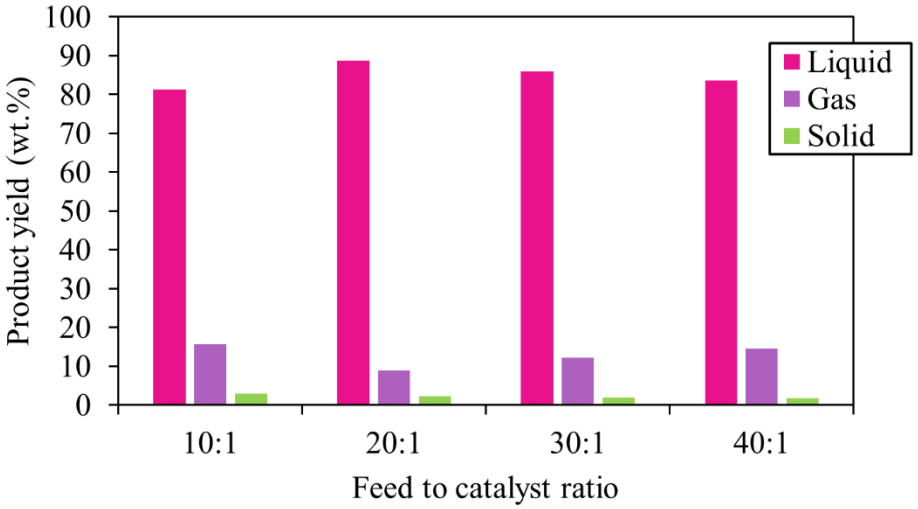

Figure 5.24 Effect of feed to catalyst ratio on product yield for A-type/liquid phase catalytic process using best red clay catalyst RC-800 at a pyrolysis temperature of 600 ^{o}C and heating rate of 15 ^{o}C/min.

It is also seen from the Table 5.19 that the solid residue of 2.35 wt.% was obtained at feed to catalyst ratio of 20:1. However, the lowest gaseous yield of 8.83 wt.% was obtained at feed to catalyst ratio of 20:1 for A-type catalytic pyrolysis using best red clay catalyst RC-800.

Table 5.19 Product yield of A-type/liquid phase catalytic pyrolysis at 600 ^{o}C and 15 ^{o}C /min using varying feed to catalyst ratio using best red clay catalyst RC-800.

Feed to catalyst ratio	Liquid (wt.%)	Gas (wt.%)	Solid (wt.%)
10:1	81.30	15.68	3.02
20:1	88.82	8.83	2.35
30:1	85.92	12.16	1.92
40:1	83.71	14.44	1.85

It should be noted that the feed to catalyst ratio of 20:1 was also found to be optimum for A-type catalytic pyrolysis using ZSM-5 ammonium powder and Nickle on silica-alumina catalyst. The liquid yield of 88.05 wt.% and 88.54 wt.% were obtained for A-type catalytic pyrolysis using ZSM-5 ammonium powder and Nickle on silica-alumina catalyst, respectively at a reaction temperature of 600 ^{o}C and heating rate of 15 ^{o}C/min.

5.3.3.3.2 Effect of temperature and holding time

Effect of temperature and holding time on liquid and solid yield were determined for each type of catalytic pyrolysis i.e., A-type, B-type and AB-type using best red clay catalyst RC-800 with feed to catalyst ratio of 20:1 as mentioned in Figure 5.25a-b. Although, the effect of temperature and holding time for B-type and AB-type catalytic pyrolysis are shown in Appendix A7. Figure 5.25a shows the effect of temperature on liquid and solid yield with zero holding time.

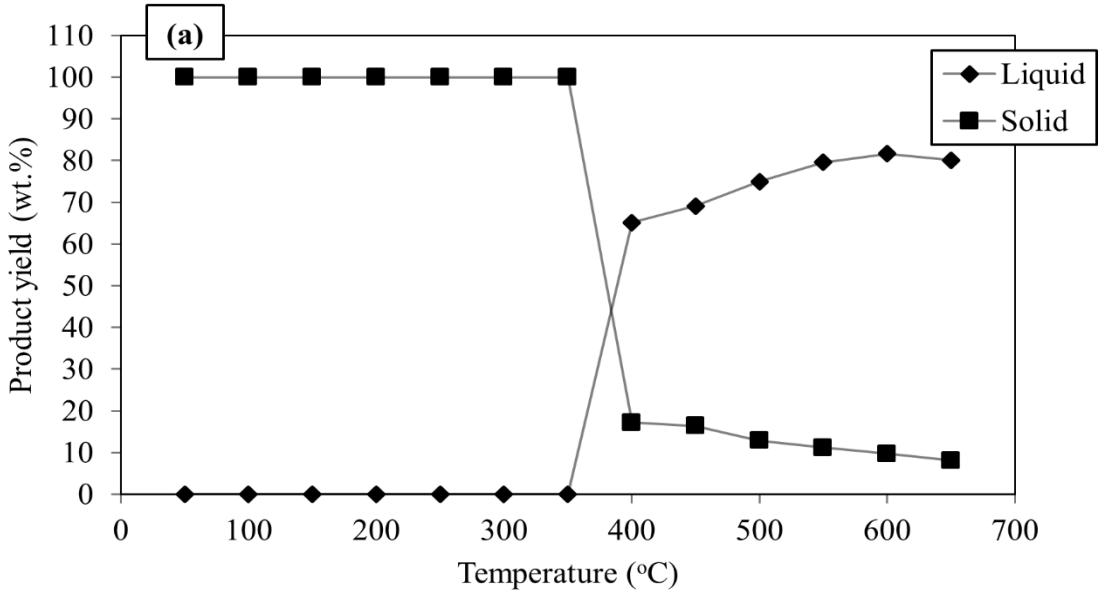

Figure 5.25a Effect of temperature on liquid and solid yield for liquid phase catalytic/A-type pyrolysis at 15 ^{o}C/min heating rate and zero hold time using red clay catalyst RC-800.

It is seen from the Figure 5.25a that the liquid yield increases with the increase in temperature up to 600 ºC and the maximum liquid yield of 81.64 wt.% was obtained at a temperature of 600 ºC with zero hold time (Figure 5.25a). It should be noted from Figure 5.25a there is no degradation of WEPS was observed up to reaction temperature of 350 ºC. Figure 5.25b shows the effect of holding time on product yield. It should be noted from Figure 5.25b that the liquid yield increases with the increases in holding time up to 30 min and remains constant beyond holding time of 30 min. The maximum liquid yield of 88.82 wt.% was obtained at a holding time of 30 min, temperature of 600 ºC and heating rate of 15 ºC/min for A-type catalytic pyrolysis. Thus, the holding time of 30 min was considered as the optimum holding time for best red clay catalyst RC-800 in terms of maximum liquid yield.

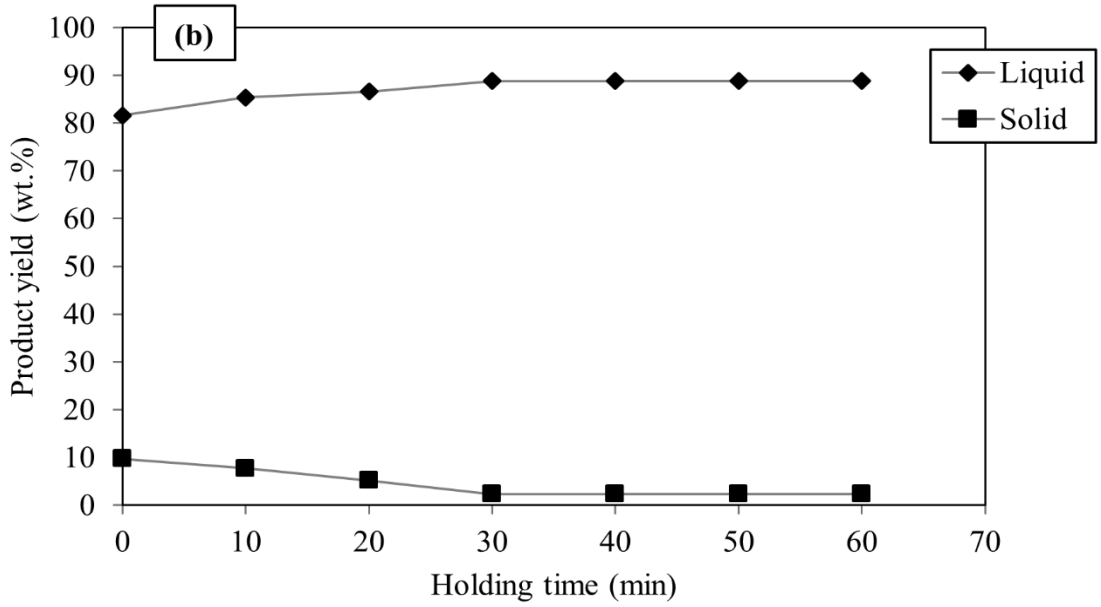

Figure 5.25b Effect of holding time on liquid and solid yield for liquid phase catalytic/A-type pyrolysis at 15 ºC/min and 600 ºC using best red clay catalyst RC-800.

It should be noted that the holding time of 30 min was also considered as the optimum for A-type catalytic pyrolysis using ZSM-5 ammonium powder and Nickel on silica-alumina catalyst. The liquid yield of 88.05 wt.% and 88.54 wt.% were obtained at a holding time of 30

min, reaction temperature of 600 ^{o}C for A-type catalytic pyrolysis using ZSM-5 ammonium powder and Nickel on silica-alumina catalyst, respectively.

5.3.3.3.3 Effect of heating rate

To determine the effect of heating rate on the product yield obtained from the catalytic pyrolysis of WEPS using RC-800 catalyst, the WEPS was subjected to pyrolysis process at a fixed reaction temperature of 550 ^{o}C with a varying heating rate ranging from 5 ^{o}C/min to 25 ^{o}C/min, optimum feed to catalyst ratio of 20:1. It is seen from Figure 5.26 that the liquid yield increases with the increase in heating rate up to 15 ^{o}C/min then starts decreasing for catalytic pyrolysis of all types reactor arrangements i.e., A-type, B-type, and AB-type. The catalytic process using A-type reactor arrangement produced the maximum liquid yield of 83.27 wt.% at a heating rate of 15 ^{o}C/min. Whereas, B-type and AB-type produced low liquid yield of 80.81 wt.% and 79.47 wt.%, respectively at a heating rate of 15 ^{o}C/min.

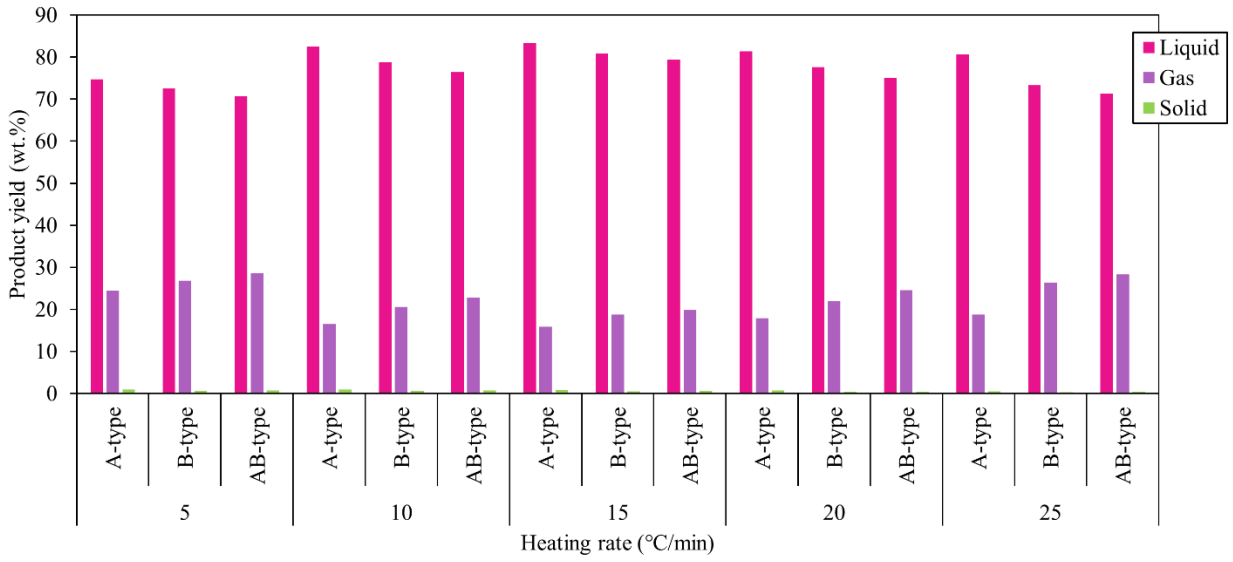

Figure 5.26 Effect of heating rate on product yield obtained from catalytic pyrolysis i.e., A-type, B-type and AB-type at a pyrolysis temperature of 550 ^{o}C using best red clay catalyst RC-800.

The heating rate beyond 15 ^{o}C/min i.e., 20 ^{o}C/min, the A-type, B-type and AB-type catalytic pyrolysis produced liquid yield of 81.39 wt.%, 77.65 wt.% and 74.98 wt.%, respectively which are lower than the liquid yield obtained by the catalytic pyrolysis of all type, at the heating rate of 15 ^{o}C/min. It may be due to β-scission reaction, which is favourable at a higher heating rate of 20 ^{o}C/min resulting in lesser liquid yield and higher gaseous yield. On the other side, lower heating rate of 5 ^{o}C/min and 10 ^{o}C/min also produced less liquid range hydrocarbons. This can be attributed to more residence time at a lower heating rate, which facilitates further cracking of hydrocarbon molecules and the same reason for such trend of liquid yield with the heating rate has already been discussed in page no. 89.

It should be observed that the heating rate of 15 ^{o}C/min was also found to be optimum for thermal as well as catalytic pyrolysis using ZSM-5 ammonium powder and Nickel on silica-alumina catalyst for each type of reactor arrangement. The maximum liquid yield of 91.69 wt.% was obtained at the optimum heating rate of 15 ^{o}C/min for thermal pyrolysis. However, the maximum liquid yield of 82.73 wt.%, 78.85 wt.% and 75.11 wt.% were obtained at the heating rate of 15 ^{o}C/min for the A-type, B-type, and AB-type reactor arrangements, respectively using ZSM-5 ammonium powder catalyst. Whereas, A-type, B-type and AB-type pyrolysis produced maximum liquid yield of 84.17 wt.%, 83.21 wt.%, and 81.15 wt.%, respectively at the heating rate of 15 ^{o}C/min using Nickel on silica-alumina catalyst.

5.3.3.3.4 Effect of temperature

The effect of temperature on the product yield for all types of reactor arrangements of catalytic pyrolysis using best RC-800 catalyst was examined at various temperatures in the range of 400-700 ^{o}C at the optimum heating rate of 15 ^{o}C/min and feed to catalyst ratio of 20:1. It is

seen from Figure 5.27 that the liquid yield increases with the increase in temperature up to 600 ^{o}C and then decreases when the temperature is further increased for the A-type catalytic pyrolysis. This can be attributed to the cracking of C-C bonds at a higher temperature which is responsible for the formation of lighter hydrocarbon with a shorter chain of carbon. The same reason for such trend of liquid yield has already been discussed in page no. 108. The liquid yield of 88.82 wt.% was obtained for A-type catalytic pyrolysis at a temperature of 600 ^{o}C. The similar trend was also observed for the B-type and AB-type catalytic pyrolysis. The maximum liquid yield of 80.81 wt.% for B-type, and 79.47 wt.% for AB-type catalytic pyrolysis were obtained at a reaction temperature of 550 ^{o}C. Among all types of catalytic pyrolysis, the AB-type catalytic pyrolysis produced the maximum gaseous yield of 19.88 wt.% at a temperature of 550 ^{o}C and it may be due to two-stage catalytic cracking of hydrocarbon molecules as already discussed earlier (page no. 92).

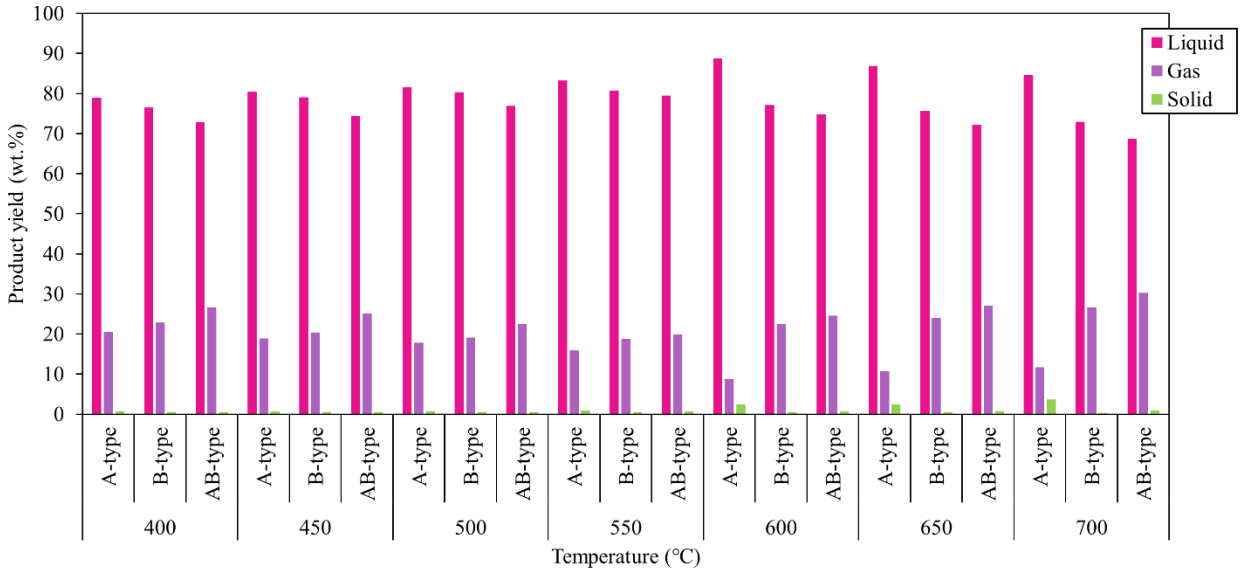

Figure 5.27 Effect of temperature on product yield obtained from catalytic pyrolysis i.e., A-type, B-type and AB-type at a heating rate of 15 ^{o}C/min using best red clay catalyst RC-800.

The B-type catalytic pyrolysis also facilitates two-stage cracking i.e., in the first stage WEPS thermally cracked and in the second stage, catalyst reacts with the vapours liberated after the thermal pyrolysis of WEPS. Thus, the slightly lower gaseous yield of 18.73 wt.% was obtained for the B-type catalytic pyrolysis as compared to the AB-type pyrolysis (19.88 wt.%) at a temperature of 550 ^{o}C and heating rate of 15 ^{o}C/min. On the other side, A-type pyrolysis provides single stage catalytic cracking of WEPS, which is in the liquid phase only. Thus, very low gaseous yield of 8.83 wt.% was obtained for the A-type catalytic pyrolysis at the optimum temperature of 600 ^{o}C and heating rate of 15 ^{o}C/min. The liquid yield for all types of catalytic pyrolysis i.e., A-type, B-type and AB-type at their optimum temperature condition is also given in Table 5.20.

Table 5.20 Product yield of WPES pyrolysis using various types of reactor arrangements at optimum temperature and heating rate of 15 ^{o}C/min using best red clay catalyst RC-800.

Type of reactor arrangement	Optimum temperature (^{o}C)	Liquid yield (wt.%)	Gas yield (wt.%)	Solid yield (wt.%)
Liquid phase/A-type	600	88.82	8.83	2.35
Vapour phase/B-type	550	80.81	18.73	0.46
Multiphase/AB-type	550	79.47	19.88	0.65

It should be noted that the temperature of 600 ^{o}C for A-type, 550 ^{o}C for B-type and AB-type catalytic pyrolysis was also found to be optimum for ZSM-5 ammonium powder and Nickel on silica-alumina catalyst. The maximum liquid yield of 88.05 wt.% (600 ^{o}C), 78.85 wt.% (550 ^{o}C) and 75.11 wt.% (550 ^{o}C) were obtained for A-type/liquid phase, B-type/vapour phase and AB-type/multiphase catalytic pyrolysis using ZSM-5 ammonium powder catalyst. However, the maximum liquid yield of 88.54 wt.%, 83.21 wt.% and 81.15 wt.% were obtained for A-

type at a temperature of 600 ^{o}C, B-type at a temperature of 550 ^{o}C, and for AB-type catalytic pyrolysis at a temperature of 550 ^{o}C, respectively using Nickel on silica-alumina catalyst.

5.3.3.4 Analysis of pyrolysis oil obtained using RC-800 catalyst

5.3.3.4.1 Estimation of aromatic content/BTE and styrene in pyrolysis oil

As it is already discussed that the quality of pyrolysis oil is mainly associated with the valuable aromatic hydrocarbons i.e., benzene, toluene, and ethylbenzene (BTE). Thus, the BTE and undesired styrene were measured using calibration characteristics (Figure 3.8, page no. 59). Table 5.21 shows the BTE and styrene content of pyrolysis oil obtained from all types of catalytic pyrolysis using best red clay catalyst RC-800 at each reaction temperature, heating rate of 15 ^{o}C/min and feed to catalyst ratio of 20:1. It is clearly seen in Table 5.21 that the highest BTE content of 27.62 wt.% was obtained for the multiphase/AB-type catalytic pyrolysis process at the optimum reaction temperature of 550 ^{o}C, among all reactor arrangements of catalytic pyrolysis. Very high production of BTE content for the AB-type/multiphase catalytic process may be due to the two stage catalytic contact and secondary reactions i.e., *in-situ* cracking and hydrogenation which takes place in the secondary reactor. The B-type catalytic pyrolysis produced slightly lower BTE content of 23.51 wt.% at the optimum reaction temperature of 550 ^{o}C as compared to the AB-type catalytic pyrolysis due to the single stage vapour phase catalytic cracking as already been discussed in page no. 92. However, the A-type catalytic pyrolysis obtained very low BTE content of 18.58 wt.% at a reaction temperature of 600 ^{o}C due to the single stage catalytic cracking in liquid phase only. The styrene content of 60.75 wt.% was obtained for the AB-type/multiphase catalytic pyrolysis at the pyrolysis temperature of 550 ^{o}C. Whereas, the styrene content of 68.86 wt.% and 63.68

wt.% were obtained for A-type and B-type catalytic pyrolysis at the same optimum reaction temperature of 600 ^{o}C and 550 ^{o}C, respectively.

Table 5.21 Product yield and BTE content obtained from catalytic pyrolysis of WEPS in the temperature range of 400 ^{o}C to 700 ^{o}C at 15 ^{o}C/min heating rate using best red clay catalyst RC-800.

Pyrolysis Temperature (^{o}C)	Reactor arrangement	Liquid (wt.%)	Gas (wt.%)	Benzene (wt.%)	Toluene (wt.%)	Ethylbenzene (wt.%)	Styrene (wt.%)	Total BTE (wt.%)
400	A-type	78.93	20.45	0.28	6.21	0.61	78.33	7.10
	B-type	76.59	22.85	0.41	8.45	2.84	76.87	11.71
	AB-type	72.84	26.65	0.83	10.68	8.25	71.58	19.76
450	A-type	80.42	18.9	0.30	8.95	1.22	77.02	10.47
	B-type	79.04	20.43	0.55	9.21	4.47	70.61	14.23
	AB-type	74.31	25.14	1.17	11.42	8.68	67.96	21.27
500	A-type	81.47	17.77	0.37	10.59	1.48	71.72	12.44
	B-type	80.38	19.12	0.69	12.77	6.22	66.98	19.69
	AB-type	76.88	22.52	1.35	14.44	10.27	61.78	26.06
550	A-type	83.27	15.88	0.43	12.46	2.43	70.03	15.32
	B-type	**80.81**	**18.73**	**0.97**	**13.86**	**8.68**	**63.68**	**23.51**
	AB-type	**79.47**	**19.88**	**1.47**	**15.42**	**10.72**	**60.75**	**27.62**
600	**A-type**	**88.82**	**8.83**	**0.48**	**12.60**	**5.50**	**68.83**	**18.58**
	B-type	77.15	22.42	0.69	13.58	8.39	61.47	22.66
	AB-type	74.71	24.56	1.03	14.12	9.28	56.48	24.43
650	A-type	86.84	10.75	0.47	12.22	4.47	65.30	17.15
	B-type	75.59	24.01	0.63	12.96	6.21	58.96	19.80
	AB-type	72.23	26.99	0.87	13.65	8.34	51.45	22.86
700	A-type	84.62	11.68	0.43	10.59	3.64	63.07	14.67
	B-type	72.98	26.65	0.57	11.44	4.36	55.96	16.36
	AB-type	68.77	30.27	0.67	13.22	6.44	47.61	20.33

Figure 5.28a shows the comparison of GC-FID characteristics of pyrolysis oil obtained from catalytic pyrolysis of WEPS at optimum heating rate i.e., 15 ^{o}C/min for all types of pyrolysis and optimum temperature of 600 ^{o}C for A-type/liquid phase, and 550 ^{o}C for B-type/vapour phase and AB-type/multiphase pyrolysis, respectively.

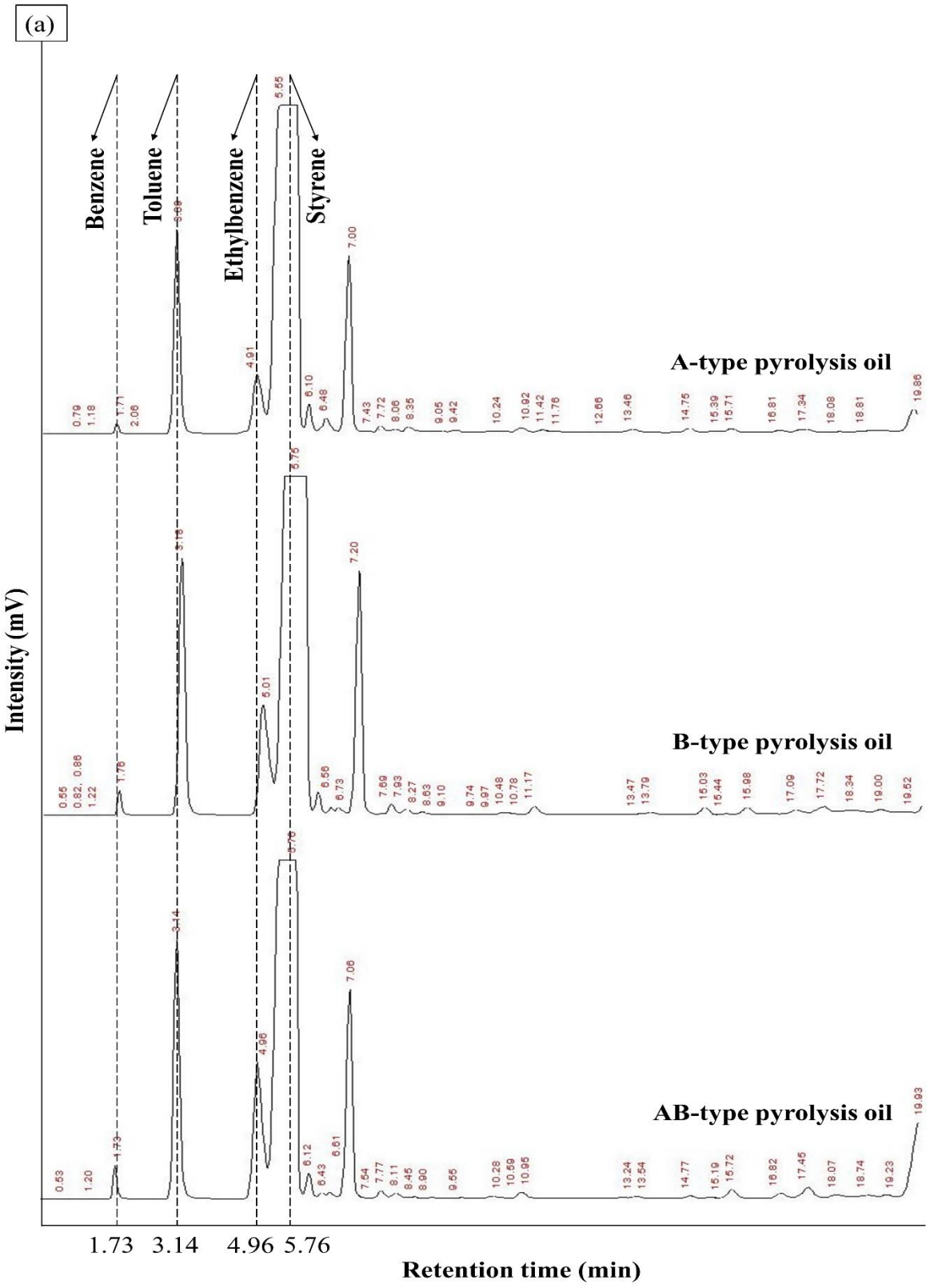

Figure 5.28a Gas chromatographs of catalytic pyrolysis oil A-type, B-type and AB-type obtained at optimum conditions using RC-800 catalyst.

It is seen from Figure 5.28a that the intensity of peaks related to the benzene, toluene, and ethylbenzene were gradually increased in the order of A-type < B-type < AB-type. Whereas, styrene content decreased in the order of A-type > B-type > AB-type. It should be noted that *in-situ* hydrogenation reaction is mainly responsible for the formation of toluene and ethylbenzene. As reported in the literature, the catalytic pyrolysis of polystyrene in the presence of a solid acid catalyst produces more benzene, toluene, and ethylbenzene than the styrene monomer as compared to the thermal pyrolysis (Park et al., 2003). It may be due to the presence of Bronsted acid sites of red clay synthesized catalyst RC-800, which is responsible for the production of aromatic hydrocarbons benzene, toluene, and ethylbenzene (Marczewski et al., 2013). The formation of ethylbenzene on RC-800 catalyst occurs by hydrogenation of styrene in hydrogen transfer reaction (Marczewski et al., 2013). Whereas, toluene is formed from the product ethylbenzene by the cleavage of the -C-C- bond of the ethyl substituent followed by hydrogenation (Onwudili et al., 2009). Moreover, the Bronsted acid sites of solid catalyst are able to protonate the styrene dimers with the formation of carbenium ions which gives the benzene after dealkylation followed by cracking (Marczewski et al., 2013). The pyrolysis of WEPS produced many intermediates along with hydrogen gas which is the main source of hydrogen during the hydrogenation reaction. Vivek et al., 2018 also reported that the plastic donate hydrogen during co-pyrolysis that helps in depolymerization of lignin. Apart from this, Zhang et al., 1995 and Adrados et al., 2012 also reported that the hydrogenation reaction is responsible for the production of valuable aromatic hydrocarbons such as toluene and ethyl benzene. The GC analysis of non-condensable gas of WEPS multiphase pyrolysis and pure hydrogen gas were carried out in thermal conductivity detector (TCD) mode and then the obtained GC characteristic was compared with the GC of pure hydrogen to ensure the

production of hydrogen gas during the degradation of WEPS. The comparison of GC characteristics between pyrolysis gas and pure hydrogen gas is shown in the Appendix A-8. It is clearly seen from the Figure A8.1, the peak of hydrogen gas is obtained at a retention time of 0.90 minute even after the consumption of hydrogen in hydrogenation reaction. Figure 5.28b shows the comparison of GC characteristics obtained for the best pyrolysis oil of AB-type pyrolysis with GC characteristics of some common commercial fuels like gasoline and kerosene.

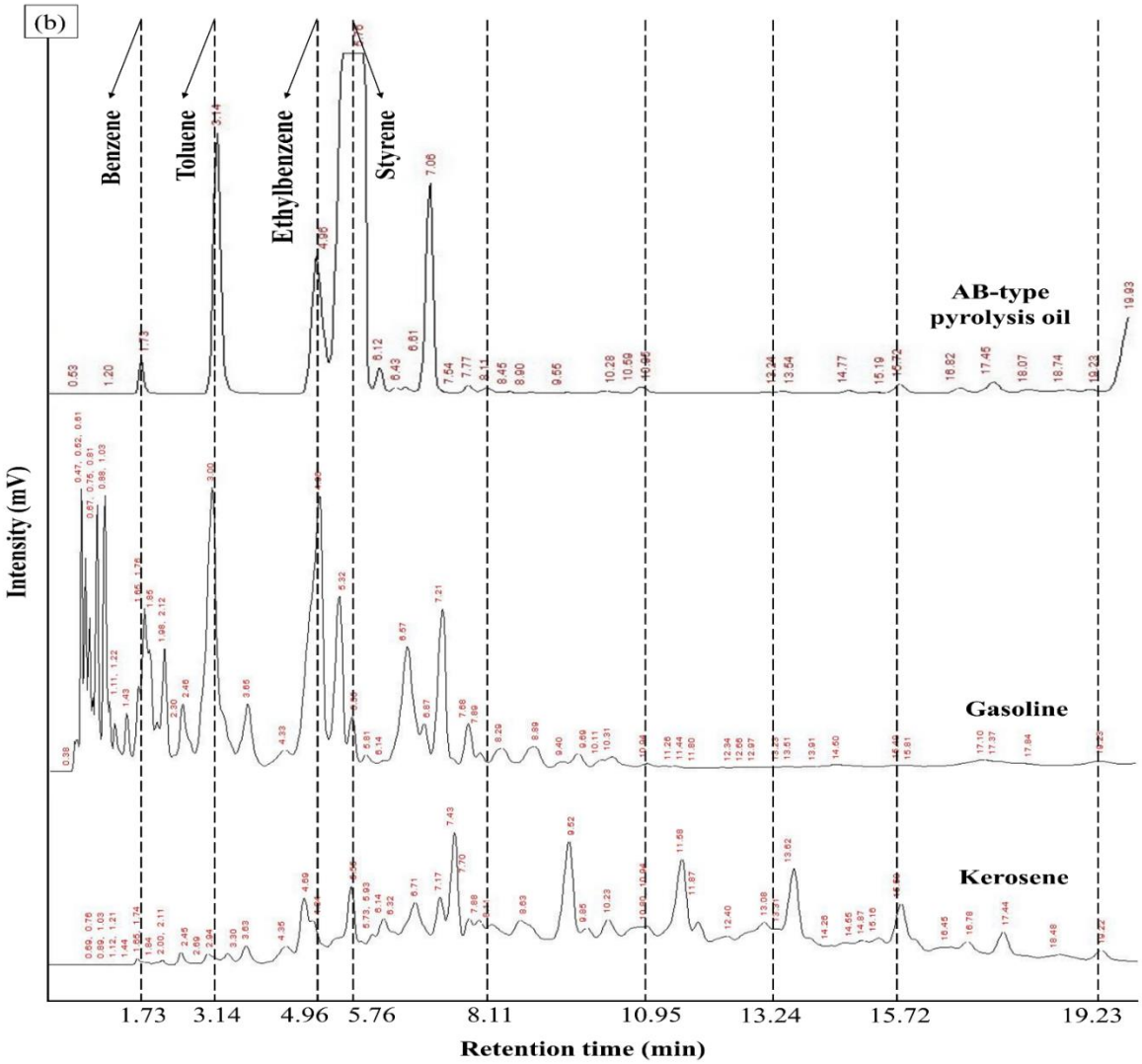

Figure 5.28b Comparison of gas chromatographs of AB-type pyrolysis oil obtained at optimum conditions using best red clay catalyst RC-800 with commercial gasoline and kerosene.

It is clearly seen from the Figure 5.28b that the traces of benzene, toluene, and ethylbenzene were found at the retention time of 1.73 min, 3.14 min, and 4.96 min for commercial gasoline and kerosene and a pyrolysis oil of AB-type, respectively. However, the peak height or % area of peak for benzene was found to be low for both the commercial fuel in comparison to oil of AB-type. Thus, separation of benzene from product oil of AB-type is essential before the use in IC engines. Surprisingly, styrene content was found to be lowest for AB-type pyrolysis, and it may be due to the conversion of styrene to other valuable aromatic hydrocarbons like benzene, toluene and ethylbenzene (BTE). Moreover, most of the components of AB-type catalytic pyrolysis oil at the higher retention time also matches with the commercial fuels gasoline and kerosene.

5.3.3.4.2 FTIR of pyrolysis oil

The FTIR spectra of catalytic pyrolysis oil obtained at the optimum condition i.e., heating rate of 15 ^{o}C/min for all types of pyrolysis and temperature of 600 ^{o}C for A-type and 550 ^{o}C for B-type and AB-type pyrolysis using red clay catalyst RC-800 is shown in Figure 5.29. The important FTIR peaks at their various finger print region of wavenumber are shown in Table 5.22. It is seen from the Table 5.22 that the catalytic pyrolysis oil contains mainly aromatic and aliphatic hydrocarbons. The absorption band found at the wavenumber of 3025.59 cm^{-1}, 3025.10 cm^{-1} and 3025.30 cm^{-1} confirmed the aromatic C-H stretching in A-type, B-type and AB-type catalytic pyrolysis oil, respectively (Budsaereechai et al., 2019). The methylene C-H asymmetric stretching vibrations were observed at a wavenumber of 2925.47 cm^{-1}, 2924.82 cm^{-1} and 2925.61 cm^{-1} for A-type, B-type and AB-type catalytic pyrolysis oil, respectively.

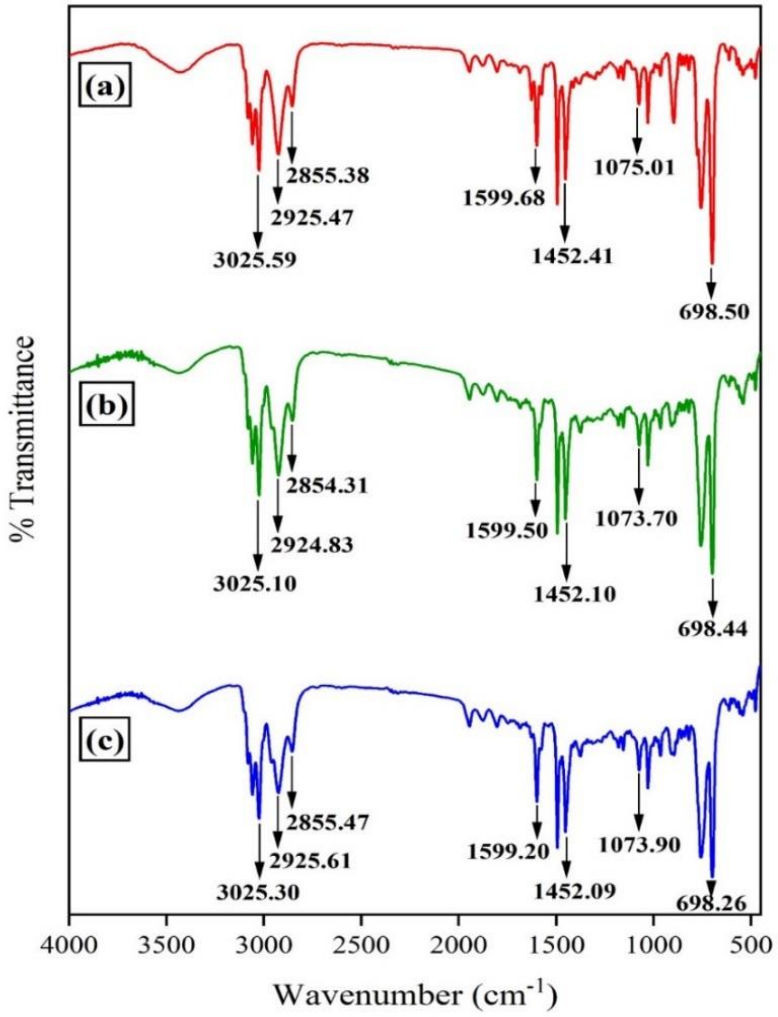

Figure 5.29 FTIR spectrum of catalytic pyrolysis oil obtained at optimum conditions using best red clay catalyst RC-800 (a) A-type/liquid phase (b) B-type/vapour phase (c) AB-type/multiphase.

Similarly, the methylene C-H symmetric stretching vibrations were noticed at a wavenumber of 28555.38 cm^{-1}, 2854.31 cm^{-1}, and 2855.47 cm^{-1} for A-type, B-type and AB-type catalytic pyrolysis, respectively. The C=C-C aromatic ring stretching were found in the A-type, B-type and AB-type catalytic pyrolysis oil at a wavenumber of 1599.68 cm^{-1}, 1599.50 cm^{-1} and 1599.20 cm^{-1}, respectively. The peaks at wavenumber of 1029.01 cm^{-1}, 1028.74 cm^{-1} and 1028.71 cm^{-1} ensured the cyclohexane ring vibrations for A-type, B-type and AB-type catalytic pyrolysis, respectively (Coates, 2006).

Table 5.22 Functional groups present in the pyrolysis oil obtained by catalytic pyrolysis of WEPS at optimum conditions using best red clay catalyst RC-800.

Functional group		Wavenumber (cm^{-1})		
	Standard finger print region	A-type/liquid phase oil	B-type/vapour phase oil	AB-type/ multiphase oil
Aromatic C−H stretching	Above 3000	3422.64 3081.57 3058.80 3025.59	3439.59 3081.19 3058.80 3025.10	3439.95 3081.22 3058.84 3025.30
Methylene C−H asym stretching	2935-2915	2925.47	2924.83	2925.61
Methylene C−H sym stretching	2865-2845	2855.38	2854.31	2855.47
C = C− C aromatic ring stretching	1615-1580	1599.68 1494.33	1599.50 1493.52	1599.20 1493.76
Methyl C−H asym bend	1470-1430	1452.41	1452.10	1452.09
Methyl C−H sym bend	1380-1370	-	1374.40	1376.34
Aromatic C−H in plane bend	1225-950	1180.12 1155.79 1075.01	1180.22 1155.36 1073.70	1180.05 1155.53 1073.90
Cyclohexane ring vibrations	1055-1000/1005-925	1029.01 964.67	1028.74 964.96	1028.71 964.95
Aromatic C−H out of plane bend	860-680	857.45, 842.06, 818.71, 755.62, 698.50	857.50, 818.92, 757.61, 698.44	857.47, 818.71, 757.32, 698.26

5.3.3.4.3 Physicochemical properties of pyrolysis oil

The physicochemical properties such as calorific value, flash and fire point, carbon residue of pyrolysis oil obtained from the catalytic pyrolysis at their respective optimum process conditions i.e., heating rate of 15 ^{o}C/min for all types of pyrolysis and temperature of 600 ^{o}C for A-type, and 550 ^{o}C for B-type and AB-type were determined (Table 5.23). In addition, physicochemical properties of pyrolysis oil were compared with standard fuels such as gasoline and kerosene for the use in IC engines and diesel generator set.

Table 5.23 Physicochemical properties of catalytic pyrolysis oil obtained at optimum conditions using best red clay catalyst RC-800.

Physicochemical properties	Catalytic pyrolysis			Commercial fuels	
	A-type	B-type	AB-type	Gasoline	Kerosene
Gross calorific value (Cal/g)	10238	11095	12810	11315	11052
Carbon residue (wt.%)	0.86	0.65	0.35	0.14	0.18
Flash point (^oC)	46	42	36	22	42
Fire point (^oC)	54	46	40	25	45

It is seen from Table 5.23 that the GCV of pyrolysis oil obtained for A-type/liquid phase (10238 Cal/g), B-type/vapour phase (11095 Cal/g) and AB-type/multiphase (12810 Cal/g) catalytic pyrolysis is higher than the thermal pyrolysis oil (9816 Cal/g). Noticeably, GCV of pyrolysis oil for the AB-type/multiphase pyrolysis is the highest (12810 Cal/g) and it may be due to the two-stage catalytic cracking which is responsible for the production of lighter hydrocarbons (Sonawane et al., 2017) as discussed earlier (page no. 101). Moreover, the calorific value of pyrolysis oil of AB-type/multiphase pyrolysis using RC-800 catalyst was higher than the commercial fuels gasoline (11315 Cal/g) and kerosene (11052 Cal/g) (Gaurh and Pramanik, 2019). It is seen from the Table 5.23 that the carbon residue of AB-type/multiphase pyrolysis oil is lowest (0.35 wt.%) and very close to standard fuels i.e., gasoline and kerosene (Shakirullah et al., 2010). It may be due to the lower amount of high molecular weight aromatics hydrocarbons (Gaurh and Pramanik, 2018a). It is also seen from the Table 5.23 that the AB-type/multiphase catalytic pyrolysis oil exhibits lowest flash point of 36 ^oC among all catalytic pyrolysis oil. Even, flash point of AB-type/multiphase catalytic pyrolysis oil is lower than kerosene (Ahmad et al., 2017) and very close to gasoline (Mukhariya

and Yadav, 2015). The lowest flash point of AB-type/multiphase catalytic pyrolysis oil also confirms the presence of a high amount of lighter paraffin and aromatic contents (Miandad et al., 2018). Thus, based on the physicochemical properties the AB-type catalytic pyrolysis oil could be recommended for the IC engines, generator sets as well as for cooking stoves.

5. 4 Performance comparison of three catalysts for the BTE production

Table 5.24 shows the performance comparison of ZSM-5 ammonium powder, nickel on silica-alumina, and red clay catalyst RC-800 in terms of BTE content for each type of reactor arrangement i.e., A-type, B-type and AB-type at optimized process conditions. The optimum temperature conditions for the multiphase and vapour phase catalytic pyrolysis using all three catalyst i.e., ZSM-5 ammonium powder, Nickel on silica-alumina and red clay catalyst RC-800 were reaction temperature of 550 ^{o}C, at the heating rate of 15 ^{o}C/min (optimum) and feed to catalyst ratio of 20:1 (optimum). However, the optimum conditions for liquid phase catalytic pyrolysis using ZSM-5 ammonium powder, Nickel on silica-alumina and red clay catalyst RC-800 were reaction temperature of 600 ^{o}C, at the heating rate of 15 ^{o}C/min (optimum), and feed to catalyst ratio of 20:1 (optimum). It is clearly seen from the Table 5.24, that the highest BTE content of 28.56 wt.% was obtained using Nickel on silica alumina catalyst at the optimized conditions for multiphase catalytic pyrolysis. Thus, nickel on silica-alumina catalyst found to be best among all three catalysts in terms of BTE content. However, ZSM-5 ammonium powder produced BTE content of 28.12 wt.% and lowest styrene content of 46.30 wt.% for multiphase catalytic pyrolysis. Interestingly, the natural low cost red clay catalyst RC-800 produced BTE content of 27.62 wt.% and styrene content of 60.75 wt.% for multiphase catalytic pyrolysis of WEPS, which is comparable with commercial catalysts ZSM-5 ammonium powder and Nickel on silica-alumina catalyst. Thus, red clay catalyst RC-800

could replace the commercial catalyst for the production of target molecules BTE which is very economical. The vapour phase catalytic pyrolysis produced BTE content of 24.28 wt.%, 21.38 wt.% and 23.51 wt.% for ZSM-5 ammonium powder, Nickel on silica-alumina, and red clay catalyst RC-800, respectively at the optimum conditions. However, the BTE content of 18.98 wt.%, 13.99 wt.% and 18.58 wt.% were obtained using ZSM-5 ammonium powder, Nickel on silica-alumina, and red clay catalyst RC-800, respectively at the optimum conditions for liquid phase/A-type catalytic pyrolysis.

Table 5.24 Comparison between liquid yield and BTE content obtained from different catalysts at optimum condition.

Catalyst type	**ZSM-5 ammonium powder**			**Nickel on silica-alumina**			**Catalyst synthesized from red clay**		
Optimum temperature ºC	**550**	**550**	**600**	**550**	**550**	**600**	**550**	**550**	**600**
Catalytic pyrolysis type	**Multi phase/ AB-type**	Vapour phase/ B-type	Liquid phase/ A-type	**Multi phase/ AB-type**	Vapour phase/ B-type	Liquid phase/ A-type	**Multi phase/ AB-type**	Vapour phase/ B-type	Liquid phase/ A-type
Liquid yield (wt.%)	75.11	78.85	88.05	81.15	83.21	88.54	79.47	80.81	88.82
Gas yield (wt.%)	24.40	21.07	11.33	17.14	15.50	7.04	19.88	18.73	8.83
Benzene (wt.%)	11.68	10.13	5.56	8.05	5.57	3.18	1.47	0.97	0.48
Toluene (wt.%)	12.18	10.14	12.10	7.55	6.53	6.48	15.42	13.86	12.60
Ethylbenzene (wt.%)	4.26	4.00	1.32	12.96	9.28	4.33	10.72	8.68	5.50
Styrene (wt.%)	46.30	46.42	55.78	55.55	65.67	69.94	60.75	63.68	68.83
Total BTE (wt.%)	**28.12**	24.28	18.98	**28.56**	21.38	13.99	**27.62**	23.51	18.58

As discussed earlier, the multiphase/AB-type catalytic pyrolysis facilitates the two stage catalytic cracking and offered enough contact between the hydrocarbon molecules and catalyst particles which accelerates the secondary reactions which are responsible for the formation of benzene, toluene and ethylbenzene (BTE) and reduction of styrene. Thus, BTE content was always higher for multiphase catalytic pyrolysis as compared to the other reactor arrangements i.e., vapour phase/B-type and liquid phase/A-type. It is also seen from the Table 5.24, the highest liquid yield of 81.15 wt.% was obtained for AB-type catalytic pyrolysis using Nickel on silica-alumina catalyst at the optimum conditions. The liquid yield of 75.11 wt.% and 79.47 wt.% were obtained using ZSM-5 ammonium powder and red clay catalyst RC-800, respectively at the optimum conditions for the same multiphase/AB-type catalytic process.

5.5 Process parameters through RSM

The detailed experimental study on pyrolysis of WEPS, shows that the multiphase/AB-type reactor arrangement gives best quality of liquid yield in terms of BTE as compared to all other types of catalytic pyrolysis. Thus, effective process parameters mainly temperature (A), heating rate (B) and feed to catalyst ratio (C) were optimized for multiphase catalytic pyrolysis using ZSM-5 ammonium powder, Nickel on silica-alumina and best natural red clay catalyst RC-800 to achieve highest liquid yield.

5.5.1 RSM coupled with BBD for maximization of liquid yield

The effect of two operating variables on liquid yield (response) was shown in this study. The State-Ease Design software used for the optimization of three operating variables i.e., temperature (A), heating rate (B) and feed to catalyst ratio (C) to produce maximum liquid

yield. As described earlier, the BBD model exhibit 17 experiments runs including 5 center point runs which are given in Table 5.25 to Table 5.27 for three different types of catalysts ZSM-5 ammonium powder, Nickel on silica-alumina and natural red clay catalyst, respectively.

Table 5.25 Box-Behnken (BBD) design matrix for three independent variables with predicted and experimental value using ZSM-5 ammonium powder as catalyst.

S. No.	Temperature (A_1) (^oC)	Heating rate (B_1) (^oC/min)	Feed to catalyst ratio (C_1)	Liquid yield (wt.%)	
				Predicted (Y_1)	Experimental
1	500	10	20:1	67.81	67.79
2	600	10	20:1	67.94	67.95
3	500	20	20:1	66.72	66.71
4	600	20	20:1	66.86	66.88
5	500	15	10:1	60.36	60.37
6	600	15	10:1	60.44	60.43
7	500	15	30:1	67.42	67.43
8	600	15	30:1	67.60	67.59
9	550	10	10:1	61.66	61.67
10	550	20	10:1	60.63	60.62
11	550	10	30:1	68.82	68.83
12	550	20	30:1	67.69	67.68
13	550	15	20:1	75.00	75.11
14	550	15	20:1	75.00	74.98
15	550	15	20:1	75.00	74.93
16	550	15	20:1	75.00	75.05
17	550	15	20:1	75.00	74.91

Table 5.26 Box-Behnken (BBD) design matrix for three independent variables with predicted and experimental value using Nickel on silica-alumina as catalyst.

S. No.	Temperature (A_2) (^oC)	Heating rate (B_2) (^oC/min)	Feed to catalyst ratio (C_2)	Liquid yield (wt.%)	
				Predicted (Y_2)	Experimental
1	500	10	20:1	75.24	75.23
2	600	10	20:1	74.24	74.25
3	500	20	20:1	75.64	75.63
4	600	20	20:1	74.60	74.61
5	500	15	10:1	73.77	73.81
6	600	15	10:1	72.90	72.92
7	500	15	30:1	77.27	77.25
8	600	15	30:1	76.10	76.06
9	550	10	10:1	71.47	71.45
10	550	20	10:1	71.81	71.78
11	550	10	30:1	74.78	74.81
12	550	20	30:1	75.19	75.21
13	550	15	20:1	81.05	81.11
14	550	15	20:1	81.05	80.91
15	550	15	20:1	81.05	80.98
16	550	15	20:1	81.05	81.15
17	550	15	20:1	81.05	81.09

Table 5.27 Box-Behnken (BBD) design matrix for three independent variables with predicted and experimental value using natural red clay as catalyst RC-800.

S. No.	Temperature (A_3) (^oC)	Heating rate (B_3) (^oC/min)	Feed to catalyst ratio (C_3)	Liquid yield (wt.%)	
				Predicted (Y_3)	Experimental
1	500	10	20:1	73.79	73.78
2	600	10	20:1	71.65	71.63
3	500	20	20:1	72.35	72.37
4	600	20	20:1	70.19	70.2
5	500	15	10:1	69.36	69.36
6	600	15	10:1	67.17	67.19
7	500	15	30:1	73.91	73.89
8	600	15	30:1	71.80	71.79
9	550	10	10:1	68.91	68.91
10	550	20	10:1	67.45	67.43
11	550	10	30:1	73.49	73.51
12	550	20	30:1	72.05	72.05
13	550	15	20:1	79.43	79.47
14	550	15	20:1	79.43	79.45
15	550	15	20:1	79.43	79.44
16	550	15	20:1	79.43	79.38
17	550	15	20:1	79.43	79.41

It is clearly seen from Table 5.25 to Table 5.27, the predicted and experimental values are very close to each other for each type of catalyst i.e., ZSM-5 ammonium powder, Nickel on silica-alumina and natural red clay catalyst. Thus, the developed model is well suited to determine the relationship between dependent variable liquid yield (Y_1) and independent variables A_1, B_1 and C_1 for ZSM-5 ammonium powder; dependent variable liquid yield (Y_2) and independent variables A_2, B_2, and C_2 for Nickel on silica-alumina catalyst; dependent variable liquid yield (Y_3) and independent variables A_3, B_3 and C_3 for red clay synthesized catalyst RC-800.

The analysis of variance (ANOVA) of the model is given in Table 5.28 for ZSM-5 ammonium powder catalyst. The Table 5.29 and Table 5.30 show ANOVA for Nickel on silica-alumina and natural red clay catalyst RC-800, respectively.

Table 5.28 ANOVA analysis for response (liquid yield) for ZSM-5 ammonium powder as catalyst.

Source	Sum of squares	Degree of freedom	Mean square	F-value	p-value (Prab> F)	Remark
model	458.52	9	50.95	11989.41	<0.0001	significant
A_1: Temperature	0.038	1	0.038	8.90	0.0204	
B_1: Heating rate	2.37	1	2.37	556.64	<0.0001	
C_1: Feed to catalyst ratio	101.10	1	101.10	23793.22	<0.0001	
A_1B_1	2.500E-005	1	2.500E-005	5.883E-003	0.9410	
A_1C_1	2.500E-003	1	2.500E-003	0.59	0.4681	
B_1C_1	2.500E-003	1	2.500E-003	0.59	0.4681	
A_1^2	74.42	1	74.42	17514.49	<0.0001	
B_1^2	50.38	1	50.38	11857.26	<0.0001	
C_1^2	196.80	1	196.80	46314.81	<0.0001	
Residual	0.030	7	4.249E-003			
Lack of Fit	1.825E-003	3	6.083E-003	0.0.87	0.9634	Not significant
Pure error	0.028	4	6.980E-003			
Correlation total	458.55	16				
Standard deviation	0.065					
Mean	68.17					
CV%	0.096					
R^2	0.9999					
Adjusted R^2	0.9999					
Predicted R^2	0.9998					
Adeq. precision	292.820					

It is clear from Table 5.28 that the p and F-values of the model were < 0.0001 and 11989.41 respectively, and these indicate that the model is significant using ZSM-5 ammonium powder as catalyst. It is also seen from the Table 5.28, the p-value for linear term A_1, B_1 and C_1 are 0.0204, <0.0001 and <0.0001, respectively. Whereas, F-value for linear term A_1, B_1 and C_1 are 8.90, 556.64 and 23793.22, respectively. Thus, the analysis of variance showed that the operating parameters i.e., temperature (A_1), heating rate (B_1) and feed to catalyst ratio (C_1) have their effect on response liquid yield (Y_1) in the order of $C_1 > B_1 > A_1$ and it means feed to catalyst ratio (C_1) has higher impact on the liquid yield, whereas temperature has the lowest impact on the liquid yield (Panjiara and Pramanik, 2020) obtained from the multiphase catalytic pyrolysis of WEPS using ZSM-5 ammonium powder catalyst. The values of R^2, adjusted R^2 and predicted R^2 are 0.9999, 0.9999, and 0.9998, respectively.

The difference between predicted R^2 and adjusted R^2 was less than 0.2, indicates the great fitness of the predicted values, and linear relationship between the actual value and predicted value (Jiang et al., 2021) as shown in Figure 5.30. The relationship between dependent parameter liquid yield Y_1 and independent parameters temperature (A_1), heating rate (B_1), and feed to catalyst ratio (C_1) in terms of actual factors, obtained for multiphase catalytic pyrolysis of WEPS using ZSM-5 ammonium powder catalyst is given in equation (5.1):

$$\text{Liquid yield } (Y_1) = -497.95100 + 1.85009\,A_1 + 4.04685\,B_1 + 3.07020\,C_1 + 1\times10^{-5}\,A_1B_1 + 5\times10^{-5}A_1C_1 - 5\times10^{-4}\,B_1C_1 - 1.68170\times10^{-3}A_1^{\,2} - 0.13837\,B_1^{\,2} - 0.068368\,C_1^{\,2} \quad (5.1)$$

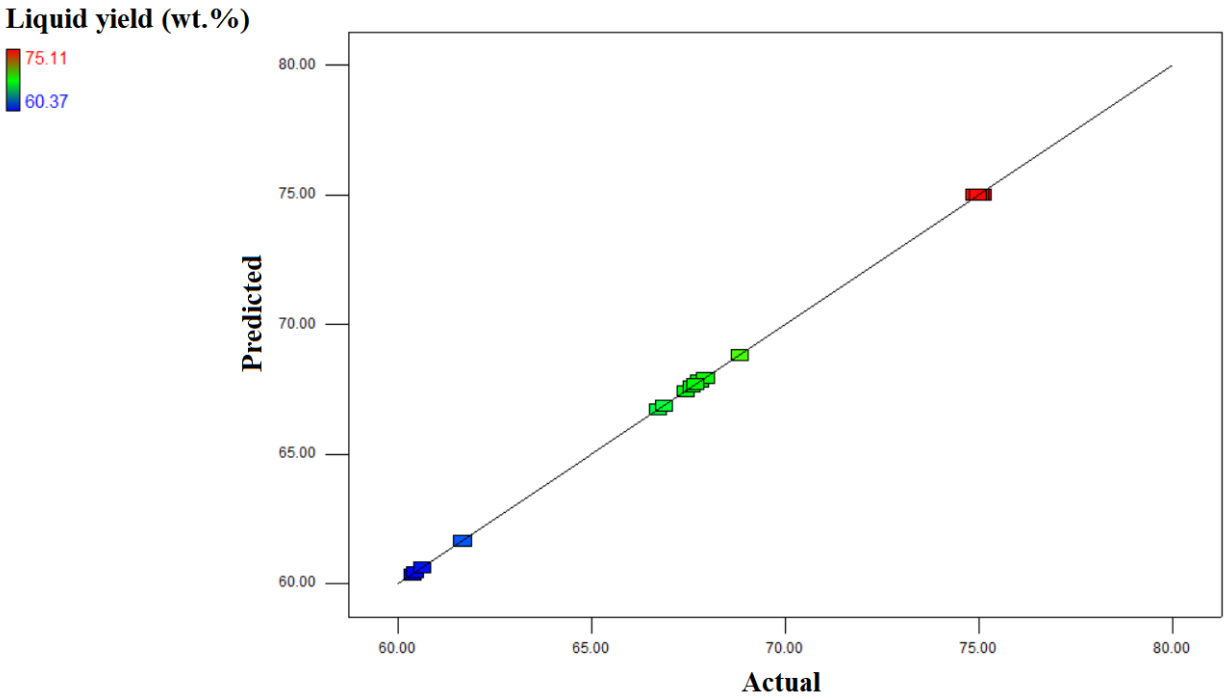

Figure 5.30 Actual vs predicted values of the model for liquid yield using ZSM-5 ammonium powder catalyst.

It is clear from Table 5.29 that the p and F-values of the model were < 0.0001 and 3158.54 respectively, and these indicate that the model was significant for multiphase catalytic pyrolysis of WEPS using Nickel on silica-alumina catalyst. The p-value for linear term A_2, B_2 and C_2 were <0.0001, 0.0003 and <0.0001, respectively (Table 5.29). Whereas, F-value for linear term A_2, B_2 and C_2 were 315.92, 42.13 and 3392.52, respectively. It can be concluded that the feed to catalyst ratio (C_2) has larger effect on liquid yield (Y_2) obtained from the multiphase catalytic pyrolysis using Nickel on silica-alumina catalyst, as compared to the heating rate and temperature. However, temperature is the second effecting factor after feed to catalyst ratio.

Table 5.29 ANOVA analysis for response (liquid yield) for Nickel on silica-alumina as catalyst.

Source	Sum of squares	Degree of freedom	Mean square	F-value	p-value (Prab> F)	Remark
Model	187.23	9	20.80	3158.54	<0.0001	significant
A_2: Temperature	2.08	1	2.08	315.92	<0.0001	
B_2: Heating rate	0.28	1	0.28	42.13	0.0003	
C_2: Feed to catalyst ratio	22.34	1	22.34	3392.52	<0.0001	
A_2B_2	4.000E-004	1	4.000E-004	0.061	0.8124	
A_2C_2	0.022	1	0.022	3.42	0.1070	
B_2C_2	1.225E-003	1	1.225E-003	0.19	0.6792	
A_2^2	20.57	1	20.57	3122.98	<0.0001	
B_2^2	64.30	1	64.30	9762.03	<0.0001	
C_2^2	61.69	1	61.69	9366.42	<0.0001	
Residual	0.046	7	6.586E-003			
Lack of Fit	6.425E-003	3	2.142E-003	0.22	0.8808	Not significant
Pure error	0.040	4	9.920E-003			
Correlation total	187.28	16				
Standard deviation	0.081					
Mean	76.37					
CV%	0.11					
R^2	0.9998					
Adjusted R^2	0.9994					
Predicted R^2	0.9991					
Adeq. precision	153.837					

It should be noted that the values of R^2, adjusted R^2 and predicted R^2 were 0.9998, 0.9994, and 0.9991, respectively. As discussed earlier, the difference between predicted R^2 and adjusted R^2 was less than 0.2, shows the great fitness of the predicted values, and linear relationship between the actual value and predicted value (Jiang et al., 2021) as shown in Figure 5.31. The

relationship between dependent parameter liquid yield (Y_2) and independent parameters temperature (A_2), heating rate (B_2), and feed to catalyst ratio (C_2) in terms of actual factors, obtained for multiphase catalytic pyrolysis of WEPS using Nickel on silica-alumina catalyst is given in equation (5.2):

$$\text{Liquid yield } (Y_2) = -237.03925 + 0.96591\ A_2 + 4.74155\ B_2 + 1.77548\ C_2 - 4\times10^{-5} A_2B_2 - 1.5\times10^{-4} A_2C_2 + 3.5\times10^{-4}\ B_2C_2 - 8.841\times10^{-4} A_2^2 - 0.15631\ B_2^2 - 0.038278\ C_2^2 \quad (5.2)$$

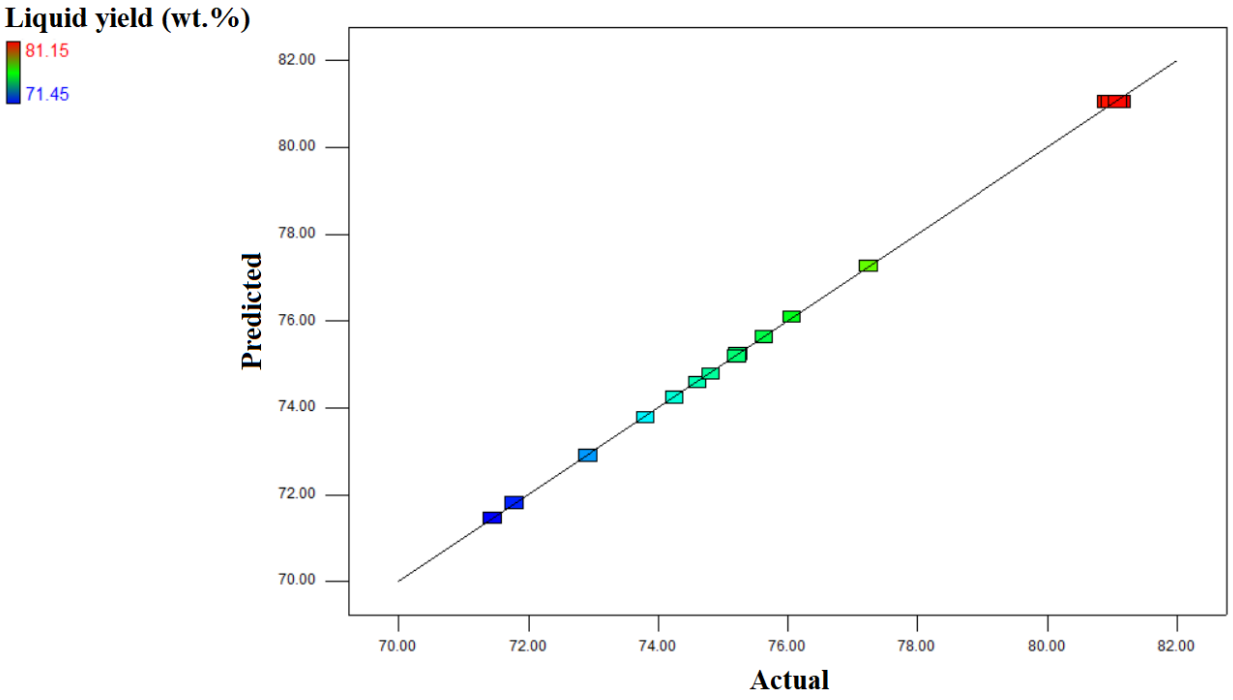

Figure 5.31 Actual vs predicted values of the model for liquid yield using Nickel on silica-alumina catalyst.

Table 5.30 shows the ANOVA for multiphase catalytic pyrolysis of WEPS using best natural red clay catalyst RC-800. The p and F-values of the model were < 0.0001 and 31994.98 respectively, and these indicate that the model is significant for multiphase catalytic pyrolysis of WEPS using RC-800 catalyst.

Table 5.30 ANOVA analysis for response (liquid yield) for natural red clay as catalyst.

Source	Sum of squares	Degree of freedom	Mean square	F-value	p-value (Prab> F)	Remark
Model	311.61	9	34.62	31994.98	<0.0001	significant
A_3:Temperature	9.22	1	9.22	8523.38	<0.0001	
B_3:Heating rate	4.18	1	4.18	3859.06	<0.0001	
C_3: Feed to catalyst ratio	42.09	1	42.09	38895.34	<0.0001	
A_3B_3	1.0000E-004	1	1.0000E-004	0.092	0.7700	
A_3C_3	1.225E-003	1	1.225E-003	1.13	0.3227	
B_3C_3	1.000E-003	1	1.000E-003	0.092	0.7700	
A_3^2	56.90	1	56.90	52585.00	<0.0001	
B_3^2	59.49	1	59.49	54971.64	<0.0001	
C_3^2	113.69	1	113.69	1.051E+005	<0.0001	
Residual	7.575E-003	7	1.082E-003			
Lack of Fit	2.575E-003	3	8.583E-004	0.69	0.6056	Not significant
Pure error	5.000E-003	4	1.250E-003			
Correlation total	311.62	16				
Standard deviation	0.033					
Mean	73.49					
CV%	0.045					
R^2	1.0000					
Adjusted R^2	0.9999					
Predicted R^2	0.9998					
Adeq. precision	485.830					

The p-value for linear term A_3, B_3 and C_3 were <0.0001, <0.0001 and <0.0001, respectively (Table 5.30). Whereas, F-value for linear term A_3, B_3 and C_3 were 8523.38, 3859.06 and 38895.34, respectively. Thus, based on the F-value for linear terms A_3, B_3 and C_3, it could be concluded that the liquid yield obtained from multiphase catalytic pyrolysis using natural red clay catalyst RC-800 catalyst strongly affected by the feed to catalyst ratio (C_3). However,

heating rate (B_3) has least effect on response liquid yield. The values of R^2, adjusted R^2 and predicted R^2 were 1.0000, 0.9999, and 0.9998, respectively. Which shows the great fitness of the predicted values, and linear relationship between the actual value and predicted value as shown in Figure 5.32. The relationship between dependent parameter (liquid yield) and independent parameters temperature (A_3), heating rate (B_3), and feed to catalyst ratio (C_3) in terms of actual factors, obtained for multiphase catalytic pyrolysis of WEPS using best red clay catalyst RC-800 is given in equation (5.3):

$$\text{Liquid yield } (Y_3) = -410.36875 + 1.59567\ A_3 + 4.37500\ B_3 + 2.28713\ C_3 - 2\times10^{-5} A_3B_3 + 3.5\times10^{-5} A_3C_3 + 1\times10^{-4}\ B_3C_3 - 1.47050\times10^{-3} A_3^2 - 0.15035\ B_3^2 - 0.051963\ C_3^2 \quad (5.3)$$

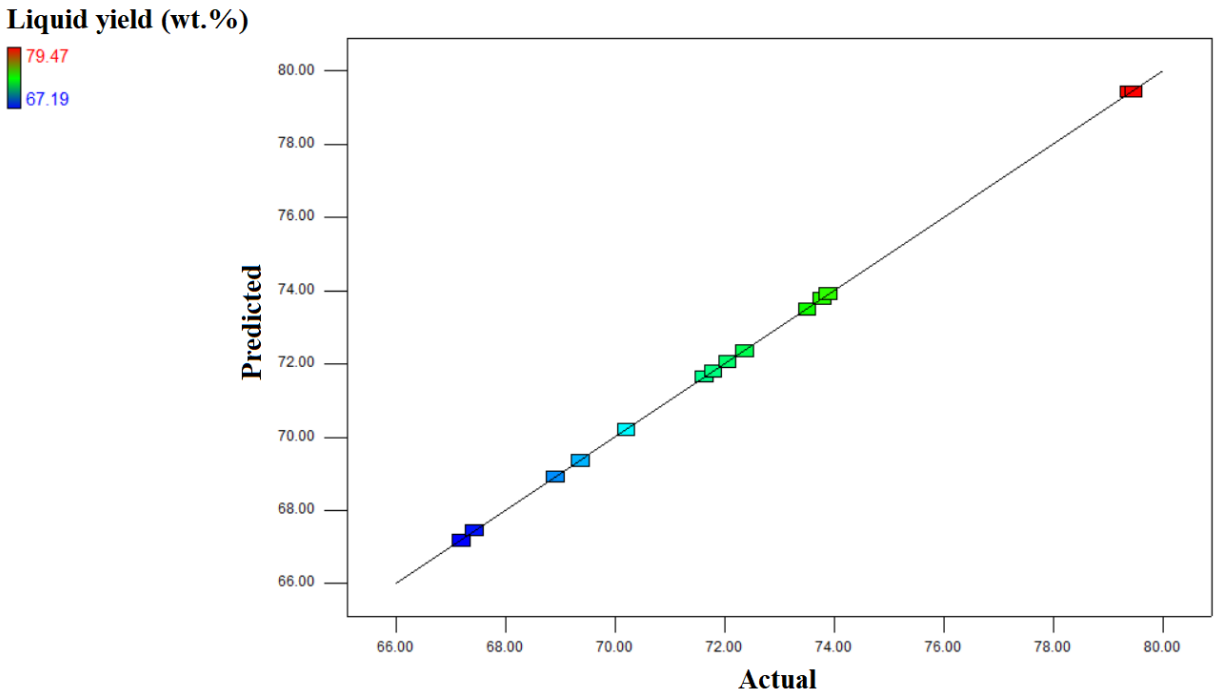

Figure 5.32 Actual vs predicted values of the model for liquid yield using best red clay catalyst RC-800.

5.5.1.1 Optimization of process variables

Figure 5.33 to Figure 5.35 shows the three dimensional (3D) plots for the response i.e., liquid yield obtained from AB-type/multiphase catalytic pyrolysis of WEPS using ZSM-5 ammonium powder, Nickel on silica-alumina and best red clay catalyst RC-800 catalyst, respectively at optimized process condition with respect to two independent operating variables at a time.

5.5.1.1.1 Optimization of process variables using ZSM-5 ammonium powder

Figure 5.33a shows the effect of temperature (A_1) and heating rate (B_1) on the liquid yield (Y_1). The temperature (A_1) was varied from 500 ^oC to 600 ^oC and heating rate (B) was varied from 10 ^oC/min to 20 ^oC/min keeping feed to catalyst ratio (C_1) fixed at its optimum value of 20.80:1. It is clearly seen from 3D plot (Figure 5.33a) that the, liquid yield increases when temperature was varied from 500 ^oC to 566.62 ^oC, and beyond the temperature 566.62 ^oC the, liquid yield goes down. This is due to the Brosnted and Lewis acid sites of ZSM-5 catalyst that facilitates to form carbonium ions appearing on the catalyst surface, which accelerates the secondary reactions at high temperature beyond 566.62 ^oC to produce more gaseous hydrocarbons (Thahir et al., 2021). Lopez et al. 2011b also concluded that the high temperature facilitates the stronger cracking of C-C bonds, which gives rise to gaseous hydrocarbons. It is also seen from the Figure 5.33a that the liquid yield (Y_1) increases with the increase in heating rate up to 15.41 ^oC/min and further increase in heating rate beyond 15.41 ^oC/min, the liquid yield decreases due to the β-scission reaction at higher heating rate resulting higher gaseous yield (Sundararajan and Bhagavathi, 2016). The maximum predicted liquid yield of 74.73 wt.% was obtained at the optimum temperature of 566.62 ^oC and heating rate of 15.41 ^oC/min.

Figure 5.33b shows the effect of temperature (A_1) and feed to catalyst ratio (C_1) on the liquid yield (Y_1) for fixed/optimum value of heating rate of 15.41 ^oC/min. The temperature (A_1) was varied from 500 ^oC to 600 ^oC and feed to catalyst ratio (C_1) was varied from 10:1 to 30:1. It is seen from the Figure 5.33b, the liquid yield increases with increase in feed to catalyst ratio up to 20.80:1 and further increase in the feed to catalyst ratio, the liquid yield decreases. It may be due to the lesser active sites of ZSM-5 catalyst available for cracking of hydrocarbon molecules (Gaurh and Pramanik, 2020). The effect of temperature on liquid yield was similar as discussed earlier (Figure 5.33a). The reason of such trend of liquid yield for varying temperature is already discussed (Figure 5.33a). Similarly, the effect of heating rate (B_1) and feed to catalyst ratio (C_1) on liquid yield for a fixed/optimum temperature of 566.62 ^oC is shown in Figure 5.33c. The trend of 3D plot for the varying heating rate and feed to catalyst ratio are similar as discussed in Figure 5.33a and Figure 5.33b. The predicted maximum liquid yield (Y_1) of 74.73 wt.% was obtained for the optimum temperature of 566.62 ^oC, heating rate of 15.41 ^oC/min and feed to catalyst ratio of 20.80:1.

(a)

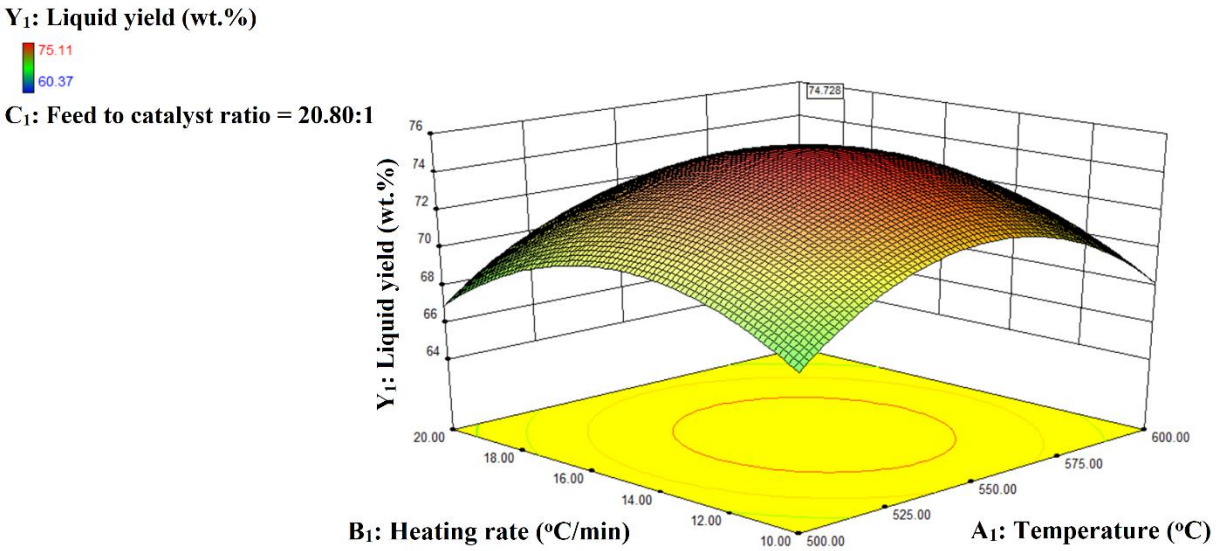

(b)

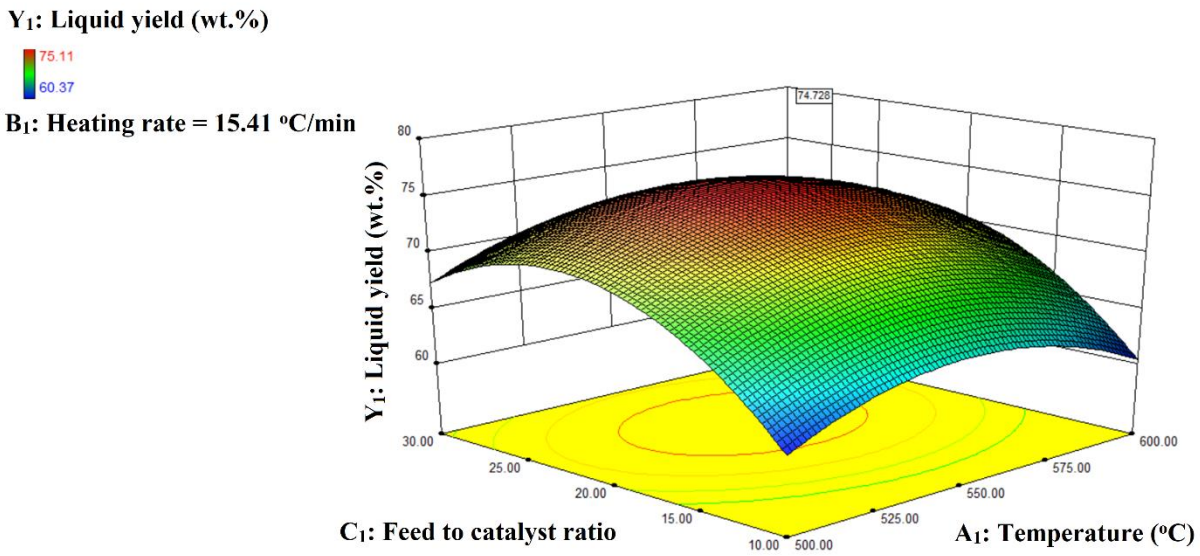

(c)

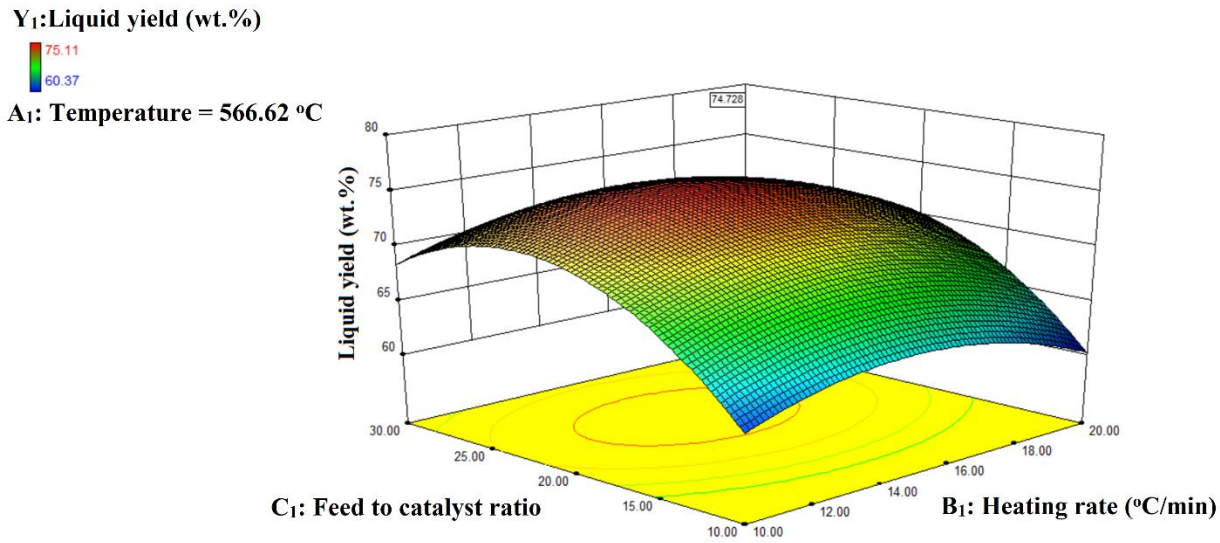

Figure 5.33 Three dimensional surface response for liquid yield showing effects of (A_1) temperature and heating rate (B_1) temperature and feed to catalyst ratio (C_1) heating rate and feed to catalyst ratio using ZSM-5 ammonium powder catalyst.

The multiphase catalytic pyrolysis experiments were carried out three times at optimum operating conditions suggested by the model to validate it. For each pyrolysis experiment, fresh feed material and catalyst were taken as per the feed to catalyst ratio. It should be noted from Table 5.31 that only 0.92 % error was found between the predicted (74.73 wt.%) and experimental value (74.04 wt.%). Very low percentage error of 0.92 % confirms that the developed RSM-BBD model is significant and applicable.

Table 5.31 predicted and experimental value of liquid yield at optimized condition using ZSM-5 ammonium powder as catalyst.

Temperature (°C)	Heating rate (°C/min)	Feed to catalyst ratio	Liquid yield (wt.%)					% Error
			Model predicted value	Exp run-1	Exp run-2	Exp run-3	Average value	
566.62	15.41	20.80:1	74.73	73.98	74.38	73.75	74.04	0.92

Additionally, to check the significance of developed RSM-BBD model equation (5.1), the multiphase catalytic pyrolysis of WEPS using ZSM-5 ammonium powder were performed at three arbitrary conditions of the effective operating variables. As per the arbitrary condition-1: A_1 = 550 °C, B_1= 15 °C/min, C_1= 30:1; arbitrary condition-2: A_1= 500 °C, B_1= 15 °C/min, C_1= 20:1; arbitrary condition-3: A_1= 600 °C, B_1= 10 °C/min, C_1= 10:1 were used to carried out the multiphase catalytic pyrolysis experiment and record the liquid yield. For each arbitrary condition liquid yield was calculated theoretically using equation (5.1) as well as experimentally. The liquid yield calculated by model equation (5.1) for arbitrary condition-1, arbitrary condition-2 and arbitrary condition-3 were 71.71 wt.%, 70.72 wt.% and 57.50 wt.%, respectively (Table 5.32). Whereas, for the same arbitrary condition-1, arbitrary condition-2 and arbitrary condition-3, the experimental values of liquid yield were 71.11 wt.%, 70.23 wt.%

and 57.06 wt.%, respectively. It is clearly shown from Table 5.32 that the percentage error between the predicted/theoretical and experimental value for arbitrary condition-1, arbitrary condition-2 and arbitrary condition-3 were 0.84 %, 0.69 % and 0.77 %, respectively. Such low errors between the predicted and experimental value of liquid yield (response) suggested that the developed RSM-BBD model is significant.

Table 5.32 Predicted and experimental value of liquid yield at random conditions using ZSM-5 ammonium powder catalyst.

Random conditions	Temperature (°C)	Heating rate (°C/min)	Feed to catalyst ratio	Predicted liquid yield (wt.%)	Experimental liquid yield (wt.%)	% Error
Arbitrary condition-1	550	15	30:1	71.71	71.11	0.84
Arbitrary condition-2	500	15	20:1	70.72	70.23	0.69
Arbitrary condition-3	600	10	10:1	57.50	57.06	0.77

5.5.1.1.2 Optimization of process variables using Nickel on silica-alumina catalyst

Figure 5.34a shows the effect of temperature (A_2) and heating rate (B_2) on the liquid yield (Y_2) obtained from multiphase catalytic pyrolysis of WEPS using Nickel on silica-alumina catalyst. The temperature (A_2) was varied from 500 °C to 600 °C and heating rate (B_2) was varied from 10 °C/min to 20 °C/min keeping feed to catalyst ratio (C_2) fixed at its optimum value of 20.54:1. It is clearly seen from 3D plot (Figure 5.34a) that the, liquid yield increases when temperature was varied from 500 °C to 536.04 °C, and beyond the temperature 536.04 °C the, liquid yield goes down. It may be due to the secondary reactions at high temperature beyond 536.04 °C to produce more gaseous hydrocarbons (Thahir et al., 2021) as discussed earlier (page no. 160). It is also seen from the Figure 5.34a that the liquid yield (Y_2) increases with the increase in heating rate up to 15.02 °C/min and further increase in heating rate beyond 15.02 °C/min, the

liquid yield decreases due to the β-scission reaction at higher heating rate (Sundararajan and Bhagavathi, 2016). This has already been discussed in page no. 160. The predicted highest liquid yield of 81.10 wt.% was obtained at the optimum temperature of 536.04 ^{o}C and heating rate of 15.02 ^{o}C/min. Figure 5.34b shows the effect of temperature (A_2) and feed to catalyst ratio (C_2) on the liquid yield (Y_2) for fixed/optimum value of heating rate of 15.02 ^{o}C/min. The temperature (A_2) was varied from 500 ^{o}C to 600 ^{o}C and feed to catalyst ratio (C_2) was varied from 10:1 to 30:1. It is seen from the Figure 5.34b, the liquid yield increases with increase in feed to catalyst ratio up to 20.54:1 and further increase in the feed to catalyst ratio, the liquid yield decreases. It may be due to the lesser active sites of Nickel on silica-alumina catalyst available for cracking of hydrocarbon molecules (Gaurh and Pramanik, 2020) as already discussed in page no. 161. The effect of temperature on liquid yield was similar as discussed earlier (Figure 5.33a). The reason of such trend of liquid yield for varying temperature is already discussed (Figure 5.33a). Similarly, the effect of heating rate (B_2) and feed to catalyst ratio (C_2) on liquid yield for a fixed/optimum temperature of 536.04 ^{o}C is shown in Figure 5.34c.

(a)

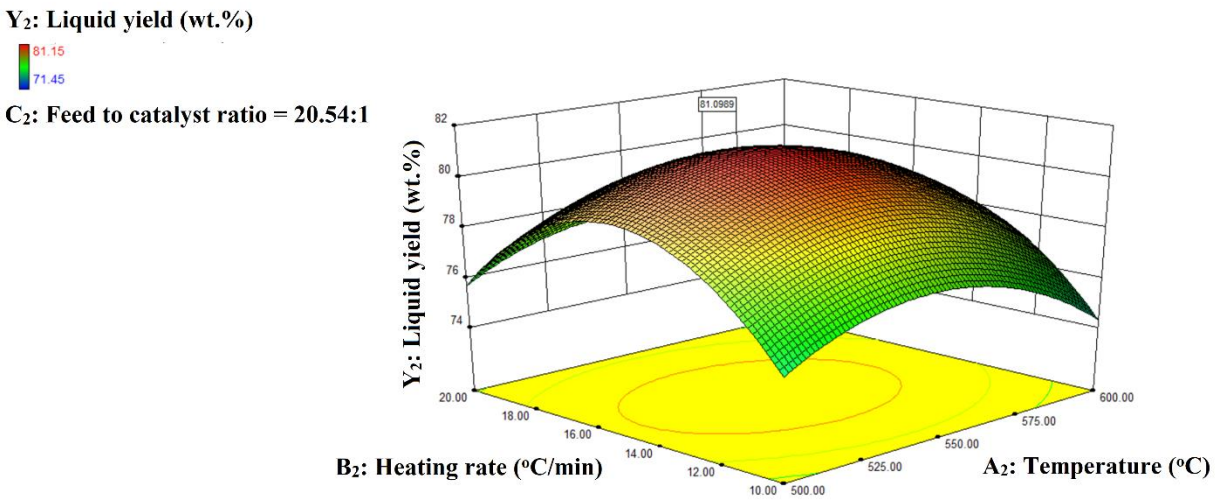

(b)

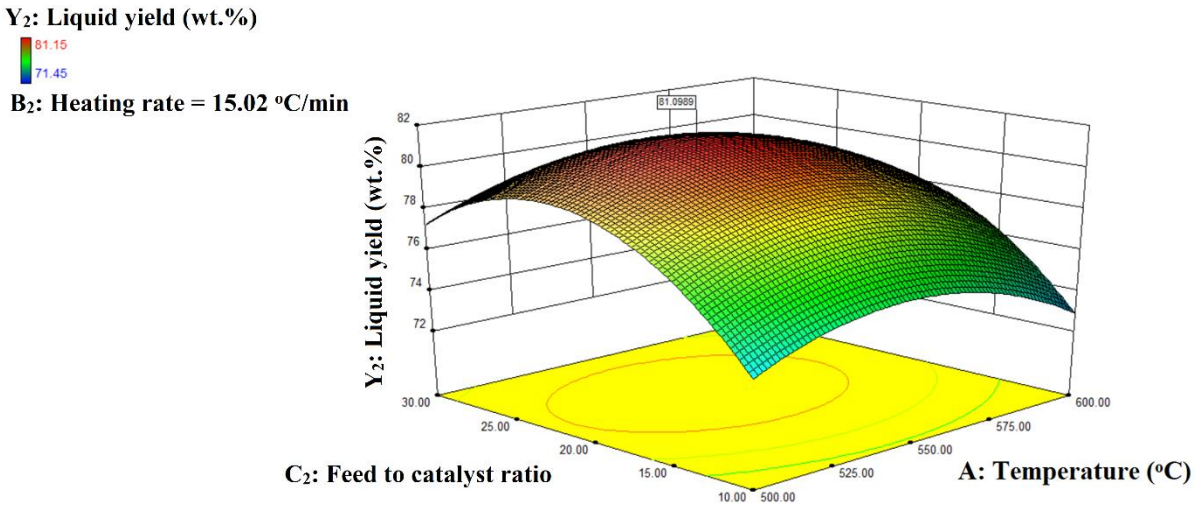

(c)

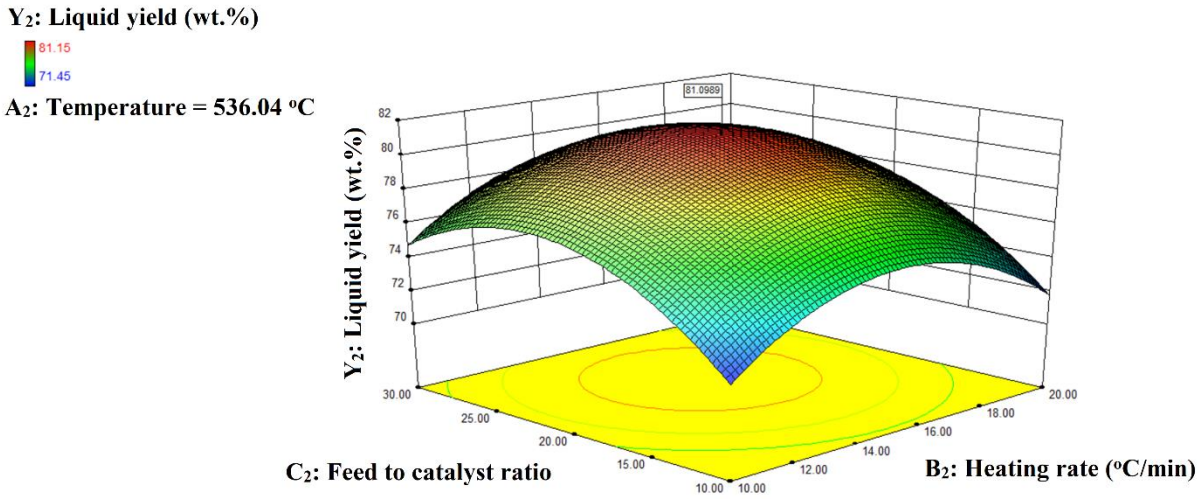

Figure 5.34 Three dimensional surface response for liquid yield showing effects of (A_2) temperature and heating rate (B_2) temperature and feed to catalyst ratio (C_2) heating rate and feed to catalyst ratio using Nickel on silica-alumina catalyst.

The trend of 3D plot for the varying heating rate and feed to catalyst ratio are similar as discussed in Figure 5.34a and Figure 5.34b. The predicted maximum liquid yield (Y_2) of 81.10 wt.% was obtained for the optimum temperature of 536.04 ^oC, heating rate of 15.02 ^oC/min

and feed to catalyst ratio of 20.54:1 using Nickel on silica-alumina catalyst. The multiphase catalytic pyrolysis experiments using Nickel on silica-alumina catalyst were carried out three times at optimum operating conditions suggested by the model to validate it. It should be noted from Table 5.33 that only 0.41 % error was found between the predicted (81.10 wt.%) and experimental value (80.85 wt.%) confirms the developed RSM-BBD model is significant and applicable.

Table 5.33 predicted and experimental value of liquid yield at optimized condition using Nickel on silica-alumina catalyst.

Temperature (°C)	Heating rate (°C/min)	Feed to catalyst ratio	Liquid yield (wt.%)					% Error
			Model predicted value	Exp run-1	Exp run-2	Exp run-3	Average value	
536.04	15.02	20.54:1	81.10	80.63	80.75	80.93	80.85	0.41

The developed RSM-BBD model equation (5.2) for multiphase catalytic pyrolysis of WEPS using Nickel on silica-alumina catalyst was also validated using three arbitrary conditions of the effective operating variables. As per the arbitrary condition-1: A_2= 550 °C, B_2= 15 °C/min, C_2= 30:1; arbitrary condition-2: A_2= 500 °C, B_2= 15 °C/min, C_2= 20:1; arbitrary condition-3, A_2= 600 °C, B_2= 10 °C/min, C_2= 10:1 were used to carried out the multiphase catalytic pyrolysis experiment and measured the liquid yield. For each arbitrary condition liquid yield was calculated theoretically using equation (5.2) as well as experimentally. The liquid yield calculated by model equation (5.2) for arbitrary condition-1, arbitrary condition-2 and arbitrary condition-3 were 78.89 wt.%, 79.35 wt.% and 68.84 wt.%, respectively (Table 5.34). Whereas, for the same arbitrary condition-1, arbitrary condition-2 and arbitrary condition-3, the experimental values of liquid yield were 78.47 wt.%, 78.89 wt.% and 68.38 wt.%, respectively.

It is clearly shown from Table 5.34 that the percentage error between the predicted/theoretical and experimental value for arbitrary condition-1, arbitrary condition-2 and arbitrary condition-3 were 0.53 %, 0.58 % and 0.67 %, respectively. Such low errors between the predicted and experimental value of liquid yield (response) suggested that the developed RSM-BBD model is significant.

Table 5.34 Predicted and experimental value of liquid yield at random conditions using Nickel on silica-alumina catalyst.

Random conditions	Temperature (°C)	Heating rate (°C/min)	Feed to catalyst ratio	Predicted liquid yield (wt.%)	Experimental liquid yield (wt.%)	% Error
Arbitrary condition-1	550	15	30:1	78.89	78.47	0.53
Arbitrary condition-2	500	15	20:1	79.35	78.89	0.58
Arbitrary condition-3	600	10	10:1	68.84	68.38	0.67

5.5.1.1.3 Optimization of process variables using best red clay catalyst RC-800

Figure 5.35a shows the effect of temperature (A_3) and heating rate (B_3) on the liquid yield (Y_3) obtained from multiphase catalytic pyrolysis of WEPS using best red clay catalyst RC-800. The temperature (A_3) was varied from 500 °C to 600 °C and heating rate (B_3) was varied from 10 °C/min to 20 °C/min keeping feed to catalyst ratio (C_3) fixed at its optimum value of 20.33:1. It is clearly seen from 3D plot (Figure 5.35a) that the, liquid yield increases when temperature was varied from 500 °C to 536.51 °C, and beyond the temperature 536.51 °C the, liquid yield goes down. The reason for such trend of liquid yield with respect to reaction temperature has already been discussed in page no. 160. It is also seen from the Figure 5.35a that the liquid

yield (Y_3) increases with the increase in heating rate up to 15.15 ^oC/min and further increase in heating rate beyond 15.15 ^oC/min. The β- scission reactions are responsible for the decrease in liquid yield beyond heating rate of 15.15 ^oC/min has already been discussed in page no. 160. The predicted maximum liquid yield of 79.49 wt.% was obtained at the optimum temperature of 536.51 ^oC and heating rate of 15.15 ^oC/min. Figure 5.35b shows the effect of temperature (A_3) and feed to catalyst ratio (C_3) on the liquid yield (Y_3) for fixed/optimum value of heating rate of 15.15 ^oC/min. The temperature (A_3) was varied from 500 ^oC to 600 ^oC and feed to catalyst ratio (C_3) was varied from 10:1 to 30:1. It is seen from the Figure 5.35b, the liquid yield increases with increase in feed to catalyst ratio up to 20.33:1 and further increase in the feed to catalyst ratio, the liquid yield decreases. Similarly, the effect of heating rate (B_3) and feed to catalyst ratio (C_3) on liquid yield for a fixed/optimum temperature of 536.51 ^oC is shown in Figure 5.35c.

(a)

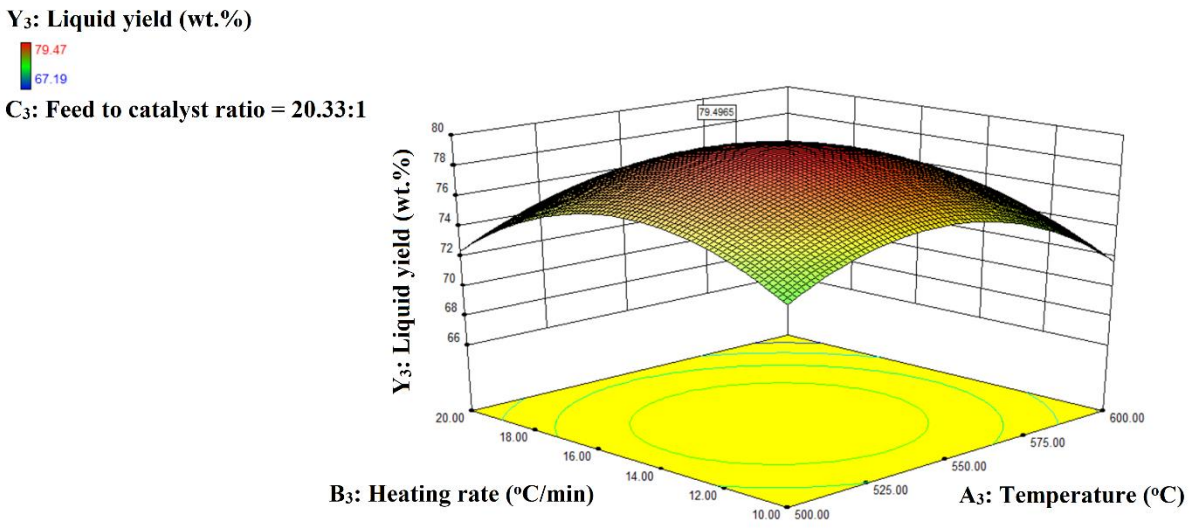

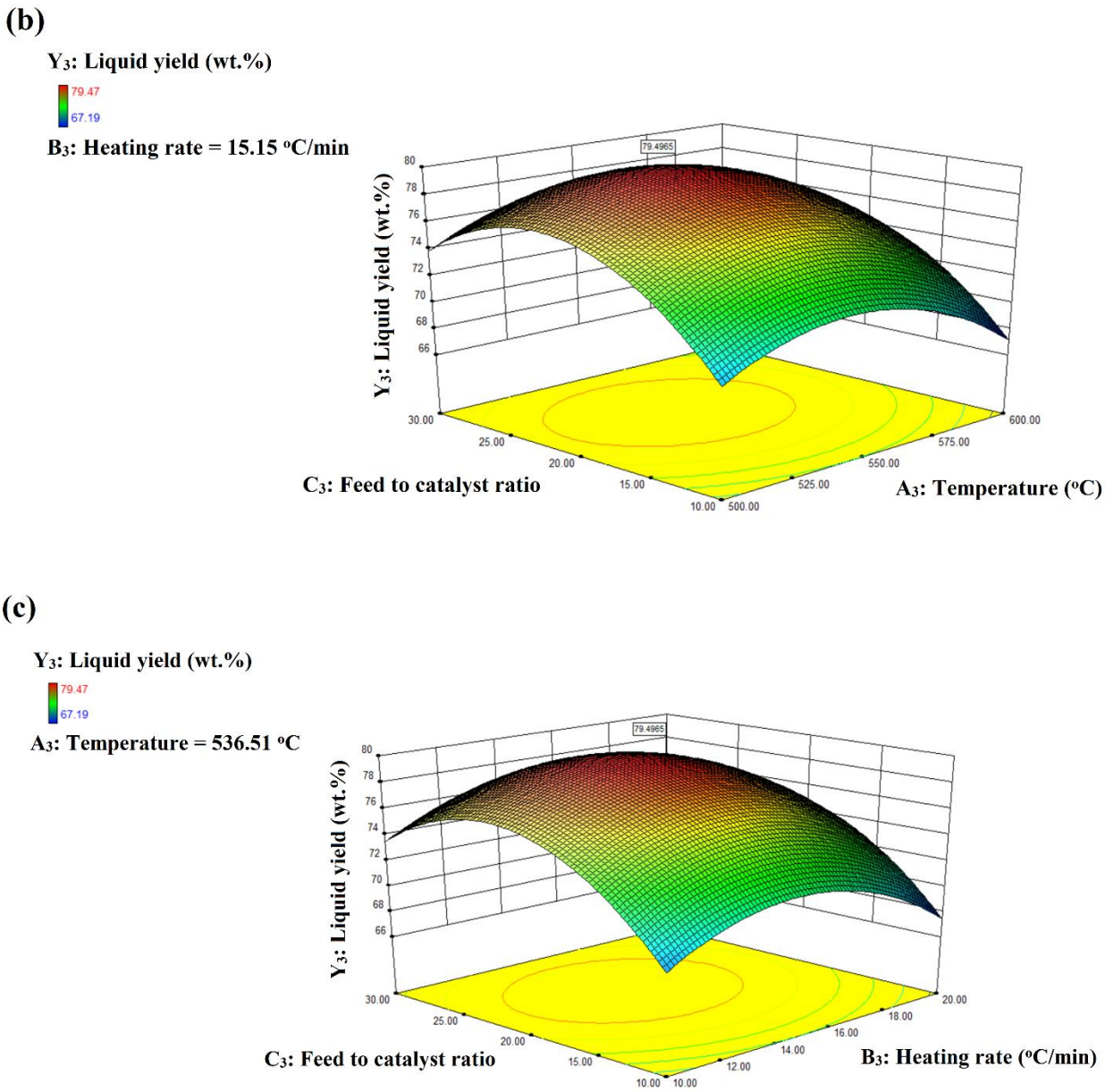

Figure 5.35 Three dimensional surface response for liquid yield showing effects of (A_3) temperature and heating rate (B_3) temperature and feed to catalyst ratio (C_3) heating rate and feed to catalyst ratio using best red clay catalyst RC-800.

The trend of 3D plot for the varying heating rate and feed to catalyst ratio are similar as discussed in Figure 5.35a (page no. 169) and Figure 5.35b (page no. 170). The predicted maximum liquid yield (Y) of 79.49 wt.% was obtained for the optimum temperature of 536.51

^{o}C, heating rate of 15.15 ^{o}C/min and feed to catalyst ratio of 20.33:1 using best red clay catalyst RC-800. The multiphase catalytic pyrolysis experiments using Nickel on silica-alumina catalyst were carried out three times at optimum operating conditions suggested by the model to validate it. It should be noted from Table 5.35 that only 0.77 % error was found between the predicted (79.49 wt.%) and experimental value (78.88 wt.%). Very low percentage error of 0.77 % confirms that the developed RSM-BBD model is significant and applicable.

Table 5.35 predicted and experimental value of liquid yield at optimized condition using best red clay catalyst RC-800.

Temperature (^{o}C)	Heating rate (^{o}C/min)	Feed to catalyst ratio	Liquid yield (wt.%)					% Error
			Model predicted value	Exp run-1	Exp run-2	Exp run-3	Average value	
536.51	15.15	20.33:1	79.49	78.96	79.01	78.68	78.88	0.77

The multiphase catalytic pyrolysis experiments using RC-800 catalyst were performed at three arbitrary conditions of the effective operating variables to validate the model equation (5.3) developed by RSM-BBD. Three arbitrary conditions are arbitrary condition-1: A_3 = 550 ^{o}C, B_3 = 15 ^{o}C/min, C_3 = 30:1; arbitrary condition-2: A_3= 500 ^{o}C, B_3 = 15 ^{o}C/min, C_3 = 20:1; arbitrary condition-3, A_3 = 600 ^{o}C, B_3 = 10 ^{o}C/min, C_3 = 10:1, which are used to carried out the multiphase catalytic pyrolysis experiments and measured the liquid yield. For each arbitrary condition liquid yield was calculated theoretically using equation (5.3) as well as experimentally. The liquid yield calculated by model equation (5.3) for arbitrary condition-1, arbitrary condition-2 and arbitrary condition-3 were 76.52 wt.%, 76.83 wt.% and 64.14 wt.%, respectively (Table 5.36). Whereas, for the same arbitrary condition-1, arbitrary condition-2 and arbitrary condition-3, the experimental values of liquid yield were 75.69 wt.%, 76.15 wt.%

and 63.87 wt.%, respectively. It is clearly shown from Table 5.36 that the percentage error between the predicted/theoretical and experimental value for arbitrary condition-1, arbitrary condition-2 and arbitrary condition-3 were 1.08 %, 0.89 % and 0.42 %, respectively. The % errors between the predicted and experimental value of liquid yield (response) in the range of 1.08 % - 0.42 % suggested that the developed RSM-BBD model is significant.

Table 5.36 Predicted and experimental value of liquid yield at random conditions using red clay catalyst RC-800.

Random conditions	Temperature (°C)	Heating rate (°C/min)	Feed to catalyst ratio	Predicted liquid yield (wt.%)	Experimental liquid yield (wt.%)	% Error
Arbitrary condition-1	550	15	30:1	76.52	75.69	1.08
Arbitrary condition-2	500	15	20:1	76.83	76.15	0.89
Arbitrary condition-3	600	10	10:1	64.14	63.87	0.42

The process parameters optimized by RSM reasonably predicted the experimental data irrespective of catalyst type for the reactor arrangement. The negligible error between predicted and experimental value of liquid yield was found for all three types of catalysts when the experiment was performed using RSM model predicted optimized process conditions.

5.5.2 Analysis of pyrolysis oil

5.5.2.1 Qualitative analysis of pyrolysis oil obtained using three different catalysts

The pyrolysis oil obtained from multiphase catalytic pyrolysis of WEPS using each catalyst i.e., ZSM-5 ammonium powder, Nickel on silica-alumina and best red clay catalyst RC-800 at their respective optimized conditions was characterized by gas chromatography in order to

identify the BTE and styrene content. As it is discussed earlier, the BTE and styrene content were determined using calibration characteristics (Figure 3.8, page no. 59). Figure 5.36a to Figure 5.36c shows the GC-characteristics of pyrolysis oil obtained at optimized condition using ZSM-5 ammonium powder, Nickel on silica-alumina and best red clay catalyst RC-800 and comparison standard fuels gasoline and kerosene, respectively.

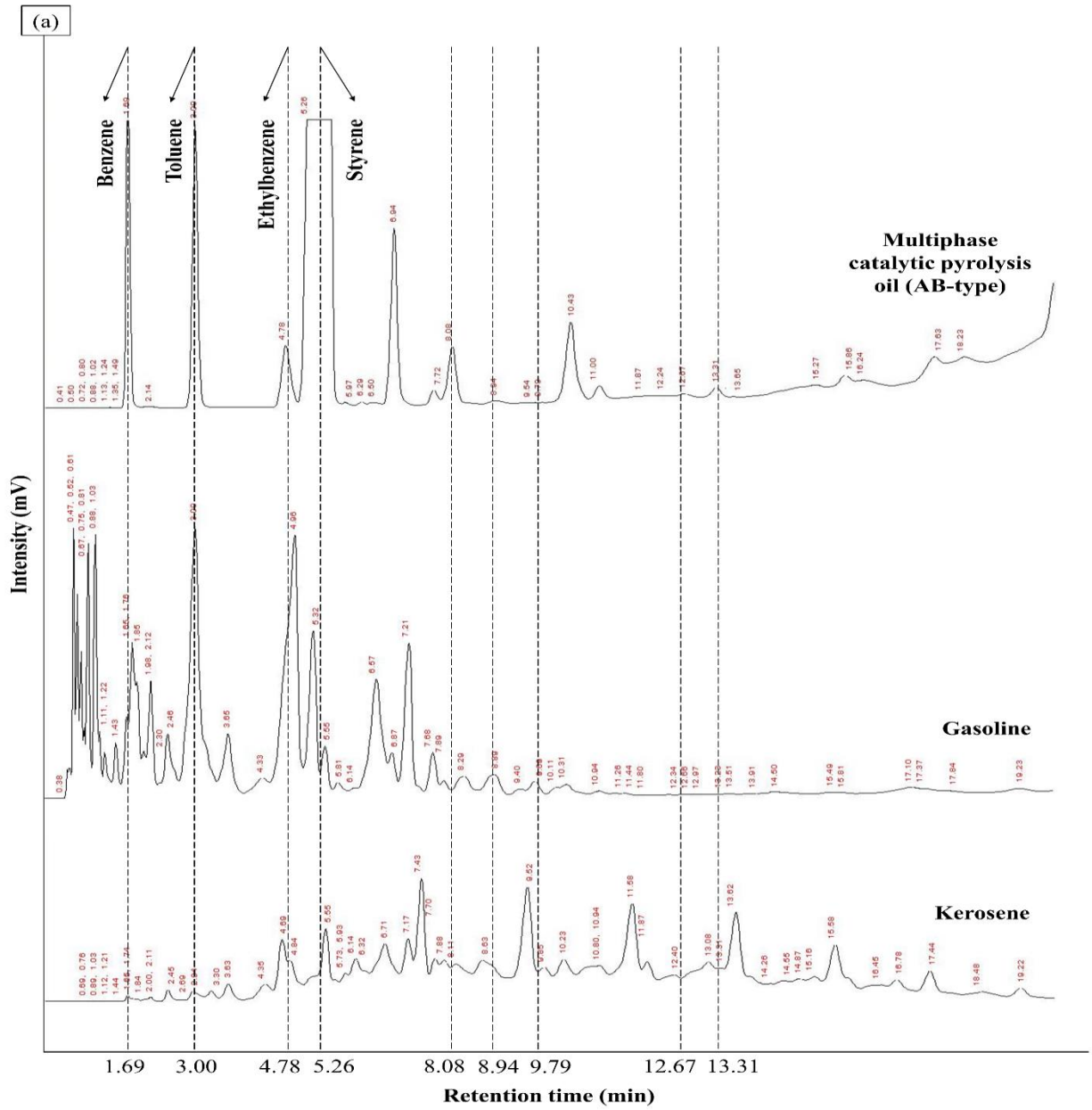

Figure 5.36a Comparison of gas chromatographs of multiphase catalytic pyrolysis oil obtained at optimized conditions using ZSM-5 ammonium powder catalyst with commercial gasoline and kerosene.

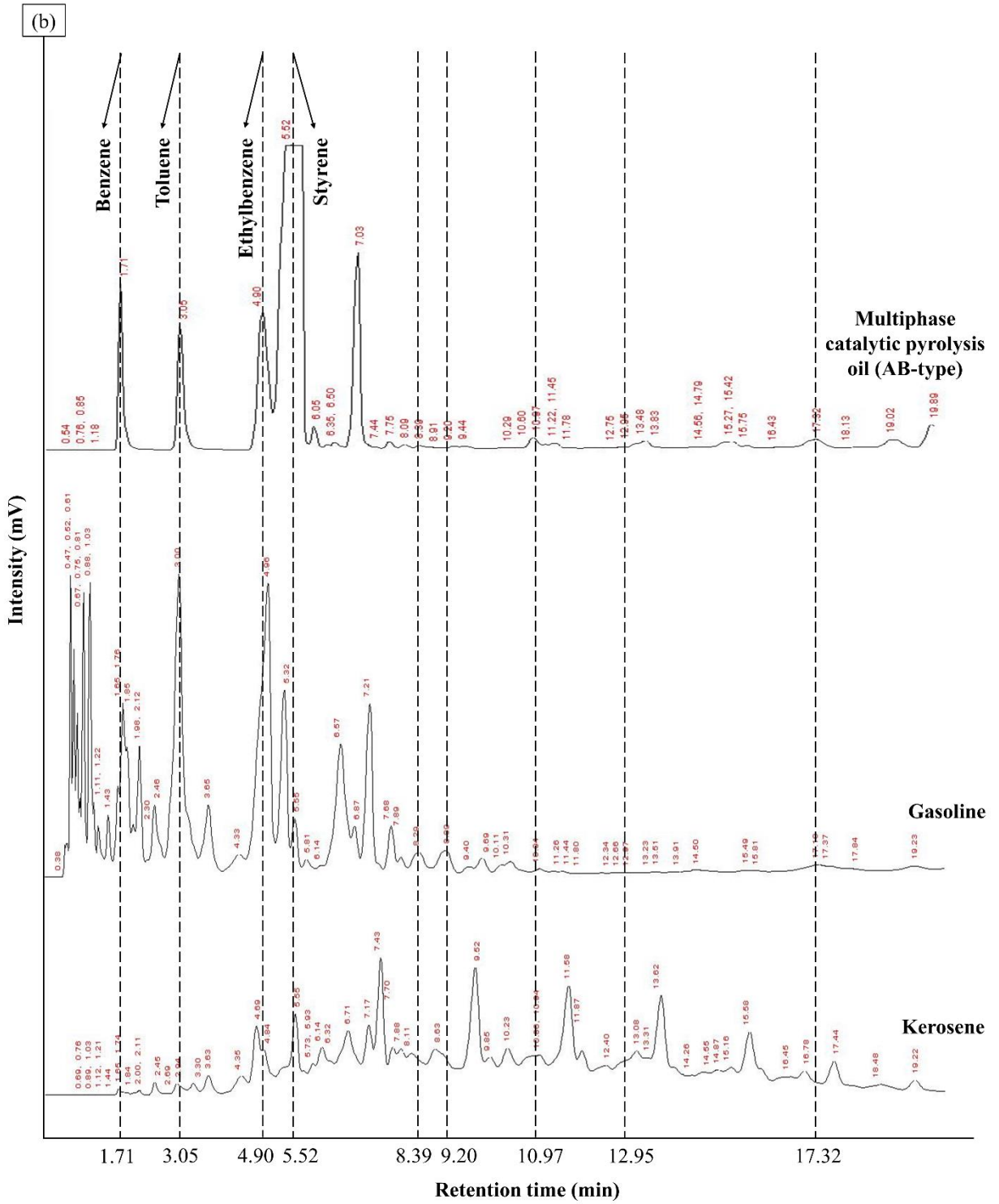

Figure 5.36b Comparison of gas chromatographs of multiphase catalytic pyrolysis oil obtained at optimized conditions using Nickel on silica-alumina catalyst with commercial gasoline and kerosene.

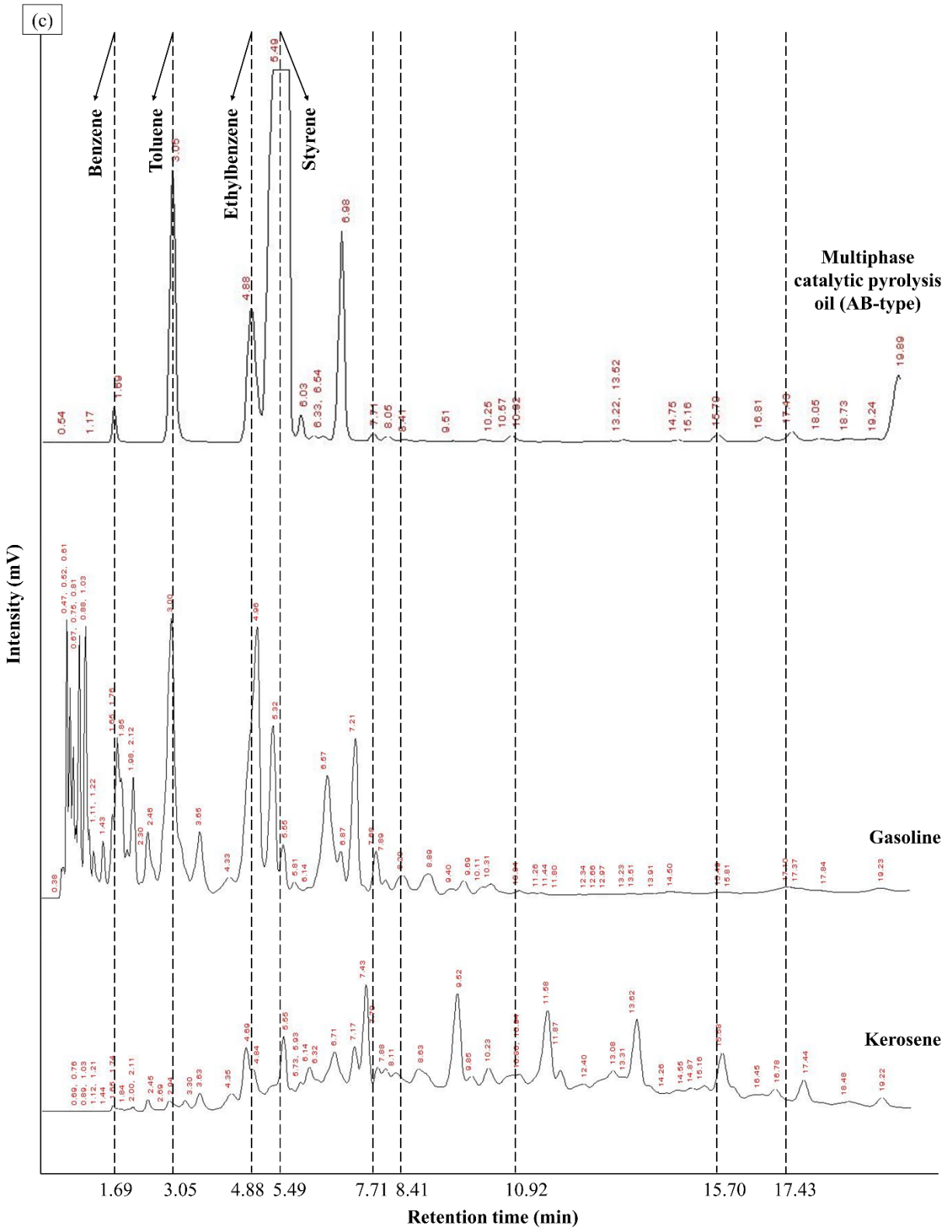

Figure 5.36c Comparison of gas chromatographs of multiphase catalytic pyrolysis oil obtained at optimized conditions using best red clay catalyst RC-800 with commercial gasoline and kerosene.

It should be noted that the Figure 5.36a to Figure 5.36c show the prominent peaks for benzene, toluene, and ethylbenzene (BTE) in the pyrolysis oil obtained from multiphase catalytic pyrolysis. However, a comparison between multiphase catalytic pyrolysis oil and commercial gasoline and kerosene fuel is shown to check the suitability of the use of pyrolysis oil in internal combustion (IC) engine. It is seen from Figure 5.36a most of the components of pyrolysis oil obtained using ZSM-5 ammonium powder, are matches with gasoline and kerosene at higher retention time between 8.08 min to 13.31 min. The pyrolysis oil obtained from multiphase catalytic pyrolysis having total BTE content of 27.86 wt.% and styrene content of 50.54 wt.% (Table 5.37). The benzene, toluene and ethylbenzene content of 11.62 wt.%, 12.16 wt.% and 4.08 wt.%, respectively were found in pyrolysis oil. Similarly, many components of pyrolysis oil obtained from multiphase catalytic pyrolysis of WEPS using Nickel on silica-alumina catalyst at optimized condition are also matches with commercial fuel gasoline and kerosene at higher retention between 8.39 min to 17.32 min (Figure 5.36b). The pyrolysis oil obtained from multiphase catalytic pyrolysis having total BTE content of 28.44 wt.% and styrene content of 56.13 wt.% (Table 5.37). The benzene, toluene and ethylbenzene content of 8.10 wt.%, 7.57 wt.% and 12.77 wt.%, respectively were found in multiphase catalytic pyrolysis oil obtained using Nickel on silica-alumina catalyst. Figure 5.36c shows the GC- characteristics of pyrolysis oil obtained using RC-800 catalyst with commercial fuel gasoline and kerosene. Most of the peaks at higher retention time in between 7.71 min to 17.43 min matches with commercial fuels gasoline and kerosene. The pyrolysis oil obtained from multiphase catalytic pyrolysis of WEPS using RC-800 catalyst having total BTE and styrene content of 26.49 wt.% and 61.78 wt.%, respectively. The benzene, toluene and ethylbenzene content of 1.41 wt.%, 14.81 wt.% and 10.27 wt.%, respectively were found in pyrolysis oil (Table 5.37).

Table 5.37 Benzene, toluene and ethylbenzene (BTE) content in the pyrolysis oil obtained at optimized conditions from multiphase catalytic pyrolysis using ZSM-5 ammonium powder, Nickel on silica-alumina, Red clay catalyst RC-800.

Catalyst	Aromatic content (wt.%)				
	Benzene	**Toluene**	**Ethylbenzene**	**Styrene**	**Total BTE**
ZSM-5 ammonium powder	11.62	12.16	4.08	50.54	27.86
Nickel on silica-alumina	8.10	7.57	12.77	56.13	28.44
Red clay catalyst RC-800	1.41	14.81	10.27	61.78	26.49

5.5.2.2 Physicochemical properties of pyrolysis oil obtained using three different catalysts

The physicochemical properties viz., gross calorific value (GCV), carbon residue, flash and fire point of multiphase catalytic pyrolysis oil obtained at the optimum condition were determined using standard test methods and given in Table 5.38. It is clear from Table 5.38 that the GCV of multiphase catalytic pyrolysis oil obtained at optimized conditions using ZSM-5ammonium powder (12547 Cal/g), Nickel on silica-alumina catalyst (12813 Cal/g) and best red clay catalyst RC-800 (11214 Cal/g) were higher than the commercial fuels gasoline (11315 Cal/g) and kerosene (11052 Cal/g) (Gaurh and Pramanik, 2019). Very high calorific value of multiphase catalytic pyrolysis oil indicates the better efficiency when used in IC engine (Romeiro et al., 2012). Furthermore, higher value of GCV confirms the presence of low molecular weight compounds in the multiphase catalytic pyrolysis oil obtained using ZSM-5 ammonium powder, nickel on silica-alumina catalyst and best red clay catalyst RC-800. As it is already discussed that the multiphase catalytic pyrolysis offers two stage catalytic cracking, responsible for the formation of low molecular weight components.

Table 5.38 Physicochemical properties of multiphase catalytic pyrolysis oil obtained at optimum conditions using ZSM-5ammonium powder, nickel on silica-alumina catalyst and best red clay catalyst RC-800 compared with commercial fuel gasoline and kerosene

Physicochemical properties	Catalytic pyrolysis oil			Gasoline	Kerosene
	ZSM-5 ammonium powder	Nickel on silica-alumina	Red clay catalyst RC-800		
Calorific value (Cal/g)	12547	12813	11214	11315	11052
Carbon residue (wt.%)	0.54	0.39	0.33	0.14	0.18
Flash point (ºC)	40	42	34	22	42
Fire point (ºC)	44	46	42	25	45

The carbon residue of pyrolysis oil obtained using ZSM-5 ammonium powder, nickel on silica-alumina catalyst and best red clay catalyst RC-800 was found to be 0.54 wt.%, 0.39 wt.% and 0.33 wt.% respectively, which was comparable with commercial fuels gasoline and kerosene (Shakirullah et al., 2010). The flash and fire point of multiphase catalytic pyrolysis oil lower than the flash and fire point of kerosene (Ahmad et al., 2017) and higher than the gasoline (Mukhraiya and Yadav, 2015). It indicates the easier ignition of pyrolysis oil in IC engines and low risk of fire hazard during storage of fuel.

5.6 Regeneration and reusability study of catalyst

It is seen from the overall study on WEPS pyrolysis using three different catalysts that the Nickel on silica-alumina catalyst comes up with highest BTE content of 28.56 wt.% for the multiphase/AB-type catalytic pyrolysis at optimum process conditions. Thus, the stability and reusability assessment of catalyst was carried out for the best catalyst Nickel on silica-alumina

for best reactor arrangement multiphase/AB-type catalytic pyrolysis only to check its activity without regeneration and after regeneration of catalyst. The multiphase/AB-type catalytic pyrolysis was conducted at above mentioned optimized experimental conditions up to five runs. After the fifth run (5^{th} run), the catalyst present in the primary reactor i.e., in liquid phase and secondary reactor i.e., vapour phase were regenerated and then further used for the production of BTE via multiphase catalytic pyrolysis process. The process of catalyst regeneration has already been discussed in the chapter-3 (page no. 57).

5.6.1 Reusability assessment of best catalyst Nickel on silica-alumina catalyst

5.6.1.1 Characterization of regenerated catalyst Nickel on silica-alumina

5.6.1.1.1 SEM analysis

The morphological changes between fresh, used and regenerated Nickel on silica alumina catalyst was determined by the SEM analysis. The SEM images of fresh, used and regenerated catalyst are presented in Figure 5.37.

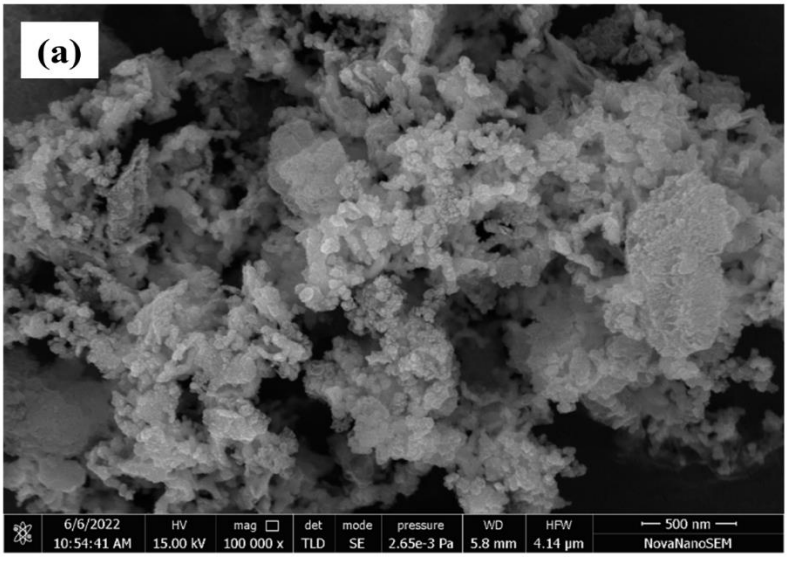

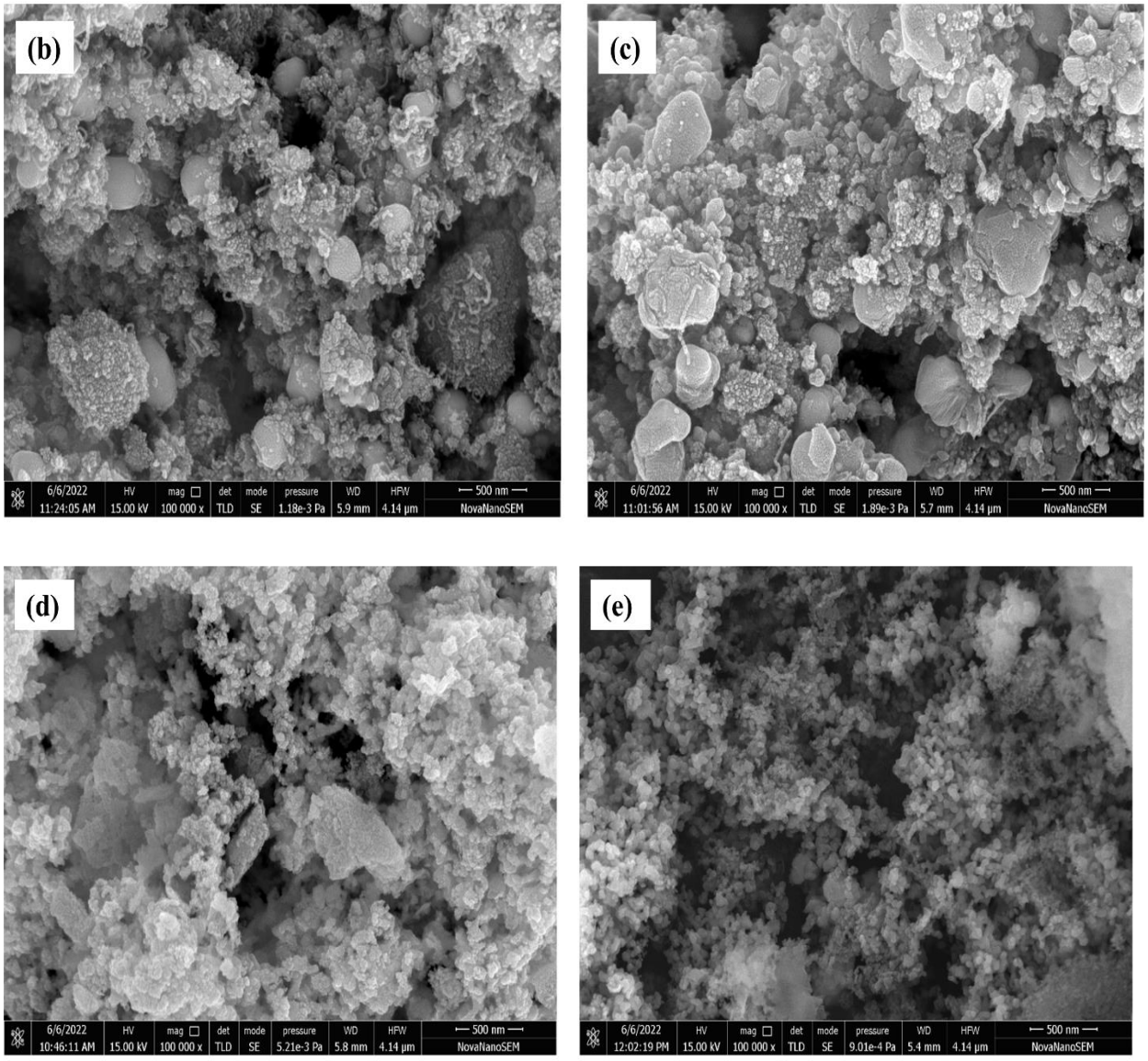

Figure 5.37 SEM image of Nickel on silica-alumina (a) fresh catalyst; (b) & (c) spent catalyst after fifth run of multiphase/AB-type i.e., liquid phase (b) and vapour phase (c); regenerated catalyst of multiphase/AB-type i.e., liquid phase (d) and vapour phase (e).

The Figure 5.37a shows the spherical nanoparticles for fresh Nickel on silica-alumina catalyst. Whereas, agglomeration of catalyst particles due to coke deposition over the surface of catalyst particles was observed for the liquid phase (Figure 5.37b) and vapour phase catalyst (Figure 5.37c) both. On the other side, the SEM images of the regenerated liquid phase (Figure 5.37d)

and vapour phase catalyst (Figure 5.37e) were very similar to the fresh nickel on silica catalyst because of coke removal after the regeneration process (Lopez et al., 2011a).

5.6.1.1.2 BET surface area analysis

The BET surface area of fresh, used and regenerated nickel on silica-alumina catalyst are listed in Table 5.39. The BET surface area of fresh catalyst was found to be 96.60 m^2/g. Whereas, surface area decreased to 6.35 m^2/g and 7.00 m^2/g for liquid phase and vapour phase catalyst, respectively because of coke deposition and agglomeration phenomenon. However, the surface area was increased to 82.70 m^2/g for liquid phase catalyst and 86.20 m^2/g for vapour phase catalyst after the regeneration process. Thus, after regeneration process the Nickel on silica-alumina can be used for further pyrolysis process, which makes the process economical.

Table 5.39 BET surface area of fresh, used and regenerated Nickel on silica-alumina catalyst for multiphase catalytic pyrolysis.

Catalyst type	AB-type pyrolysis catalyst position or location in reactor	Surface area (m^2/g)
Fresh catalyst	-	96.62
Spent catalyst after 5th run	Liquid phase catalyst	6.35
	Vapour phase catalyst	7.00
Regenerated catalyst	Liquid phase catalyst	82.70
	Vapour phase catalyst	86.20

5.6.1.2 Product yield of AB-type pyrolysis

The product yield obtained from multiphase catalytic pyrolysis using fresh, used/spent and regenerated catalyst are shown in Figure 5.38. The liquid yield of 81.15 wt.% and gaseous yield of 17.14 wt.% was obtained from multiphase catalytic pyrolysis using fresh nickel on

silica-alumina catalyst at a temperature of 550 ^{o}C and heating rate of 15 ^{o}C/min (Table 5.40). The liquid yield was decreased due to the cracking ability of fresh catalyst (Run-1), which enhanced the gaseous range molecules (Miandad et al., 2016). After fresh run/run-1, the liquid yield with the increase in as the number of runs up to 5th run.

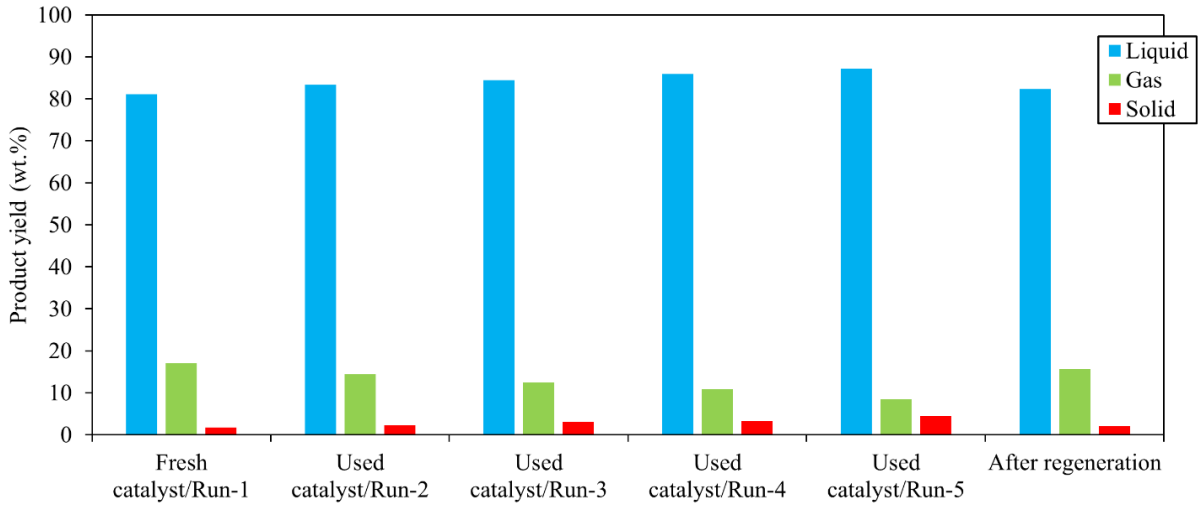

Figure 5.38 Comparison of product yield obtained from multiphase catalytic pyrolysis of WEPS using fresh, used/spent and regenerated Nickel on silica-alumina catalyst at a temperature of 550 ^{o}C, heating rate of 15 ^{o}C/min using feed to catalyst ratio of 20:1.

The liquid yield of 87.15 wt.% was obtained at the fifth run of pyrolysis experiment (Table 5.40). It may be due to the coke deposition over the surface of the catalyst, which reduced the surface area and cracking ability of the catalyst. It is also seen from the Table 5.40 that the very high solid yield of 4.42 wt.% was obtained at the fifth (5th) experimental run, which also confirms the coke deposition over the surface of the catalyst. However, the liquid yield of 82.31 wt.% and solid yield of 2.08 wt.% was obtained using regenerated catalyst. The liquid, gaseous and solid of regenerated catalyst were very close to fresh catalyst. This study confirms that the regenerated study could be performed to reduce the consumption of fresh catalyst and thereby making the process more economical as the catalyst is very expensive.

Table 5.40 Product yield obtained from multiphase catalytic pyrolysis for different experimental runs using fresh, used/spent and regenerated Nickel on silica-alumina catalyst.

Catalyst type	Liquid (wt.%)	Gas (wt.%)	Solid (wt.%)
Fresh catalyst/Run-1	81.15	17.14	1.71
Used catalyst/Run-2	83.34	14.40	2.26
Used catalyst/Run-3	84.47	12.44	3.09
Used catalyst/Run-4	85.91	10.82	3.27
Used catalyst/Run-5	87.15	8.43	4.42
After regeneration	82.31	15.61	2.08

5.6.1.3 Analysis of pyrolysis oil

5.6.1.3.1 Quantification of aromatic content/BTE and styrene in pyrolysis oil

The quality of pyrolysis oil obtained using fresh, spent/used and regenerated catalyst was measured in terms of target molecules benzene, toluene, and ethylbenzene (BTE) content using calibration characteristics (Figure 3.8, page no. 59). The BTE and styrene content of pyrolysis oil obtained from multiphase catalytic pyrolysis using fresh, used and regenerated Nickel on silica-alumina catalyst is mentioned in Table 5.41.

Table 5.41 Aromatics BTE and styrene content of multiphase catalytic pyrolysis oil obtained using fresh, spent/used and regenerated Nickel on silica-alumina catalyst.

Catalyst	Benzene (wt.%)	Toluene (wt.%)	Ethylbenzene (wt.%)	Styrene (wt.%)	Total BTE (wt.%)
Fresh run/run-1	8.05	7.55	12.96	55.55	28.56
Run-2	7.15	7.12	11.56	60.12	25.83
Run-3	6.23	6.89	9.91	63.78	23.03
Run-4	6.95	6.13	5.26	71.98	18.34
Run-5	5.24	5.19	3.84	78.33	14.27
After regeneration	8.10	7.57	12.77	56.13	28.44

It is seen from the Table 5.41, that multiphase catalytic pyrolysis using fresh Nickel on silica-alumina catalyst produced very high BTE content of 28.56 wt.% because of secondary reactions, mainly cracking and hydrogenation. These secondary reactions are responsible for the production of target molecules BTE. Moreover, the reactor arrangement used for the multiphase catalytic pyrolysis facilitates the two-stage catalytic cracking, which also accelerates the secondary reactions. After the fifth (5^{th}) run , the BTE content drastically decreased to 14.27 wt.% due to the reduction in the surface area of the catalyst. Accordingly, the Brosnted acid sites, which are responsible for the formation of target molecules BTE, also decreases because of the coke deposition (Marczewski et al., 2013). The BTE content of 25.83 wt.%, 23.03 wt.% and 18.34 wt.% were obtained at experimental run-2, run-3 and run-4, respectively. However, almost the same BTE content of 28.44 wt.% was obtained using regenerated nickel on silica-alumina catalyst.

5.6.1.3.2 Physicochemical properties of pyrolysis oil

The physicochemical properties such as gross calorific value (GCV), carbon residue and flash and fire point of pyrolysis oil obtained from multiphase catalytic pyrolysis using fresh, used and regenerated Nickel on silica-alumina catalyst were measured as per the standard methods given in the experimental section. It is seen from the Table 5.42, the calorific value of pyrolysis oil obtained from multiphase catalytic pyrolysis using fresh catalyst was found to be highest (12750 Cal/g), even higher than the commercial fuel gasoline and kerosene (Gaurh and Pramanik, 2019). Whereas, the calorific value get decreased to 9826 Cal/g after fifth (5^{th}) run. It may be due to the presence of high molecular weight molecules in the pyrolysis oil because

after fifth (5^{th}) run catalyst loosed its cracking ability and not able to produce lighter molecules of high calorific value.

Table 5.42 Physicochemical properties of pyrolysis oil obtained from multiphase catalytic pyrolysis using fresh, used and regenerated Nickel on silica-alumina catalyst.

Physicochemical properties	Catalytic pyrolysis/ Run-1	Catalytic pyrolysis/ Run-5	After regeneration	Gasoline	Kerosene
GCV (Cal/g)	12750	9826	11440	11315	11052
Carbon residue (wt.%)	0.45	0.89	0.51	0.14	0.18
Flash point (^oC)	40	56	42	22	42
Fire point (^oC)	44	62	48	25	45

The calorific value of pyrolysis oil obtained using regenerated catalyst was found to be 11440 Cal/g, which indicates that after the regeneration process, catalyst significantly improved the quality of pyrolysis oil. The carbon residue of pyrolysis oil obtained using fresh and regenerated catalyst were comparable with commercial fuel gasoline and kerosene (Shakirullah et al., 2010). Furthermore, the flash and fire point of pyrolysis oil obtained using fresh catalyst was found to be lower than kerosene (Ahmad et al., 2017) and higher than gasoline (Mukhraiya and Yadav, 2015). Whereas, the flash and fire point of pyrolysis oil obtained from regenerated catalyst was very close to the commercial fuel kerosene (Ahmad et al., 2017). Thus, it is recommended that the, pyrolysis oil obtained using regenerated catalyst could be used in diesel generator sets and cooking stoves.

5.7 Comparison of the present study with other works available in open literature

There are various studies available in literature based on the simple liquid phase catalytic pyrolysis of polystyrene (PS). However, in present study the effect of various effective process parameters such as feed to catalyst ratio, heating rate, reaction temperature, reactor arrangement on the product yield and product composition has been examined in detail. Such type of detailed study based on the pyrolysis of waste expanded polystyrene (WEPS) has not been found in open literature. However, the comparison of the present work with other studies available in open literature is presented in Table 5.43. Gaurh and Pramanik, 2020 carried out the catalytic pyrolysis of polystyrene (PS) using ZSM-5 catalyst in the range of temperature 400 ^{o}C to 700 ^{o}C. The highest liquid yield of 86.2 wt.% was obtained at a temperature of 700 ^{o}C mainly contains benzene (0.80 wt.%), toluene (16.57 wt.%) and ethylbenzene (3.57 wt.%). However, the styrene content of pyrolysis oil was not reported by Gaurh and Pramanik 2020. The benzene and ethylbenzene content in the present study (Table 5.43) is higher than the benzene and ethylbenzene content reported by Gaurh and Pramanik 2020. Adnan et al., 2014 employed Zinc bulk catalysts Zn, ZnO, and $ZnCl_2$ to conduct the catalytic pyrolysis of expanded polystyrene (EPS). They reported that the Zn catalyst performed best for the catalytic pyrolysis of EPS. The catalytic pyrolysis using Zn catalyst produced toluene of 2.47 wt.%, ethylbenzene of 1.16 wt.% and styrene of 47.96 wt.% in the pyrolysis oil. The toluene and ethylbenzene content reported by Adnan et al., 2014 was very less as compared to the present study (Table 5.43). However, the ZSM-5 ammonium powder used in the present study produced the styrene content of 46.30 wt.% of styrene in the pyrolysis oil. Furthermore, another catalysts ZnO and $ZnCl_2$ reported by Adnan et al., 2014 also produced less toluene and ethylbenzene as compared to the present work (Table 5.43). Similarly, Shah et al., 2014 used Mg, MgO and $MgCO_3$ for the catalytic pyrolysis expanded polystyrene (EPS).

Table 5.43 Comparison of the present study with other pyrolysis works based on the pyrolysis of polystyrene (PS) available in the open literature.

Catalyst used	Pyrolysis Temperature (°C)	Reactor	Liquid yield (wt.%)	Aromatic content (wt.%)	References
ZSM-5	400-700	Semi-batch reactor	Temperature: 700 °C 86.2	Benzene: 0.80 Toluene: 16.57 Ethylbenzene: 3.57 Styrene: not available	Gaurh and Pramanik, 2020
Zn, ZnO, $ZnCl_2$	450-500	Semi-batch reactor	Catalyst: Zn Temperature: 450 °C Liquid yield: 96.73±0.12	Benzene: not available Toluene: 2.47 Ethylbenzene-: 1.16 Styrene: 47.96	Adnan et al., 2014
			Catalyst: ZnO Temperature: 450 °C Liquid yield: 84.73±2.31	Benzene: not available Toluene: 1.80 Ethylbenzene: 0.60 Styrene: 41.45	
			Catalyst: $ZnCl_2$ Temperature: 500 °C Liquid yield: 79.60±4.20	Benzene: not available Toluene: 2.11 Ethylbenzene: 1.93 Styrene: 40.88	
Mg, MgO, $MgCO_3$	Catalyst: Mg Temperature: 450 Catalyst: MgO, $MgCO_3$ Temperature-400	Batch reactor	Catalyst: Mg 82.20	Benzene: not available Toluene: 2.73 Ethylbenzene: 0.88 Styrene: 66.56	Shah et al., 2014
			Catalyst: MgO 91.60	Benzene: not available Toluene: 4.05 Ethylbenzene: 2.23 Styrene: 54.53	
			Catalyst: $MgCO_3$ 81.80	Benzene: not available Toluene: 6.28 Ethylbenzene: 7.59 Styrene: 55.23	

Catalyst used	Pyrolysis Temperature (°C)	Reactor	Liquid yield (wt.%)	Aromatic content (wt.%)	References
Silica-alumina	410	Semi-batch reactor	97.3	Benzene: not available Toluene: Not available Ethylbenzene: 0.2 Styrene: 80.98	Moqadam et al., 2015
ZSM-5 ammonium powder, Nickel on silica-alumina, Red clay catalyst RC-800	550 °C	Semi-batch reactor (**Multi phase catalytic pyrolysis)**	Catalyst: ZSM-5 ammonium powder Liquid yield: 75.11	Benzene: 11.68 Toluene: 12.18 Ethylbenzene: 4.26 Styrene: 46.30	**Present work**
			Catalyst: Nickel on silica-alumina Liquid yield: 81.15	Benzene: 8.05 Toluene: 7.55 Ethylbenzene: 12.96 Styrene: 55.55	
			Catalyst: Red clay RC-800 Liquid yield: 79.47	Benzene: 1.47 Toluene: 15.42 Ethylbenzene: 10.72 Styrene: 60.75	

The catalytic pyrolysis of EPS using Mg as a catalyst obtained toluene, ethylbenzene and styrene content of 2.73 wt.%, 0.88 wt.% and 66.56 wt.%, respectively in the pyrolysis oil. The MgO catalyst produced the slightly more toluene (4.05 wt.%), ethylbenzene (2.23 wt.%) and less styrene content of 54.53 wt.% as compared to the Mg catalyst. Whereas, $MgCO_3$ obtained highest toluene (6.28 wt.%) and ethylbenzene (7.59 wt.%) in the pyrolysis oil as compared to the other catalysts i.e., Mg and MgO. However, the toluene and ethylbenzene content in the present work (Table 5.43) is higher than the toluene and ethylbenzene content reported by Shah et al., 2014. Moqadam et al., 2015 conducted the catalytic pyrolysis of polystyrene (PS) using silica-alumina catalyst. The pyrolysis oil mainly composed of styrene monomer (80.98 wt.%). However, the minute ethylbenzene (0.2 wt.%) was also found in the pyrolysis oil. However, the styrene content was found to be very less (Table 5.43) as compared to the styrene content reported by Moqadam et al., 2015.